PART ONE: FURTHER INVESTIGATION OF ENERGY TRANSFER PROCESSES IN THE UNIMOLECULAR DECOMPOSITION OF NITRYL CHLORIDE

PART TWO: DECOMPOSITION OF NITROGEN PENTOXIDE IN THE PRESENCE OF NITRIC OXIDE. IV. EFFECT OF NOBLE GASES

PART THREE: THEORETICAL PRE-EXPONENTIAL FACTORS FOR HYDROGEN ATOM ABSTRACTION REACTIONS

PART FOUR: CARBON ISOTOPE EFFECT DURING OXIDATION OF CARBON MONOXIDE WITH NITROGEN DIOXIDE

Thesis by

David James Wilson

In Partial Fulfillment of the Requirements

For the Degree of

Doctor of Philosophy

California Institute of Technology

Pasadena, California

1958

TO MY WIFE

Acknowledgments

It is a pleasure to express my appreciation to the people who have helped me in the pursuit of this work.

My association with Dr. Harold S. Johnston has been a source of great satisfaction to me. I am deeply grateful for his encouragement, advice, direction, and friendship during the past seven years. Not only has he directed my research work, but he has strongly influenced the course of study that I have followed.

Mr. Burt Bubb and Mr. Robert Perthel were of much help in designing and constructing the apparatus. Mrs. Sylvia Teem, who typed the thesis, was most helpful and obliging.

The faculties and graduate students of the Institute and of Stanford University provided a friendly, helpful, and challenging environment. I am especially indebted to Herman Cordes, Milton Volpe, Ted Harrison, and Donald Rapp.

We are obligated to the California Research Corporation and to the Office of Naval Research for their financial support of this work. My family and I are especially grateful to the National Science Foundation for the three fellowships they have given us.

And lastly, I am deeply grateful to my wife, whose typing, computing, editing and proofreading have been of great assistance, and who has been a source of comfort and of strength.

Abstract

The unimolecular decomposition of nitryl chloride was investigated in the pressure range 10 to 500 mm. and the temperature range 141 to 205°C. Relative efficiencies of foreign gases were found to vary slightly, if at all, over this range of conditions. The reaction was observed to be partially heterogeneous in the Pyrex reaction cell used. The results of this work are in agreement with those of Volpe and Cordes at low pressures and with those of Casaletto at high pressures. The discrepancies between the relative efficiencies obtained by Volpe and those obtained by Schumacher and Sprenger are probably due to effects of heterogeneity in the work of Schumacher and Sprenger.

The data obtained in this work were interpreted in terms of the Lindemann mechanism. Relative efficiencies were calculated by means of the Schwartz-Slawsky-Herzfeld theory and the Landau-Teller theory; the latter theory gave results in qualitative agreement with the available experimental data.

Relative efficiencies of the noble gases and of carbon tetrachloride for the decomposition of nitrogen pentoxide at 50°C. in the pressure range 0.1 to 3.0 mm., are reported in Part Two of this thesis. It was found that deactivation of activated reactant molecules does not occur on every collision.

Part Three of this thesis, "Theoretical Pre-exponential Factors for Hydrogen Atom Abstraction Reactions," contains its own abstract. Pre-exponential factors were calculated by means of Eyring's activated complex theory for ten bimolecular reactions. Part Four of this thesis "Carbon Isotope Effect during Oxidation of Carbon Monoxide with Nitrogen Dioxide," contains its own abstract.

Table of Contents

Table of Contents (Cont'd)

PART ONE: FURTHER INVESTIGATION OF ENERGY TRANSFER PROCESSES IN THE UNIMOLECULAR DECOMPOSITION OF NITRYL CHLORIDE

I. Introduction

The thermal decomposition of nitryl chloride was first investigated by Schumacher and Sprenger (1,2,3). The reaction was investigated over a pressure range of from ten mm.* to ten atmospheres and over a temperature range of from 100 to 150°C. The progress of the reaction was followed by observing the change in pressure as the reaction proceeded. The pressure after the reaction had gone to completion was found to be greater than the initial pressure by one half of the initial nitryl chloride pressure. The concentration of nitryl chloride at any time during a run was found to follow the first-order integrated rate expression. The empirical first-order rate constant was found to be dependent upon the total initial pressure of the gas and to be independent of the size of the vessel in which the reaction was carried out.

Schumacher and Sprenger proposed that the stoichiometry of the reaction is

$$NO_2Cl \rightarrow NO_2 + \tfrac{1}{2} Cl_2 .$$

They also proposed the following mechanism for the reaction:

$$NO_2Cl \rightarrow NO_2 + Cl \qquad k_1,$$
$$Cl + NO_2Cl \rightarrow NO_2 + Cl_2 \qquad k_2.$$

---

* A list of the abbreviations used in this dissertation is given in Appendix I.

If a steady state concentration of chlorine atoms is assumed, the empirical first-order rate constant can be identified with $2k_1$.

Cordes and Johnston (4) investigated the thermal decomposition of nitryl chloride over a temperature range of 180 to 250°C. and over a pressure range of five to one hundred mm. of argon and of one to fifteen mm. of nitryl chloride. Their work was done in a fifty-liter Pyrex flask to avoid possible heterogeneity; and the reaction was followed colorimetrically, by measuring the absorption by nitrogen dioxide of the 436 millimicron line of an A-H4 mercury arc. They confirmed the stoichiometry suggested by Schumacher and Sprenger and also confirmed that the reaction is first order with respect to time. The empirical first-order rate constant was found to be first order with respect to concentration of argon and with respect to initial concentration of nitryl chloride. Cordes and Johnston found an activation energy for the reaction of 27.5 ± 0.1 kcal/mol. This work is a clear-cut example of the second-order region of a unimolecular reaction. It also shows that argon does not deactivate excited nitryl chloride upon every collision (5). Cordes and Johnston also made a study of several variations of the mechanism proposed by Schumacher and Sprenger and concluded that the original mechanism was in all probability correct.

Volpe and Johnston (6,7) made a study of the decomposition of nitryl chloride at 203°C. in the presence of each of sixteen foreign gases at total pressures between two and six mm. The rate under such conditions is the rate of activation of nitryl chloride by collision. They listed relative rate constants for activation by the various foreign gases and also listed the relative efficiency of energy transfer,

collision per collision. They concluded, in agreement with previous findings (4,5), that deactivation does not occur upon every collision of an excited nitryl chloride molecule. The relative efficiency of energy transfer shows several strong empirical correlations with molecular interaction parameters (such as boiling point and the constants from the Lennard-Jones potential function). Gases with permanent dipole moments were found to have higher relative efficiencies than comparable non-polar molecules. They found, however, very little correlation between relative efficiency and the number of atoms or number of oscillators in the foreign gas molecules. Their relative efficiencies, obtained at the low-pressure limit of the reaction at 203°C., were quite different from those obtained by Schumacher and Sprenger in the intermediate pressure range at 140°C. (Table I). One of the objectives of this dissertation is to clear up this point — to see if relative efficiencies really do display the temperature or pressure dependence these results indicate, or if one study or the other was subject to some unknown systematic error.

Table I. Comparison of Volpe and Johnston's Results with Those of Schumacher and Sprenger

M-gas	Relative Efficiency (Volpe and Johnston)	Relative Efficiency (Schumacher and Sprenger)
NO_2Cl	1.00	1.00
NO_2	1.15	0.54
Cl_2	0.35	0.17
O_2	0.29	0.19
CO_2	0.38	0.16
H_2	0.35	0.17

Volpe and Johnston (7) also made a detailed analysis of the effects of the time-dependent change in composition of the reaction mixture upon the rate of energy transfer during the course of the reaction. Their work is applicable to the low-pressure region of the reaction, where the observed rate is the rate of activation of reactant molecules.

Casaletto and Johnston (8) attempted to reach the high-pressure limit of the reaction but were unsuccessful. They made runs at pressures as high as 115 atmospheres, using nitrogen as the added foreign gas, at 123 and 147°C. Calculations by Herschbach (9) using Slater's theory of unimolecular reactions (10,11,12) indicate that the high-pressure limit lies at pressures above 4000 atmospheres.

There was a wide gap in experimental conditions between the work of Cordes, Volpe, and Johnston (4,6) and the work of Casaletto and Johnston (8). There were discrepancies between the relative efficiencies of foreign gases found by Volpe (6) and those found by Schumacher and Sprenger (1,2,3). The present study is designed to close the gap and clear up the discrepancy.

II. Theory

A. The Lindemann Theory

If a chemical species, A, decomposes according to the rate law

$$-\frac{dA}{dt} = kA,$$

then the decomposition is said to be first order with respect to time. (Capital letters used in this and subsequent equations refer to concentrations, and t refers to time.) The quantity k is the empirical first-order rate constant. Gas-phase unimolecular decompositions are experimentally observed to obey this rate law; the subsequent discussion will be limited to this class of reactions.

The Lindemann theory of unimolecular gas reactions has been discussed in great detail by Mills and Johnston (13); it will be only briefly outlined here, except for some aspects of the theory which were developed after that paper was written. The Lindemann theory proposes that a molecule of species A obtains sufficient internal energy to decompose by colliding with molecules M, of the same or different species as A. The resulting activated A molecules, which will be denoted by A*, can either be deactivated by a second collision; or they can decompose into products. It is assumed that only two-body collisions contribute appreciably to the process and that the individual quantum states i of A* are not dependent upon the composition or temperature of the bulk gas.

Let the activating rate constant be denoted by a_{im} (where the subscript m denotes the identity of the activating gas), the deactivating rate constant by b_{im}, and the decomposition rate constant by c_i. Then the above-mentioned process is described by the chemical equations:

$$
\begin{aligned}
A + M &\rightarrow A_i^* + M \qquad a_{im}, \\
A_i^* + M &\rightarrow A + M \qquad b_{im}, \\
A_i^* &\rightarrow \text{Products} \qquad c_i .
\end{aligned}
\tag{1.1}
$$

In this mechanism the a_{im} and b_{im} have been averaged over the non-reactive states of A and M, where it is assumed that the distributions are those found at equilibrium (14). Such averaging is certainly not valid if activation and deactivation take place by a stepwise process; i.e., if the collisions result only in transitions to the next higher or next lower vibrational state of the reactant molecule. This statement is proved, for a highly over-simplified model, in Appendix II. It is assumed that there is only one gas species, M, that contributes toward the activation and deactivation processes. (This restriction will later be relaxed.) The rate of the reaction is given by the sum of the rates of disappearance of reactant from the various quantum states i:

$$
-\frac{dA}{dt} = \sum_i c_i A_i^* . \tag{1.2}
$$

A value for A_i^* may be found by calculating $\frac{dA_i^*}{dt}$ from the mechanism 1.1 and then making use of the steady state assumption (15) (see also Appendix III) to set $\frac{dA_i^*}{dt}$ equal to zero:

$$
\frac{dA_i^*}{dt} = 0 = AM\, a_{im} - A_i^* M\, b_{im} - A_i^* c_i . \tag{1.3}
$$

From this equation and the rate expression 1.2 it follows that

$$
-\frac{dA}{dt} = \sum_i \frac{a_{im} c_i M A}{b_{im} M + c_i} = kA. \tag{1.4}
$$

The coefficient of A in this equation is the expression for the empirical first-order rate constant k in terms of the microscopic molecular rate constants of the theory.

R. C. Tolman (16) has shown, by means of the principle of microscopic reversibility, that the rate constants a_{im} and b_{im} are related by the expression $a_{im} = b_{im}P_i$, where P_i is the equilibrium probability of the state i of molecule A. The quantities a_{im}, b_{im}, and P_i are functions of temperature and of the molecular parameters of A. The quantities a_{im} and b_{im} are also functions of molecular parameters of M. c_i is a function only of the molecular parameters of A. Substituting the above relationship ($a_{im} = b_{im}P_i$) into the expression for k gives

$$K = \sum_i \frac{b_{im} P_i c_i M}{b_{im} M + c_i} \quad . \tag{1.5}$$

If more than one species of molecule contribute to the collisional activation of A, the following steps are included in the mechanism:

$$\begin{aligned} &A + A \rightarrow A_i^* + A \quad a_{ia}, && A + N \rightarrow A_i^* + N \quad a_{in}, \\ &A + A_i^* \rightarrow A + A \quad b_{ia}, && N + A_i^* \rightarrow A + N \quad b_{in}, \\ &A + M \rightarrow A_i^* + M \quad a_{im}, && \text{etc.} \\ &A_i^* + M \rightarrow A + M \quad b_{im}, && A_i^* \rightarrow \text{Products} \quad c_i. \end{aligned} \tag{1.6}$$

The expression for k becomes

$$K = \sum_i \frac{P_i c_i \left[b_{ia}A + b_{im}M + b_{in}N + \cdots \right]}{\left[b_{ia}A + b_{im}M + b_{in}N + \cdots \right] + c_i} \quad . \tag{1.7}$$

B. The Functional Form of b_{im}

From relation 1.7 one would like to obtain information about the functions b_{im}. (In the following discussion the quantities P_i and c_i will be left perfectly general.) One would like to know, first, the nature of the dependence of b_{im} upon the identity of M and, second, the nature of the dependence of b_{im} upon the quantum state i of the activated reactant molecule. This paper is concerned with the first of these two questions.

As one makes runs at lower and lower pressures of reactant and added foreign gas, a point is reached below which $b_{im} M \ll c_i$ for all states i that contribute to the reaction. In this pressure region the function k can be expanded in positive powers of M:

$$K = \sum_{n=1}^{\infty} \left[\sum_i P_i c_i \left(\frac{b_{im}}{c_i} \right)^n \right] M^n \cong \sum_i b_{im} P_i M$$
$$= \langle b_m \rangle P M = a_m M, \qquad (1.8)$$

where $P = \sum_i P_i$, and $a_m = \sum_i a_{im}$.

If one has both reactant and foreign gas present at low pressures, the observed rate is $a_m M + a_a A$ (5,6). If for a set of runs one maintains constant the initial reactant concentration and varies the foreign gas concentration, one can obtain a plot of k versus M. The slope of this plot is a_m; and the intercept is $a_a A_o$, where A_o is the constant initial concentration of reactant used in making the runs. The ratio a_m/a_a will be denoted by $R^o(M/A)$; it is the efficiency at the low-pressure limit of M relative to A for activation of A. In

terms of the microscopic quantities,

$$R^{o}(M/A) = \frac{\sum_i b_{im} P_i}{\sum_i b_{ia} P_i} = \frac{\sum_i a_{im}}{\sum_i a_{ia}} . \qquad (1.9)$$

By virtue of the principle of microscopic reversibility, this ratio is also the corresponding relative efficiency for deactivation. Volpe (6) obtained values of $R^{o}(M/A)$ for sixteen different foreign gases for the decomposition of nitryl chloride.

There are several other ways of defining relative efficiencies that are applicable over the entire pressure range, instead of just at the low-pressure limit.

The differential efficiency of N relative to M is defined as

$$R^{d}(N/M) = \left(\frac{\partial K_n}{\partial N} \Big/ \frac{\partial K_m}{\partial M} \right)_{\substack{K_n = K_m \\ T_n = T_m}} = \frac{\sum_i \frac{P_i c_i^2 b_{in}}{(b_{in}N + b_{ia}A + c_i)^2}}{\sum_i \frac{P_i c_i^2 b_{im}}{(b_{im}M + b_{ia}A + c_i)^2}} , \qquad (1.10)$$

where T_n and T_m are the temperatures at which the two sets of runs are made.

The integrated efficiency of N relative to M is defined as

$$R^{i}(N/M) = \left(\frac{M}{N} \right)_{\substack{K_n = K_m \\ T_n = T_m}} = \frac{\sum_i \frac{P_i c_i^2 b_{in}}{L_i(A,M,N)}}{\sum_i \frac{P_i c_i^2 b_{im}}{L_i(A,M,N)}} , \qquad (1.11)$$

where $L_i(A,M,N) = (b_{im}M + b_{ia}A + c_i)(b_{in}N + b_{ia}A + c_i)$

Lastly, a relative efficiency may be expressed in terms of finite differences as follows:

$$R^f(N/M) = \left(\frac{\Delta M}{\Delta N}\right)_{\substack{K_n = K_m \\ K_{n+\Delta n} = K_{m+\Delta m} \\ T_n = T_m}} \tag{1.12}$$

This is expressed implicitly in terms of the microscopic rate constants as

$$\sum_i \frac{(M b_{im} - N b_{in}) P_i c_i^2}{L_i(A, M+\Delta M, N+\Delta N)} = \sum_i \frac{(\Delta N b_{in} - \Delta M b_{im}) P_i c_i^2}{L_i(A, M+\Delta M, N+\Delta N)}. \tag{1.13}$$

Note that these last three relative efficiencies all depend upon the pressures at which they are measured and that the last one depends upon the sizes of the finite differences as well.

A wide variety of functional forms can be hypothesized for the quantity b_{im}. It was often assumed previously (see references 11, 12, and 17, for example) that b_{im} was equal to the kinetic theory collision constant z_{ma} for collisions between molecules A and M. This assumption was subsequently proven false (5,6). The possibility was raised by Johnston (18) that the function b_{im} might be factorable into a constant, dependent only upon the identity of the foreign gas, and a function, dependent only upon the quantum state i of the reactant molecule: $b_{im} = b_m f_i$.

It is of interest to see what effect this assumption has upon the various relative efficiencies previously defined. It is shown in Appendix IV that, if this factoring can be made, then all these relative efficiencies are constant and equal over the entire pressure range

at a given temperature. One merely substitutes $b_{in} = R(N/M)b_{im}$ into the expressions, makes use of the fact that $k_n = k_m$ to derive $N\,R(N/M) = M$, and simplifies.

A simple argument (19) due to Johnston and Professor Paul Garabedian, of Stanford University, is closely related to the above treatment of relative efficiencies. Let there be a set of runs made in which the only species contributing to reactant activation is M and another set made in which the activating species is N. Then

$$K_m(M) = \sum_i \frac{b_{im} P_i c_i M}{b_{im} M + c_i} \tag{1.14}$$

and

$$K_n(N) = \sum_i \frac{b_{in} P_i c_i N}{b_{in} N + c_i} \,. \tag{1.15}$$

Denote the low-pressure efficiency of N relative to M by R. Define a variable z such that $z = M$ for the set of runs made with species M and $z = RN$ for the set of runs made with species N. This serves to change the independent variable of k_n in such a way that $k_n(z)$ and $k_m(z)$ have the same slope at the origin.

$$K_m(z) = \sum_i \frac{P_i c_i z}{z + \left(\frac{c_i}{b_{im}}\right)} \,; \tag{1.16}$$

$$K_n(z) = \sum_i \frac{P_i c_i z}{z + \left(\frac{c_i R}{b_{in}}\right)} \,. \tag{1.17}$$

Postulate that $k_n(z) = k_m(z)$ over a range of real positive z. Since k_n and k_m are analytic functions of z, they can be analytically

continued throughout the z-plane if z is made a complex variable. Since the functions are identical over a range of z, their analytic continuations are identical throughout the z-plane (20). In particular, the functions have poles at the same points on the negative real axis, and at these poles they have the same residues. The condition that the poles occur at the same places gives the relation $b_{in} = Rb_{jm}$, where i does not necessarily equal j. The condition that the residues be equal gives the relation $P_i c_i = P_j c_j$, which implies either that $P_i c_i = P_j c_j$ for any i and j or that $i = j$. The first assumption is physically unreasonable in view of the exponential temperature dependence of P_i. Therefore one concludes that $b_{in} = Rb_{im}$, or that the function b_{im} can be factored into $b_m f_i$. Recall the assumption from which this conclusion was derived: a change of the scale of the independent variable can be made which identically superimposes plots of k_m versus M for different species M over a finite pressure range.

The last paragraph shows that $b_{im} = b_m f_i$ is a necessary condition for this superposition to take place. Sufficiency follows by merely substituting $z = RN$, $b_{in} = Rb_{im}$ in the expression for $k_n(N)$ and substituting $z = M$, $b_{im} = b_{im}$ in the expression for $k_m(M)$.

If $b_{im} = b_m f_i(T)$, where b_m is not a function of temperature and $f_i(T)$ is, then all of the previously defined relative efficiencies are independent of temperature as well as of pressure. For, if one refers to the expressions for the relative efficiencies in terms of the microscopic rate constants (equations 1.9, 1.10, 1.11, and 1.12), it becomes apparent that the temperature dependence in the numerator cancels that in the denominator. Therefore, if temperature dependence

of relative efficiencies is observed, then either $b_{im} = b_m(T)f_i(T)$ or b_{im} cannot be factored.

To summarize: if there is neither pressure nor temperature dependence of relative efficiency, then $b_{im} = b_m f_i(T)$. If there is temperature dependence but not pressure dependence, then $b_{im} = b_m(T)\, f_i\,(T)$. If one finds pressure dependence or both pressure and temperature dependence, then b_{im} cannot be factored. One of the objects of this investigation is to determine which of these alternatives is correct for the thermal decomposition of nitryl chloride. The large discrepancy between the results of Volpe and Johnston and those of Schumacher and Sprenger made it appear plausible that a large temperature or pressure effect existed. If this effect did exist, it could give interesting information on the form of the function b_{im}.

Let $\mathcal{R}$ be any one of the relative efficiencies defined by equations 1.9, 1.10, 1.11, or 1.12. If $b_{im} = b_m(T)f_i(T)$, the quantity $RT^2 \frac{\partial \log \mathcal{R}}{\partial T}$ is the difference in activation energy at the low-pressure limit of the reactions involving the foreign gases being compared. This follows from the fact that for this case the relative efficiencies under consideration are all numerically equal to the relative efficiency at the low-pressure limit.

$$R^\circ(N/M) = \frac{K_n'}{K_m'}, \qquad K_n' = \frac{K_n}{N},$$

$$\log R^\circ(N/M) = \log K_n' - \log K_m', \tag{1.18}$$

and $$RT^2 \frac{\partial \log R^\circ(N/M)}{\partial T} = E_n^\circ - E_m^\circ.$$

This temperature derivative at the low-pressure limit has an interesting interpretation in terms of the most general form of the Lindemann theory (14). This derivative is the quantity

$$\left[\langle \epsilon^a + \epsilon^n \rangle_n^* - \langle \epsilon^a + \epsilon^n \rangle^e \right] - \left[\langle \epsilon^a + \epsilon^m \rangle_m^* - \langle \epsilon^a + \epsilon^m \rangle^e \right].$$

$\langle \ \rangle_n^*$ signifies averaging over the distribution of reacting A molecules which were activated in A-N collisions, and $\langle \ \rangle^e$ signifies averaging with respect to the equilibrium distribution of all molecules. A proof of this statement is given in Appendix V.

Kassel (21) and Johnston and White (22) have developed a large number of theorems which can be used to test experimental data to see if they are consistent with the Lindemann theory. For other papers on the theory of unimolecular gas reactions, see also references (23-28).

C. Computation of Relative Efficiencies

1. Introduction

During the last few years the theoretical treatment of collisional activation probabilities, which was first developed by Zener (29), has been refined and extended (30-36). Unfortunately these treatments all contain approximations that are of dubious validity when they are applied to the very highly excited, strongly anharmonic vibrational states involved in chemical reactions.

Relative efficiencies, collision per collision, were calculated using the theory of Schwartz, Slawsky, and Herzfeld (30, 31, 32) for the decomposition of nitryl chloride in the presence of twelve different gases. The results are compared with the relative efficiencies,

collision per collision, found by Volpe and Johnston for these gases.

2. The Theory of Schwartz, Slawsky, and Herzfeld

Let Ψ be the wave function which describes two molecules in space as they undergo collision. It satisfies the Schroedinger equation,

$$H^{(s)}\Psi - \frac{\hbar^2}{2\mu}\left[\frac{1}{r^2}\frac{\partial}{\partial r}\left(r^2\frac{\partial\Psi}{\partial r}\right) + \frac{1}{r^2\sin\theta}\frac{\partial}{\partial\theta}\left(\sin\theta\frac{\partial\Psi}{\partial\theta}\right)\right] + V\Psi = W\Psi. \tag{1.19}$$

$V = V_r(r)V_{int}(s)$; $H^{(s)}$ is the Hamiltonian operator of the internal vibrational motion; W is the total energy of the system; μ is the reduced mass of the two molecules; r is the distance between their centers of mass; θ is the angle between the vector $\vec{r}$ and the apse-line; and s represents internal coordinates describing the vibrations. The molecules are considered rotationless during the collision.

This equation is solved by perturbation theory, using an exponential interaction potential. The wave functions used are the harmonic oscillator functions and the solutions to the problem of elastic scattering from an exponential potential. The number of molecules which are inelastically scattered from a uniform beam of unit amplitude and of given initial velocity and which have caused a particular vibrational transition, is obtained by integrating the corresponding wave function, multiplied by the ratio of the final velocity to the initial velocity, over the surface of a sphere about the scattering center. This quantity is then averaged over an equilibrium distribution of initial velocities. The integrations performed in evaluating the perturbation theory matrix elements and in averaging over the initial velocity distribution are done approximately.

3. Application of the Theory to the Computation of Relative Efficiencies

For most calculations nitryl chloride was regarded as a diatomic gas; one group of calculations was made considering nitryl chloride as a polyatomic gas with two oscillators taking part in energy transfer.

For one set of calculations made, set A, the constants in the exponential intermolecular potential were chosen to cause the potential to match in value and in slope the Lennard-Jones potential where it has a value of 6kT, which corresponds to the "most effective energy of collision" in the Schwartz-Slawsky-Herzfeld theory.

For another set of calculations, set B, the constants in the exponential intermolecular potential were chosen to cause the potential to match in value and in slope the potentials obtained by Amdur and coworkers (37-40) where these potentials have the value 6kT. Nitryl chloride was assumed to have the same potential parameters as those Amdur reported for argon (corresponding to collisions with the chlorine atom in the molecule) in one group of this set of calculations. In another group, nitryl chloride was assumed to have the same potential parameters as Amdur found for neon (corresponding to collisions with an oxygen or nitrogen atom). Amdur's potentials, obtained by scattering experiments with noble gases, presumably give a more accurate picture of the repulsive portion of the intermolecular potential than do potentials determined from viscosity and virial coefficient data.

The first formula used in set A of the calculations was calculated from the following equations derived by Schwartz, Slawsky and Herzfeld, (reference (30), p. 717):

$$Z_{ma} = Z_0 \cdot \frac{2 m_{a1} m_{a2} (m_m + m_a)}{m_m (m_{a1}^2 + m_{a2}^2)} \cdot Z_{vib.}^{ma} \cdot Z_{trans.}^{ma}, \tag{1.20}$$

$$Z_{vib.}^{ma} = \frac{1}{2\pi^2} \frac{\theta'_{ma}}{\theta_a},$$

$$Z_{trans.}^{ma} = \pi^2 \sqrt{\frac{3}{2\pi}} \left(\frac{\theta_a}{\theta'_{ma}}\right)^2 \left(\frac{T}{\theta'_{ma}}\right)^{\frac{1}{6}} \cdot \exp\left\{\frac{3}{2}\left(\frac{\theta'_{ma}}{T}\right)^{1/3} - \frac{\theta_a}{2T} - \frac{\epsilon_{ma}}{KT}\right\},$$

$$\theta_a = \frac{h\nu}{k}, \quad \theta'_{ma} = 1{,}687 \frac{m_m m_a}{m_m + m_a} \nu^2 \ell_{ma}^2.$$

Z_{ma} is the average number of M-A collisions required to de-excite a diatomic molecule A by one quantum level; Z_0 is a steric factor; m_{a1} and m_{a2} are the masses of the atoms constituting A; ν is the vibration frequency of A; ϵ_{ma} is the depth of the well in the M-A intermolecular potential; and ℓ_{ma} is a parameter in the exponential approximation to the intermolecular potential, $V = H \cdot \exp(-r/\ell_{ma})$.

It was assumed that the efficiency, collision per collision, of M relative to A (5,6) is given by

$$P_m = R^o(M/A) \cdot \frac{\mathcal{Z}_{aa}}{\mathcal{Z}_{am}} = \frac{Z_{aa}}{Z_{am}}. \tag{1.21}$$

$\mathcal{Z}_{aa}$ and $\mathcal{Z}_{am}$ are kinetic-theory collision constants; $R^o(M/A)$ is the relative efficiency defined by equation 1.9; and Z_{aa} and Z_{am} are defined by equation 1.20. On substituting equation 1.20 into equation 1.21 and simplifying, one obtains

$$P_m = \left(\frac{2m_m}{m_a+m_m}\right)^{13/6}\left(\frac{\ell_{am}}{\ell_{aa}}\right)^{7/3} \cdot$$
$$\cdot \exp\left\{\left[1-\left(\frac{2m_m}{m_m+m_a}\cdot\frac{\ell_{am}^2}{\ell_{aa}^2}\right)^{\frac{1}{3}}\right]\frac{3}{2}\left(\frac{\theta'_{aa}}{T}\right)^{\frac{1}{3}} - \frac{1}{T}\left(\frac{\epsilon_{aa}-\epsilon_{am}}{K}\right)\right\}. \qquad (1.22)$$

This equation was then solved for $\frac{3}{2}\left(\frac{\theta'_{aa}}{T}\right)^{\frac{1}{3}}$, which should be constant for all different species of M for relative efficiencies obtained with a given reactant at constant temperature:

$$\frac{3}{2}\left(\frac{\theta'_{aa}}{T}\right)^{\frac{1}{3}} = \frac{\log\left[\left(\frac{m_a+m_m}{2m_m}\right)^{13/6}\left(\frac{\ell_{aa}}{\ell_{am}}\right)^{7/3}P_m\right] + \frac{1}{T}\left(\frac{\epsilon_{aa}-\epsilon_{am}}{K}\right)}{1-\left(\frac{2m_m}{m_m+m_a}\cdot\frac{\ell_{am}^2}{\ell_{aa}^2}\right)^{1/3}}. \qquad (1.23)$$

The quantities ℓ_{aa}/ℓ_{am} were assumed to be proportional to the corresponding ratios of Lennard-Jones collision diameters for the calculations based on Lennard-Jones potential parameters. Values of collision diameters and well-depths were taken from references (41) and (6) and combined by means of the rules

$$\sigma_{am} = \frac{1}{2}\left(\sigma_{aa}+\sigma_{mm}\right),$$
$$\epsilon_{am} = \left(\epsilon_{aa}\cdot\epsilon_{mm}\right)^{1/2}. \qquad (1.24)$$

The quantity $\frac{3}{2}\left(\frac{\theta'_{aa}}{T}\right)^{1/3}$ was then computed for twelve different foreign gases. The quantities P_m were obtained from reference (6). It was found that $\frac{3}{2}\left(\frac{\theta'_{aa}}{T}\right)^{1/3}$ showed a great deal of variation, even when the interaction potential parameters of nitryl chloride were given somewhat different values from those first used. Nevertheless, an

average value of $\frac{3}{2}\left(\frac{\theta'_{aa}}{T}\right)$ was computed, and this value was used in equation 1.22 to compute the quantities P_m. Agreement with the experimental values of P_m was very poor. The calculated values showed the same qualitative trends as the observed values; but the calculated values varied by a factor of about a hundred, whereas the observed values varied by a factor of less than ten.

One might think that the effects of having more than one oscillator excited or de-excited in the reactant molecule could possibly account for the above-mentioned discrepancy. Herzfeld, in reference (30), p. 721, gives the following formula for the case where A contains two oscillators:

$$Z_{sjam} = 2Z_0\left[\frac{\pi\, m_m (m_{a1}^2 + m_{a2}^2)\, b_s b_j}{m_{a1} m_{a2} (m_m + m_a)}\right]^{-2}\left(\frac{\theta'_{sam}\,\theta'_{jam}}{\theta_{sa}\,\theta_{ja}}\right)\cdot$$
$$\cdot\left(\frac{\theta_{sa} \pm \theta_{ja}}{\theta'_{sjam}}\right)^2\left(\frac{3T}{2\pi\,\theta'_{sjam}}\right)^{\frac{1}{2}}\cdot \qquad (1.25)$$
$$\cdot\exp\left\{\frac{3}{2}\left(\frac{\theta'_{sjam}}{T}\right)^{1/3} - \frac{\theta_{sa} \pm \theta_{ja}}{2T} - \frac{\epsilon_{am}}{KT}\right\},$$

$$\theta'_{sjam} = \theta'_{sam} + \theta'_{jam} \pm 2\sqrt{\theta'_{sam}\,\theta'_{jam}}\ .$$

The subscripts s and j refer to the two modes of vibration; b_s and b_j are amplitude factors from the corresponding normal coordinates.

If one makes the assumptions used in the single-oscillator case, the formula for P_m is

$$P_m = \exp\left\{\frac{3}{2}\left(\frac{\theta'_{sjaa}}{T}\right)^{\frac{1}{3}}\left[1 - \left(\frac{2m_m}{m_m + m_a}\,\frac{l_{am}^2}{l_{aa}^2}\right)^{\frac{1}{3}}\right] - \frac{1}{T}\left(\frac{\epsilon_{aa} - \epsilon_{am}}{K}\right)\right\}\cdot \qquad (1.26)$$
$$\cdot\left(\frac{2m_m}{m_m + m_a}\right)^{5/2}\frac{l_{am}}{l_{aa}}\ .$$

This equation was solved for $\frac{3}{2}\left(\frac{\theta'_{5\frac{1}{2}aa}}{T}\right)^{1/3}$, which should be constant for a given reactant at constant temperature.

$$\frac{3}{2}\left(\frac{\theta'_{5\frac{1}{2}aa}}{T}\right)^{\frac{1}{3}} = \frac{\log\left[\rho_m\left(\frac{m_m+m_a}{2m_m}\right)^{5/2}\frac{l_{aa}}{l_{am}}\right] + \frac{1}{T}\left(\frac{\epsilon_{aa}-\epsilon_{am}}{K}\right)}{1-\left(\frac{2m_m}{m_m+m_a}\cdot\frac{l_{am}^2}{l_{aa}^2}\right)^{1/3}}. \qquad (1.27)$$

Experimental values of ρ_m were inserted in equation 1.27, and $\frac{3}{2}\left(\frac{\theta'_{5\frac{1}{2}aa}}{T}\right)^{1/3}$ was computed. This quantity showed much variation. An average value was taken, and ρ_m was computed by means of equation 1.26. The results were very similar to those obtained using the single-oscillator formula.

For set B of the calculations, in which values of l_{aa}/l_{am} were calculated from Amdur's formulas, the procedure was the same as for the set A. l_{aa} was given values varying from that found for neon to that found for argon, as no experimental determination of the nitryl chloride potential has yet been made by Amdur's method. The results looked moderately promising until the absolute values of de-excitation probabilities were computed. All of these probabilities were much larger than unity. When θ'_{aa} was computed by means of equation 1.20, it turned out to be almost one hundred times larger than the value obtained by means of equation 1.23 and the observed relative efficiencies.

Other attempts to strain the theory to fit the data were also unsuccessful.

One is therefore forced to the conclusion that the transition-probability calculations currently used in sound-dispersion work do not account satisfactorily for the relative efficiencies of foreign gases observed in the decomposition of nitryl chloride. One might suspect that the approximations made by using first-order perturbation theory and a crude physical model are the rocks upon which the calculation founders.

The failure of the approximate quantum-mechanical treatment of relative efficiencies discussed above, suggested the use of the classical theory of Landau and Teller (reference 30, pp. 705-708). Landau and Teller assumed that the probability of de-excitation in an A-M collision was

$$P_{am} = \frac{1}{Z_0'} \exp\left(\frac{-4\pi^2 \nu \ell_{am}}{w}\right). \qquad (1.28)$$

Z_0' is a constant; ν is the vibration frequency of the oscillator being de-excited; ℓ_{am} is a parameter of the intermolecular potential; and w is the relative velocity of the colliding molecules. This probability was then averaged over an equilibrium distribution of relative velocities, and a value was obtained for the average number of collisions required to de-excite the oscillator.

By the same method as was used in the previous treatment (see equation 1.21), it was found that

$$P_m = \sqrt{\frac{2m_m}{m_m+m_a}} \cdot \frac{\ell_{ma}}{\ell_{aa}} \cdot \exp\left\{\frac{3}{2}\left(\frac{m_a \ell_{aa}^2 \pi \nu^2}{kT}\right)^{1/3}\left[1 - \left(\frac{2m_m}{m_m+m_a} \cdot \frac{\ell_{ma}^2}{\ell_{aa}^2}\right)^{\frac{1}{3}}\right]\right\} . \qquad (1.29)$$

If one assumes that $\nu \cong 0$ and that the ℓ's are proportional to the corresponding collision diameters, this formula reproduces the relative efficiencies of non-polar gases fairly well. It is not, however, applicable to polar gases; and the results obtained by the above formula were corrected for the polarity of nitryl chloride by being multiplied by 0.489.

The numerical results of this work are given in Table II.

Table II. Comparison of Calculated and Observed Relative Efficiencies, Collision per Collision

M	a.	b.	c.	d.	e.	f.	g.
NO_2Cl	1.00	1.00	1.00	1.00	1.00	.49	—
He	.15	.02	.02	.05	.08	.12	.09
Ne	.22	.25	.27	.34	.38	.25	.16
A	.30	.55	.61	.61	.36	.35	.30
Kr	.36	.90	1.06	.66	.32	.44	.47
Xe	.46	1.09	1.23			.47	
H_2	.15	.01	.006			.09	
N_2	.34	.40	.39			.32	
O_2	.34	.46	.48			.33	
Cl_2	.50	.96	.99			.46	
HCl	.63	.68	.76			.42	
CO_2	.50	.65	.65			.39	
N_2O	.48	.65	.59			.41	
SF_6	.49	.92	.82			.62	

M identity of foreign gas

a. observed relative efficiency, collision per collision;

b. set A, single-oscillator formula, equation 1.22;

c. set A, two-oscillator formula, equation 1.26;

d. set B, single oscillator formula, $\ell_{aa} = .43$;

e. set B, single oscillator formula, $\ell_{aa} = .20$;

f. Landau-Teller theory, $\ell_{am} \propto \sigma_{am}$ (Lennard-Jones parameter), equation 1.29;

g. Landau-Teller theory, ℓ_{am} computed from Amdur's data.

III. Experiment

A. Preparation of Materials

1. Preparation of Nitryl Chloride

Nitryl chloride was prepared by the method of Wise and Volpe (42) as described by Volpe and Johnston (6). Anhydrous hydrogen chloride was passed through a porous glass disk and into a tower containing 50 cc. of 90% nitric acid, 120 cc. of 95% sulfuric acid, and 130 cc. of 30% fuming sulfuric acid. The resulting mixture of nitryl chloride and chlorine was caught in a trap cooled with a solid carbon dioxide-acetone bath. This mixture was then transferred to a vacuum distillation apparatus, and the chlorine was largely removed by distillation from a trap cooled with pentane slurry (-95°C.) to a trap cooled with liquid nitrogen. The nitryl chloride produced in this way was shown by Volpe (6) to be more than 98% pure. The nitryl chloride was then distilled into Pyrex ampules with break-off seals, and it was stored in those ampules. In order to avoid the possibility of contamination, the nitryl chloride was not permitted to come in contact with stopcock grease from the time it was distilled into the ampules until after it was reacted.

2. Preparation of Other Gases

Nitrogen dioxide was obtained in a steel cylinder from the Matheson Company, Joliet, Illinois. This material was transferred from the cylinder into a storage trap, where it was protected from water by phosphorus pentoxide and kept at ice temperature. Oxygen was then passed

into the trap, and the trap was shaken until the green color of dissolved nitrogen sesquioxide was replaced by an orange-yellow color. Before use for optical calibration, this material was distilled from a trap at ice temperature to a trap at -80°C., at which temperature it was a white solid.

Helium, hydrogen, and carbon monoxide were Matheson's "reagent gases of highest purity", obtained in sealed glass bulbs. Matheson's "spectroscopically pure" oxygen was obtained in a steel tank. None of these gases were further purified.

Dichlorodifluoromethane was obtained in a steel cylinder from E. I. du Pont de Nemours and Company, Wilmington, Delaware. Dichlorotetrafluoroethane, chlorotrifluoromethane, bromotrifluoromethane, and trichlorofluoromethane were obtained from Matheson in lecture bottles. These compounds were purified by taking the middle third during distillation from solid carbon dioxide to liquid nitrogen temperatures.

The carbon tetrachloride used was Baker's Reagent Grade, from J. T. Baker Chemical Company, Phillipsburg, New Jersey; and the nitromethane was Eastman's Practical Grade, from Eastman Kodak Company, Rochester, New York. These compounds were purified by taking the middle third during distillation from 0°C. to -80°C.

Nitric acid was prepared by reacting Baker's Reagent Grade potassium nitrate with Baker's Reagent Grade sulfuric acid. The product was redistilled from 0°C. to -80°C., and the middle third was taken.

Argon was obtained in a tank from the Matheson Company. It was condensed out in a trap with liquid nitrogen, and then it was distilled

at a temperature slightly above that of liquid nitrogen. The middle third of the distillate was used.

B. Apparatus Design

The apparatus was designed to permit the making of measurements over a range of temperatures from 140°C. to 200°C. and over a pressure range of from 10 to 600 mm. First-order rate constants were to be found for mixtures containing relatively small concentrations of nitryl chloride and widely varying concentrations of inert gas. The comparatively large pressures of added inert gas to be used made the use of a large reaction vessel inconvenient; so a cylindrical cell 30 cm. long and 2 cm. in diameter was used. Cordes and Johnston (4) had shown that the colorimetric method was well-suited for determining the rate of advancement of the reaction; and this method, with some modifications to be mentioned later, was used. The concentration of nitrogen dioxide was measured by its absorption of light in the wave length band 400-475 millimicrons.

The apparatus consisted of three basic units: one, a purification and pipet system for mixing added inert gas with nitryl chloride and for introducing the mixture into the reaction cell; two, the reaction cell and its thermostat; and three, the optical system and phototube and recording voltmeter.

1. Pipet System

The pipet system consisted of several one- and two-liter glass bulbs, used for storing inert gases, and a three-liter stainless steel tank, used for storing nitryl chloride and mixtures of nitryl chloride

and inert gas. Pressure measurements of nitryl chloride mixtures were made both with a large stainless steel vacuum gage obtained from the Crosby Company, Boston, Massachusetts, and with a glass Bourdon gage used as a null instrument in conjunction with a mercury manomenter. Liquid nitryl chloride was stored in a glass bulb with a break-off seal that led to a Kovar seal, needle valve, and thence to the stainless steel pipet. A small quantity of nitryl chloride was introduced from the glass bulb into the pipet. Then inert gas was added. (At 205°C. and 170°C. the concentration of nitryl chloride in the mixture was obtained by letting its decomposition in the reaction cell go to completion and determining the terminal concentration of nitrogen dioxide optically. At 141°C. larger amounts of nitryl chloride were used, and these were measured with the Bourdon gage. When this procedure was used, the gases were given two hours to mix in the pipet before runs were made.)

The gases were then expanded into the evacuated reaction cell; and the valve between the pipet and the cell was left open until pressure equilibrium was attained, which occurred within a period of less than five seconds. The pressure of gas in the pipet was then measured with the Bourdon gage. Concentrations were in all cases computed by means of the perfect gas law. In certain cases this introduced errors of less than ½%; these could not be avoided without determining the second virial coefficients of some of the Freons, carbon tetrachloride, nitromethane, and nitric acid. This correction is negligible compared to the uncertainties introduced by the heterogeneous reaction.

The nitryl chloride storage bulb, the stainless steel pipet, the Bourdon gage, and the reaction cell were joined by means of glass,

stainless steel, and Kovar tubing. Stainless steel diaphragm valves were used in this portion of the line to avoid the possibility of stopcock grease catalysis of the decomposition of nitryl chloride.

2. Reaction Cell and Thermostat

The reaction cell, shown in Figure 2, was constructed of Pyrex glass. It included a glass bellows to prevent the thermal expansion of the steel thermostat tank from breaking the cell. Optically flat Pyrex windows were sealed on both ends of the cell. The cell was clamped into the thermostat by means of two liquid-tight compression seals, shown in Figure 2. Teflon "O" rings were used as gasket material; they were quite satisfactory at the temperatures (141°C. to 205°C.) at which they were used.

The thermostat tank was constructed of auto body steel (one sixteenth of an inch thick). An empty tube ran the full length of the tank, and ports for mounting the reaction cell were located at either end of the tank. The outside of the tank was covered with one inch of magnesia board and a layer of asbestos paper.

The thermostat was filled with about four gallons of Dow Corning 550 Fluid, obtained from the Dow Corning Corporation, Midland, Michigan. The bath was heated by four knife-type, 250-watt heating elements, supplied by the Central Scientific Company, Chicago, Illinois. Two of these heaters were connected in parallel to a Powerstat variable transformer (made by the Superior Electric Company, Bristol, Connecticut). One heater was used only as a booster to initially bring the thermostat up to operating temperature. One heater was connected in series with a

FIGURE 1

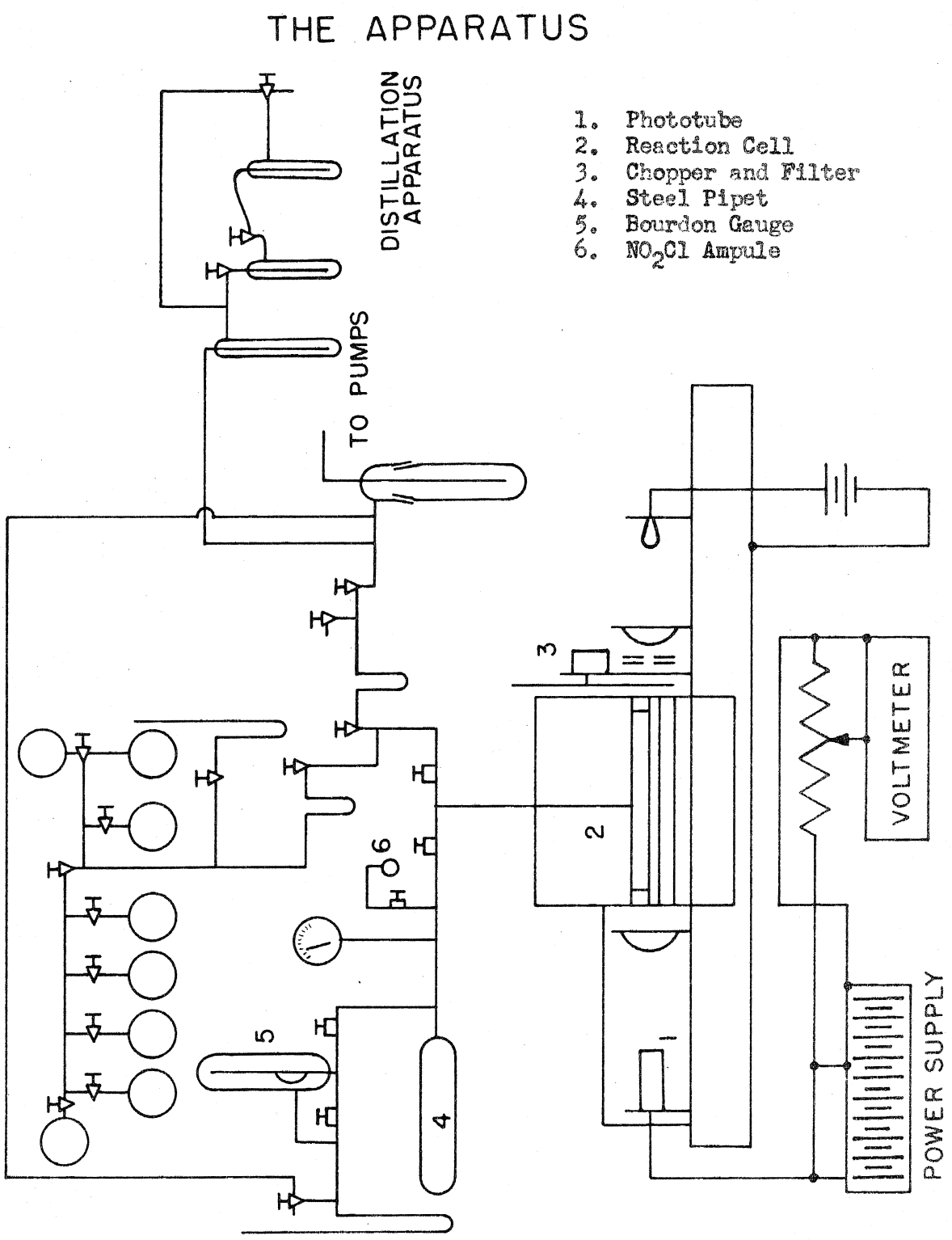
THE APPARATUS
DISTILLATION APPARATUS
TO PUMPS
1. Phototube
2. Reaction Cell
3. Chopper and Filter
4. Steel Pipet
5. Bourdon Gauge
6. NO_2Cl Ampule
VOLTMETER
POWER SUPPLY

FIGURE 2

REACTION CELL

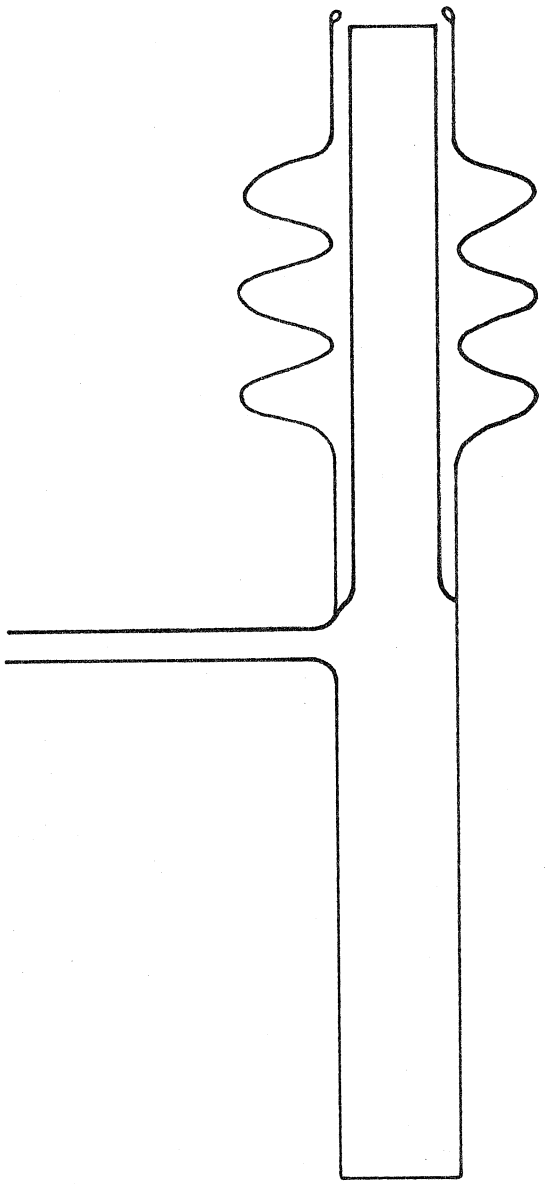

FIGURE 3

CELL MOUNTING

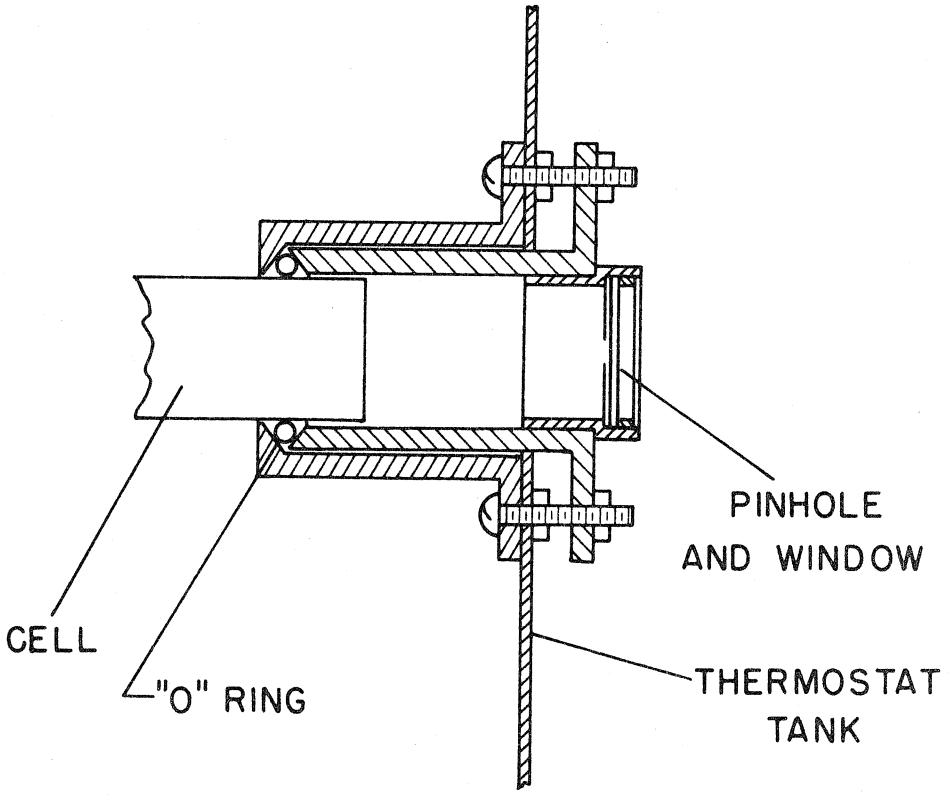

mercury switch (obtained from Minneapolis-Honeywell, Philadelphia, Pennsylvania) which was controlled by a mercury thermoswitch (supplied by Philadelphia Scientific Glass Company, Philadelphia, Pennsylvania). This last heater was used to control the temperature of the thermostat. The fluid in the thermostat was stirred by a variable-speed electric stirrer (Precision Scientific Company, Chicago, Illinois, catalog number 65748). The bath temperature remained constant within about a tenth of a centigrade degree, and readings taken at different locations were constant within the same limit. The thermoswitch seems to provide an excellent and simple method of controlling the temperature of a liquid-filled thermostat, expecially when long-term stability is desired.

3. Optical System, Phototube, and Recording Voltmeter

The thermostat was bolted to a seven-foot aluminum casting (Figure 1) which served as an optical bench for the light source, lenses, and phototube. A casting was used to avoid the warping and twisting that might be produced in a wooden or rolled-iron beam by the heat of the thermostat.

Nitrogen dioxide absorbs light strongly at 436 millimicrons; neither reactant, nitryl chloride, nor any of the foreign gases used absorb in this region to any appreciable extent. Chlorine does absorb light in this region slightly, but a correction for this absorption was made. Therefore the rate of decomposition of nitryl chloride can be determined by colorimetric measurement of the rate of appearance of nitrogen dioxide. The optical system passed light of wave lengths in

the band 400 to 475 millimicrons through alternately the reaction cell and an empty tube; the light was then focused on a photomultiplier tube. The light source was a 6-volt, 50-candlepower lamp, number 1183 from the General Electric Company, Schenectady, New York. The filters were numbers 3389 and 5113 from the Corning Glass Works, Corning, New York. The photomultiplier tube was type 6292 from the Allen B. Du Mont Laboratories, Inc., Passaic, New Jersey. The phototube was powered by twenty 67½-volt radio "B" batteries. The lenses were 4½-inch condensing lenses of 7-inch focal length and unknown antecedents. The output from the phototube was sent through a voltage divider, from which the signal was sent to a Minneapolis-Honeywell Brown recording voltmeter with a response time of a quarter of a second.

The light beam was collimated by a 4½-inch condensing lens and then chopped by a slotted disc driven by a Telechron synchronous motor obtained from the General Electric Company, Ashland, Massachusetts. The chopper was designed to give a dark-current reading, an initial intensity reading, and a cell intensity reading per cycle; and the cycles were 3 3/4, 7½, and 15 seconds long, depending on the disc used. This permitted corrections to be made for light source and phototube drift occurring during a run.

C. Treatment of Data

The data obtained during the course of a run appeared on a roll of recorder chart paper. The dark current reading, blank tube intensity reading, and cell intensity reading were then tabulated; and the dark current reading was subtracted from the other two. The ratio of the

corrected initial cell intensity to the corrected initial blank tube intensity was computed, and the blank tube intensities were multiplied by this factor. This corrected for the slight difference in size of the pinholes in the two light paths. The corrected blank tube intensity will be denoted by I_o and the corrected cell intensity by I. The ratio I_o/I was tabulated, and its logarithm was taken. This logarithm will be denoted by D; its value when the reaction has gone to completion will be denoted by D_∞. $D_\infty - D$ was then computed, and its logarithm was tabulated. $\log_{10}(D_\infty - D)$ was then graphed as a function of time, and the negative of the slope of the resulting straight line was computed. This quantity multiplied by 2.303 gives the value of the empirical first-order rate constant for the run. Points were taken through no more than the first half-life of the reaction; and the initial point and any other isolated, obviously erroneous points were ignored in determining the slope.

The resulting rate constants were then corrected for the foreign gas effect of the reactant in the following way. A plot of rate constant (k) versus reactant concentration (A) was made for a series of runs made with reactant only, and a line was drawn through the resulting set of points. The value of the rate constant for a run made with an initial concentration A_1 of reactant and no added foreign gas, was subtracted from the value of the rate constant of a run made with added inert gas and an initial concentration A_1 of reactant.

There was unmistakable evidence of some heterogeneous reaction at all temperatures. Rate constants were high and erratic after air had been admitted to the cell unless the cell was treated with nitryl chloride

and evacuated several times. At low total pressures the experimental error was unusually high; and the extrapolation to zero pressure of plots of k versus reactant pressure gave a finite intercept on the k-axis, even though the work of Cordes and Johnston indicated that the data being extrapolated at 170 and 205°C. were within the low-pressure, second-order region. It is believed that the correction for reactant-gas effect described in the preceding paragraph also corrects, at least to a first approximation, for the heterogeneous portion of the reaction.

All rate constants are given in Appendix VIII, and plots of k versus M appear in figures 7 through 25.

Integrated relative efficiencies were then computed by means of equation 1.11. At 205°C., values of $R^i(N/M)$ were computed for several different values of the rate constants to see if $R^i(N/M)$ is a function of pressure.

D. Errors

The largest single source of error in this work was the uncertain effect of heterogeneity mentioned under section C above. The error introduced by heterogeneity could conceivably be quite large, possibly of the order of 20-30% at 141°C. The reproducibility of results in the system used is, unfortunately, no measure of the magnitude of the error introduced by the effects of heterogeneity.

The purity of the nitryl chloride used was probably about 98 mole %. The method used by Volpe (6) for preparing and purifying this material was followed exactly, and Volpe's rather exhaustive investigation of the

purity of the resulting product indicated a purity of about 98 mole % for the material. The only significant impurity was a small amount of chlorine.

The cell and optical system were calibrated both with nitrogen dioxide and with the mixture obtained on allowing the decomposition of a known amount of nitryl chloride to go to completion. A plot was made of log (I_o/I) versus initial nitryl chloride concentration, and Beer's Law was observed to be followed over the range studied. One error in the calibration that must be mentioned is that caused by the possible absorption of nitrogen dioxide and/or nitryl chloride by stopcock grease. This error was minimized by letting the stopcock of the small storage pipet stand in the presence of the gas for fifteen minutes; then the gas pressure in the pipet was quickly measured; the gas was immediately admitted to the reaction cell; and the valve leading to the cell was closed.

Pressure readings made on manometers and the glass Bourdon gage were accurate to about $\pm$ 0.5 mm. This introduced an uncertainty of as much as 5% in the nitryl chloride pressures of some of the runs made at 141°C. Usually, however, this error was less than 1%. Uncertainty in pressure readings also introduced a very small error (about 0.5%) in the volume calibrations of the cell and of some of the pipets.

Errors in the optical system and voltmeter were apparently of the order of 0.5% or less. Such errors were, of course, magnified during the calculation of rate constants. It is estimated that they produced about a 2% error in the rate constants. The voltmeter was very sensitive to dusty air, however. Until filters were installed on the ventilator in

the room, very frequent cleaning of the voltmeter slide wire was necessary to maintain the sensitivity of the instrument. The design of the optical system was found to be quite satisfactory in eliminating errors due to light source drift.

The errors subject to estimation, therefore, introduce an uncertainty of about 2.5% in the concentration of nitryl chloride (except for some of the runs at 141°C., where the error may be as much as 7%), an uncertainty of less than 1% for the total pressure readings, and an error of about 2% in the values of the rate constants. The reader is again reminded, however, that the effects of heterogeneity are by far the greatest potential source of error in this work, and that only a rough estimate could be made of this error.

E. Results

The experimental data obtained in this work are reported in Appendix VIII, in a table and as graphs of k versus M. It was observed that the plots of log $(D_\infty - D)$ versus time, from which the first-order rate constants were calculated, were linear. Figures 10 through 21 in Appendix VIII indicate that the runs were made in the intermediate-pressure range between the low-pressure second-order region and the high-pressure first-order region.

Activation energies were calculated from the data at 170 to 205°C. and at 141 to 170°C. by means of the formula

$$E = \frac{2.303\ RT_1T_2\log(k_2/k_1)}{T_2 - T_1}\ .$$

The value 28.1 ± .4 kcal/mol. was found. This is in good agreement with

the value of 27.5 ± .1 kcal/mol. found at the low-pressure limit (4) and with the value of 29.0 kcal/mol. found at a pressure of seven atmospheres (8). On the basis of Slater's theory (12), one expects an increase of about 2.2 kilocalories in the activation energy as one goes from the low-pressure to the high-pressure limit. (One merely substitutes n = 6 into the equation

$$E_L = E_H - \frac{(n - 1)kT}{2},$$

where n is the number of normal modes occurring in the reaction coordinate, and E_L and E_H are the activation energies at the low- and the high-pressure limits.) Therefore the observed variations are in the right direction and are presumed to be a real effect.

The value of the activation energy obtained sets a limit of about one kilocalorie on the magnitude of the change in enthalpy for the decomposition of nitryl chloride (4). If one then inserts values for the change in enthalpy, the rate of the reaction, the radius of the cell, and the thermal conductivity of the reacting mixture into equation 7.59 of Appendix VII; one finds that thermal gradients were totally negligible in the runs made in a 50-liter bulb (4,6). The maximum calculated temperature difference between the walls and any point in the body of reacting gas was less than 0.5 centigrade degrees.

The reaction was found to be partially heterogeneous in the Pyrex cell at all temperatures, and the heterogeneous reaction was especially rapid after the cell had been exposed to the atmosphere. The extent of the heterogeneous reaction was determined by plotting k against concentration of nitryl chloride for runs made with nitryl chloride alone.

Plots of k versus reactant concentration extrapolate through the origin if the data are obtained in the low-pressure region. Such data obtained in the reaction cell used in this study extrapolated to give a finite intercept at zero reactant concentration.

The effects of heterogeneity are shown in figures 7, 8, 9, and 25, in Appendix VIII. The straight lines passing almost through the origins of the plots of k versus reactant concentrations shown in figures 7, 8, and 9 are the results of Cordes and Johnston's work with a 50-liter bulb at 180 and 203°C., corrected to the temperatures used in the present investigation. The clusters of points lying above Cordes' lines are the results of this investigation, and are regarded as demonstrating the effect of the heterogeneous reaction.

The effects of exposure of the interior of the reaction cell to air are shown in figures 7 and 25. In both of these cases, two sets of runs were made. One set, the results of which are indicated by circles, was made without previous exposure of the cell to air. The other set, indicated by crosses, was made after accidental exposure of the cell to air. In both cases it is seen that previous exposure of the cell to air materially increased the rate of the reaction.

The size of the spherical flask that must be used to reduce the heterogeneous reaction to an effect of 5% at a nitryl chloride concentration of 2×10^{-7} mol/cc. was computed for the temperatures 205, 170, and 141°C. It was assumed that the rate of the heterogeneous reaction is proportional to the surface-to-volume ratio of the cell. The results were as follows: at 205°C., a bulb of 0.35 liters capacity is necessary; at 170°C., a bulb of 65 liters capacity is necessary; and

at 140°C., a bulb of 780 liters capacity is necessary. These size requirements might be relaxed by careful pre-treatment of the reaction cell. Also, the size requirements decrease as one goes to higher pressures of added inert gas.

An estimate of the activation energy of the heterogeneous reaction was made, and a value of 16 $\pm$ 4 kcal/mol. was obtained. The nitryl chloride runs made at 205 and 170°C. were used for this calculation, since the previous history of the cell was roughly the same for these two sets of data.

One suspects that the activation energy of 20.5 kcal/mol. reported by Schumacher and Sprenger in (2) for work done at and below 150°C. is the result of considerable heterogeneity in their reaction cell. They varied the surface-to-volume ratios of their reaction vessels by a factor of three, and failed to observe any effect on the rate of the reaction. If this was done only at the upper portions of the temperature and pressure ranges through which they studied the reaction, their negative result is not too surprising. No mention was made in their work of the size of the cell; but a glass cell of, say, 1-liter capacity could easily explain their low activation energy in terms of heterogeneity.

Integrated relative efficiencies were computed by means of equation 1.11, and are listed in Table III below. $R^i(N/CO_2)$ was determined experimentally and then multiplied by $R^o(CO_2/NO_2Cl) = 0.38$ to obtain a value for $R^i(N/NO_2Cl)$. Attempts to determine the relative efficiencies of hydrogen, nitromethane, and nitric acid failed: chemical reactions other than the thermal decomposition of nitryl chloride

Table III

Relative Efficiencies of Foreign Gases

in the Decomposition of Nitryl Chloride

$R^i(M/NO_2Cl)$ at 205°C.

$K \cdot 10^3 sec^{-1}$	0*	2.3	4.6	6.9	9.2	11.5	13.8
M							
CO_2	.38	.38	.38	.38	.38	.38	.38
O_2	.26	.37	.30	.29	.27	.27	.27
CO	—	.29	.29	.29	—	—	—
A	.21	.19	.17	.17	.18	.17	.16
He	.25	.41	.28	.26	—	—	—
CCl_2F_2	.49	.56	.52	.54	.56	.57	.56
$CClF_3$	—	.67	.60	.63	.65	.66	.66
CCl_4	—	—	.98	1.08	1.14	—	—
$CBrF_3$	—	—	.79	.76	.76	.76	.74
$C_2Cl_2F_4$	—	—	.87	.84	.83	.83	.83

*Obtained from (6)

Table III (cont'd)

Relative Efficiencies of Foreign Gases in the Decomposition of Nitryl Chloride

$R^i(M/NO_2Cl)$ at 170°C.

M	K	$11.5 \cdot 10^{-4} sec^{-1}$
CO_2		.38
A		.16
CCl_2F_2		.52

$R^i(M/NO_2/Cl)$ at 141°C.

M	K	$2.0 \cdot 10^{-4} sec^{-1}$	**
CO_2		.38	.16
A		.16	—
CCl_2F_2		.48	—
O_2		.19	.19
NO_2Cl		1.21	1.00

**Schumacher and Sprenger's data, as reported in (6)

FIGURE 4

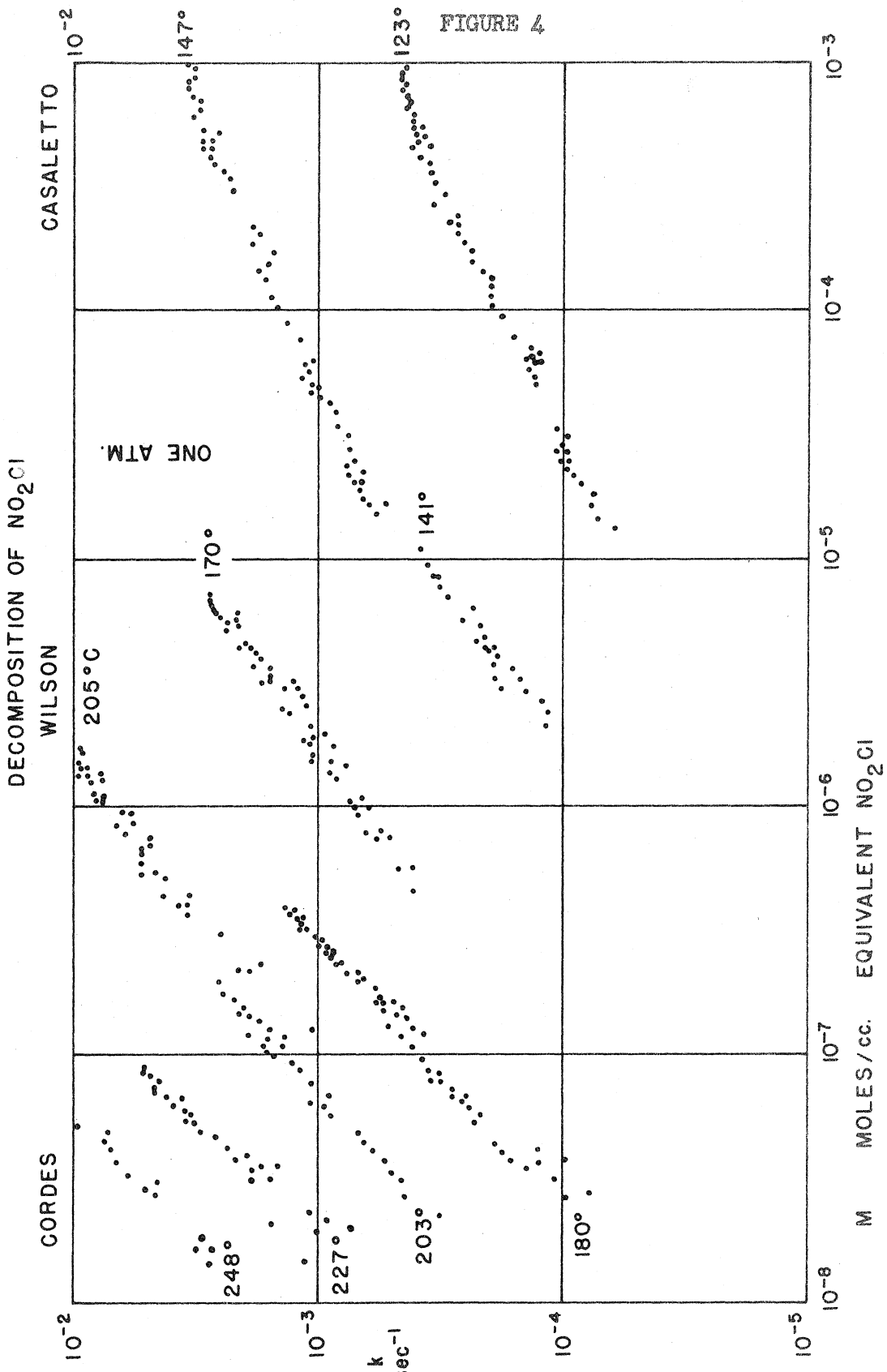
DECOMPOSITION OF NO_2Cl
WILSON
CORDES
CASALETTO
ONE ATM.
205°C
170°
141°
147°
123°
248°
227°
203°
180°
10^{-2}
10^{-3}
10^{-4}
10^{-5}
k sec^{-1}
10^{-8}
10^{-7}
10^{-6}
10^{-5}
10^{-4}
10^{-3}
M MOLES/cc. EQUIVALENT NO_2Cl

occurred. The values of relative efficiencies obtained by Volpe and Johnston (6) and by Schumacher and Sprenger (1,2,3) are listed in the table for comparison.

It would appear from Table III that relative efficiencies are functions at most slowly varying with temperature and pressure. The relative efficiencies of Schumacher and Sprenger are probably erroneous because of the unrecognized effects of heterogeneity.

In view of the large and uncertain effects of heterogeneity, the small variation of relative efficiencies with pressure at constant temperature does not eliminate the hypothesis that $b_{im} = b_m f_i$. Even had no variation at all been observed in data much more precise than those reported here, one could not conclude that $b_{im} = b_m f_i$: the discussion in II, B, of this thesis requires that data of infinitely high precision show no variation of relative efficiency with pressure if the proof given in that section is to be applicable to the situation where one suspects that $b_{im} = b_m f_i$. That, however, this hypothesis is not a bad approximation can be seen in Figure 4, in which $R^o(M/NO_2Cl)$ values obtained at 203°C. were used to "normalize" the concentrations of foreign gases. The variation in pressure under which the data in this figure were taken is about 100,000-fold, and the temperature varied over a range of 125 centigrade degrees.

Aside from heterogeneity, which is rather slight at 205°C., it can be said that the present work in a Pyrex glass tube of about 20 millimeters inside diameter is in essential agreement with the work of Cordes and Johnston at 203°C. in a 50-liter flask. Also, the high-pressure points observed in this study join satisfactorily to the low-pressure extreme of Casaletto's work, corrected to 141°C.

IV. Conclusions

This investigation has filled the gap between the low-pressure work of Cordes and of Volpe and the high-pressure work of Casaletto. This work was designed to provide an understanding of the different relative efficiencies obtained by Volpe and Johnston and by Schumacher and Sprenger; these differences might have been a very interesting real effect (see Part II, B).

At high temperatures and low pressures, the present work is in agreement with the results of Johnston, Cordes, and Volpe. At lower temperatures and higher pressures, it is in agreement with the results of Casaletto and Johnston. At low pressures a heterogeneous reaction was found. The rate of this heterogeneous reaction was almost doubled by previous exposure of the cell to air, and this effect was long-lasting.

It is presumed that the interpretation of the work of Schumacher and Sprenger is obscured by the effects of heterogeneity.

Previous work (see reference 7 and Part Two of this thesis) has shown that deactivation of an activated molecule does not occur on every collision. The complete breakdown of the calculations made in Part II, C, of this thesis shows that the theory of energy transfer applicable to diatomic molecules in low-lying vibrational states is not applicable to polyatomic molecules in highly excited vibrational states. However, the classical theory of Landau and Teller gives relative efficiencies that are in adequate, although not brilliant, agreement with those observed experimentally.

PART TWO: DECOMPOSITION OF NITROGEN PENTOXIDE IN THE PRESENCE OF NITRIC OXIDE. IV. EFFECT OF NOBLE GASES

[Reprinted from the Journal of the American Chemical Society, **75**, 5763 (1953).]

Decomposition of Nitrogen Pentoxide in the Presence of Nitric Oxide. IV. Effect of Noble Gases

By David J. Wilson and Harold S. Johnston

Received June 22, 1953

The rate of the reaction $N_2O_5 + NO \rightarrow 3NO_2$ has been shown by Smith and Daniels[1] and by Mills and Johnston[2] to be that of an elementary unimolecular reaction. At around 0.1 mm. pressure in a 22-liter flask, the reaction is homogeneous and definitely within the second-order region.[3] The low-concentration second-order rate constants of a series of gases have been reported.[4]

Using the 22-liter bulb, and the same method of interpreting the data as was used previously,[3,4] we have determined the low-concentration second-order rate constants of the noble gases and carbon tetrachloride. Reactant pressures were each about 0.08 mm., and foreign gas pressures ranged from 3 to 0.02 mm. Experimental results are given in Table I.

Table I

Experimental Results

M gas	No. of points	Intercept, sec.$^{-1}$	Low concn. second-order rate constant, cc. mole^{-1} sec.$^{-1}$ × 10^5 Value	Standard error	Ratio to pure N_2O_5
He	27	0.0132	2.80	0.26	0.124
Ne	17	.0129	2.02	.32	.090
Kr	26	.0119	3.57	.23	.159
Xe	11	.0134	3.30	.95	.147
CCl_4	30	.0130	12.4	1.3	.551

As shown previously, the activating efficiency function of the state i above the critical energy, a_{Mi}, can be written as $a_{Mi} = b_{Mi}P_i$, that is, the relative activating efficiency is also the relative deactivating efficiency. The function b_{Mi} is further factored, $b_{Mi} = b_M f_{Mi}$, where b_M is the kinetic collision constant

$$b_M = N_0 \left[8\pi RT \left(\frac{1}{M_1} + \frac{1}{M_2}\right)\right]^{1/2} \left(\frac{\sigma_1 + \sigma_2}{2}\right)^2 \quad (1)$$

where N_0 is Avogadro's number; σ_1 and σ_2, the collision diameters of the colliding particles; M_1 and M_2, the molecular weights of the colliding particles; and R and T have their usual meaning. The function f_{Mi} is the efficiency factor for deactivation which in general may be a function of each state i and a different function for each foreign gas M.

If the collision constant can be calculated by 1, then the relative efficiencies with b_M factored out give the ratios $\overline{(f_M)}/\overline{(f_1)}$, where 1 stands for nitrogen pentoxide, and the bar indicates an average with respect to P_i over the excited states. If deactivation occurred at every collision or if f_{Mi} depended on the quantum states i of the reactant molecule only but not on the identity of the foreign gas M, this ratio would be unity every time. It is not. (See Table II. This table includes data calculated from reference 4.)

Table II

Efficiency and Relative Efficiency

M gas	Mol. wt.	Collision diameter, Å.	Low concn. rate const./kinetic collision const., $\overline{(f_M)} \times 10^{10}$	$\overline{(f_M)}/\overline{(f_1)}$
He	4	2.18[a]	6.02	0.0650
Ne	20	2.59[a]	7.95	.0855
A	40	3.64[a]	14.3	.154
Kr	83.8	4.16[a]	19.3	.208
Xe	131.3	4.85[a]	17.5	.189
N_2	28	3.75[a]	21.2	.228
NO	30	3.75	27.9	.300
CO_2	44	4.59[a]	35.9	.387
CCl_4	154	5.46	62.5	.673
SF_6	146	4.52	41.2	.443
N_2O_5	108	6.00	93.0	1.000

[a] From E. H. Kennard, "Kinetic Theory of Gases," McGraw-Hill Book Co., Inc., New York, N. Y., 1938, p. 149.

Furthermore, it is impossible to adjust the collision diameters of either nitrogen pentoxide or of the various M gases to obtain ratios $\overline{(f_M)}/\overline{(f_1)}$ that are equal to unity. For the molecular weights are accurately known, and the ratio, $(2\sigma_{N_2O_5}/\sigma_{N_2O_5} + \sigma_M)^2$, can never be greater than 4, which is not sufficiently large to account for the observed relative efficiencies of the noble gases and nitrogen. Thus, the efficiency function f_{Mi} does differ markedly from one gas to another. (These results do not answer the question as to whether or how the efficiency function varies over the states i of the reactant molecule.)

Relative efficiency increases slowly with molecular weight through at least krypton for the noble gases. It increases at constant molecular weight as one goes from noble gases to diatomic or polyatomic gases, and nitrogen pentoxide is much more efficient than anything else we have yet used. A study of the relative efficiencies of diatomic and polar gases is now in progress.

We are grateful to the National Science Foundation for a Fellowship in support of this work, and to the Office of Naval Research, Project NR-051-246, Contract N6 onr 25131.

Department of Chemistry
Stanford University
Stanford, Cal.

(1) J. H. Smith and F. Daniels, This Journal, **69**, 1735 (1947).
(2) R. L. Mills and H. S. Johnston, *ibid.*, **73**, 938 (1951).
(3) H. S. Johnston and R. L. Perrine, *ibid.*, **73**, 4782 (1951).
(4) H. S. Johnston, *ibid.*, **75**, 1567 (1953).

PART THREE: THEORETICAL PRE-EXPONENTIAL FACTORS FOR HYDROGEN ATOM ABSTRACTION REACTIONS

[Reprinted from the Journal of the American Chemical Society, **79**, 29 (1957).]

[CONTRIBUTION FROM THE DEPARTMENT OF CHEMISTRY AND CHEMICAL ENGINEERING]

Theoretical Pre-exponential Factors for Hydrogen Atom Abstraction Reactions[1]

BY DAVID J. WILSON[2] AND HAROLD S. JOHNSTON[2]

RECEIVED AUGUST 29, 1956

For a series of bimolecular reactions involving hydrogen atom abstraction, pre-exponential factors in the Arrhenius equation $k = A \exp(-E/RT)$ have been calculated by means of activated complex theory. The structure and mechanical properties of the activated complex are unambiguously assigned from a set of empirical rules from the fields of molecular structure and molecular spectroscopy. Bond distances around the transferred hydrogen atom are evaluated by Pauling's rule for fractional bonds, stretching force constants are assigned by means of Badger's rule, reduced moments of inertia for internal rotation are evaluated by means of Pitzer's simple approximate method, bending force constants are assigned by analogy with hydrogen-bonded molecules, and the reaction coördinate is explicitly introduced as the (highly perturbed) antisymmetric vibrational mode of the atom transferred. With these assignments of structure and force constants, a vibrational analysis was carried out by Wilson's FG matrix method; for the larger activated complexes this detailed vibrational analysis was made only for degrees of freedom close to the transferred hydrogen atom. For 8 cases out of 9 the agreement between calculated and observed pre-exponential factors is quite satisfactory. For the reaction of bromine with isobutane calculated and observed pre-exponential factors disagree by a factor of 10^5. It is argued that this method of assigning properties to the activated complex is realistic enough to constitute strong theoretical grounds for suspecting that the experimental results were interpreted by means of an incorrect mechanism.

Introduction.—The general theory of bimolecular gas phase reactions is presented in several well known books [3] To use the theory one needs to know the structure and mechanical properties of the activated complex. Semi-empirical rules have been formulated for constructing potential energy surfaces from which to estimate the structure, mechanical properties and electronic energies for especially simple activated complexes.[3] For complexes of many atoms, 4 or more in cases of low symmetry, this procedure becomes forbiddingly complicated. For quite complicated complexes one surrenders the hope of calculating activation energies and concentrates on the pre-exponential factor A in $k = A \exp(-E/RT)$. Rules have been proposed[3] whereby one makes a realistic guess of the moments of inertia of the activated complex, and the vibrational frequencies are assumed to be so high that the vibrational partition functions are unity. Computations based on this level of approximation give pre-exponential factors lower than observed ones by a factor of 10^2 to 10^6 for activated complexes containing 4, 5, or 6 atoms.[4] This discrepancy is removed if one makes a realistic estimate of vibration frequencies and makes an adequate allowance for the effect of internal rotations.[4] In an effort to refine and extend the method proposed in ref. 4 for computation of pre-exponential factors, we are following a suggestion made by Professor Pauling for the calculation of bond distances in activated complexes. For calibration of the method we have treated the well-known reactions $H + H_2$ and $Br + H_2$, and the calculations are extended to cover typical cases of hydrogen atom abstractions from organic molecules by methyl free radicals and by bromine atoms.

Method of Computation.—In order to calculate pre-exponential factors A for bimolecular reactions, one needs to know, both for reactants and the activated complex, the molecular weight, moments of inertia for over-all rotation, moments of inertia for internal rotation, barriers to internal rotation, all vibration frequencies and electronic degeneracy. (One also needs the transmission coefficient.) These data can be obtained for the reactants from spectroscopy. The problem is thus reduced to one of determining the structure and mechanics of the activated complex. It is assumed[3] that the excitation energy of the reactants has gone into the potential energy of a single separable reaction coördinate, so that the rest of the activated complex is like a normal molecule. Thus, except for the reaction coördinate, one may make heavy use of analogy with ordinary molecules. This analogy means, in particular, that normal bond distances and normal force constants are to be expected.

For purposes of kinetics any of the rules or the tables of normal covalent radii are adequate, and for single, double or triple bonds we use the convenient tables in Pauling's "Nature of the Chemical Bond."[5] However, for the H_3 complex or for a methyl radical abstracting a hydrogen from an organic compound, the bonds are more nearly "half-bonds" than any integral order, and in this treatment these bonds will be formally regarded as "half-order." There are various rules for the length of a bond of any order; the most convenient of these is Pauling's rule[6]

$$R_1 - R = 0.30 \log_{10} n \qquad (1)$$

where R is the bond radius in Å., R_1 is the radius of the corresponding single bond, and n is the order of the bond. Long standing arguments[6a] justify a linear complex for H_3, and this structure was assigned to the C–H–C links in methyl radical reactions and C–H–Br links in the bromine reactions. By these arguments and rules the detailed geometric structure of the activated complex was determined.

From Badger's rule[7] stretching force constants

(1) In support of this work one of us (DJW) is indebted to the National Science Foundation for a Fellowship. Also this work was supported in part by the Office of Naval Research, Project NR-051-246, Contract N6 onr 25131.

(2) Department of Chemistry, California Institute of Technology, Pasadena, California.

(3) S. Glasstone, K. L. Laidler and H. Eyring, "Theory of Rate Processes," McGraw-Hill Book Co., Inc., New York, N. Y., 1941.

(4) D. R. Herschbach, H. S. Johnston, K. S. Pitzer and R. E. Powell, *J. Chem. Phys.*, **25**, 736 (1956).

(5) L. Pauling, "Nature of the Chemical Bond," Cornell University Press, Ithaca, N. Y., 1940.

(6) L. Pauling, THIS JOURNAL, **69**, 542 (1947).

(6a) F. London, "Probleme der modernen Physik," Sommerfeld Festschrift, 1928.

(7) R. M. Badger, *J. Chem. Phys.*, **2**, 128 (1933); **3**, 710 (1934).

were assigned to all bonds in the complex. We know of no equivalent to Badger's rule for bending force constants, so we used analogy with the bending force constants in the bifluoride ion. The bending force constant was taken as the bending force constant in the bifluoride ion reduced by the ratio of bending force constants in CH_4 and CF_4. Skeletal internal rotations were regarded as essentially free; usually the methyl group internal rotations cancelled out pairwise between numerator and denominator, that is, between activated complex and the reactant. The electronic degeneracy of the complex was assumed to be the same as for the methyl radical. Transmission coefficients were taken as unity. Thus by these rules and analogies, the mechanical properties of the activated complex, aside from the reaction coördinate, were assigned.

The reaction coördinate was treated as previously.[4] The reaction coördinate for these atom-transfer reactions can be made to appear very naturally by including an interaction term in the potential energy which reduces the restoring force on the anti-symmetric vibration to zero. For the H_3 complex, the potential energy expression was taken to be

$$2V = k_s r_1^2 + k_s r_2^2 + 2k_s r_1 r_2 + k_b \alpha_1^2 + k_b \alpha_2^2 \quad (2)$$

The magnitude of the cross-product term is not an adjustable parameter; in this case it must have the value $2k_s$ in order to cause the antisymmetric stretching frequency to vanish. If the two stretching force constants differ, the interaction constant is $2(k_1 k_2)^{1/2}$.

For reactions 1, 2, 3 and 9 in Table I, a detailed vibrational analysis (including a reaction coördinate such as eq. 2) was made for the entire complex by the Wilson FG matrix method,[8] and the vibration frequencies were used to calculate the pre-exponential factor.[3,4] For reaction 4, the frequencies were classified by the method of ref. 4, and most frequencies were assigned from the corresponding type in ethane and deuteroethane, but the stretching and bending frequencies including the transferring atom were calculated by the Wilson FG matrix method on the assumption that the complex was a five-atomic molecule. Thus as many frequencies as possible were cancelled out between reactants and activated complex, and all frequencies which do not match-up for cancellation were computed as carefully as possible[8]; this procedure is spoken of here as an "approximate vibrational analysis." For reactions 5, 6, 7, 8 and 10, this approximate vibrational analysis was carried out. For these cases further approximations were made: all moments of inertia for both the hydrocarbons and the complex were computed as if the hydrogens were located at the nuclei of the carbon atoms to which they are attached. The same approximation was made for skeletal internal rotations[4]; methyl group internal rotations were cancelled out between reactants and complex.

For the long-chain hydrocarbons calculations were made for abstraction of secondary hydrogens only, since the activation energy for abstraction of primary hydrogens is known[9] to be about 2 kcal. higher (a factor of 8 at these temperatures) than for secondary hydrogens. Calculations were made for the reaction of a methyl radical with one specific hydrogen atom, and then this result was multiplied by the total number of secondary hydrogen atoms. In this way the symmetry numbers were included in the rotational partition functions of the hydrocarbons and of the activated complexes in reactions 6, 7 and 8. For the reaction of the bromine atom with 2-methylpropane, the calculation is based on abstraction of the tertiary hydrogen atom; it is known from analysis of products[10] that this is the only reaction occurring in this system.

TABLE I

THEORETICAL AND EXPERIMENTAL PRE-EXPONENTIAL FACTORS FOR BIMOLECULAR REACTIONS WITH ABSTRACTION OF HYDROGEN ATOMS

Reaction	T, °K.	$\log_{10} A$ Calcd.	$\log_{10} A$ Obsd.	Ref.
(1) $H + H_2 \rightarrow H_2 + H$	1000	13.7	13.7	*a*
(2) $CH_3 + H_2 \rightarrow CH_4 + H$	455	12.0	11.5–12.5	*b*
(3) $H + CH_4 \rightarrow H_2 + CH_3$	455	13.6		
(4) $CD_3 + CH_4 \rightarrow CD_3H + CH_3$	455	11.3	11.5	*c*
(5) $CD_3 + C_2H_6 \rightarrow CD_3H + C_2H_5$	455	11.3	11.3	*d*
(6) $CH_3 + n\text{-}C_4H_{10} \rightarrow CH_4 + C_4H_9$	455	11.8	11.0–11.5	*e*
(7) $CH_3 + n\text{-}C_5H_{12} \rightarrow CH_4 + C_5H_{11}$	455	11.7	11.0	*d*
(8) $CH_3 + n\text{-}C_6H_{14} \rightarrow CH_4 + C_6H_{13}$	455	11.7	11.1	*d*
(9) $Br + H_2 \rightarrow HBr + H$	523	14.1	13.6–14.2	*f*
(10) $Br + (CH_3)_3CH \rightarrow HBr + (CH_3)_3C$	393	12.4	17.6	*g*

[a] A. Farkas, *Z. physik. Chem.*, **10B**, 419 (1930). A. Farkas and L. Farkas, *Proc. Roy. Soc.* (*London*), **152A**, 124 (1935). M. Van Meersche. *Bull. soc. chim. Belg.*, **60**, 99 (1951). [b] T. G. Marjury and E. W. R. Steacie, *Disc. Faraday Soc.*, **14**, 45 (1953). E. Whittle and E. W. R. Steacie, *J. Chem. Phys.*, **21**, 993 (1953). R. E. Rebbert and E. W. R. Steacie, *Can. J. Chem.*, **32**, 113 (1954). [c] J. R. McNesby and A. S. Gordon, THIS JOURNAL, **76**, 4196 (1954). [d] Reference 9. [e] R. E. Rebbert and E. W. R. Steacie, *J. Chem. Phys.*, **21**, 1723 (1953). M. H. Steacie and E. W. R. Steacie, *Can. J. Chem.*, **31**, 505 (1953). [f] M. Bodenstein and S. C. Lind, *Z. physik. Chem.*, **57**, 168 (1907); M. Bodenstein and G. Jung, *ibid.*, **121**, 127 (1926). G. B. Kistiakowsky and E. R. Van Artsdalen, *J. Chem. Phys.*, **12**, 469 (1944). [g] Reference 10.

Results of the Calculations.—The activated complexes deduced from these rules are given in Fig. 1 together with the structure assumed for the methyl radical. In this figure small circles represent hydrogen atoms, medium circles stand for carbon atoms, large circles are bromine atoms, and the ovals represent CH_2 or CH_3 groups. From these structures the moments of inertia and symmetry numbers were evaluated, and these quantities are listed in Tables II and III. By use of Badger's rule the stretching force constants given in Table IV were found. With the data in Tables II–IV the contribution of each degree of freedom to the pre-exponential factor A_p was computed, and these

(8) Wilson, Decius and Cross, "Molecular Vibrations," McGraw-Hill Book Co., Inc., New York, N. Y., 1955.

(9) A. F. Trotman-Dickenson, J. R. Birchard and E. W. R. Steacie, *J. Chem. Phys.*, **19**, 163 (1951).

(10) B. H. Eckstein, H. A. Scheraga and E. R. Van Artsdalen, *ibid.*, **22**, 28 (1954).

TABLE II

PROPERTIES DEDUCED FOR ACTIVATED COMPLEXES

Complex	Moments of inertia (A.M.U. Å.²)	I internal rotation (A.M.U. Å.²)	Vibration freq. (cm.⁻¹)
(1)	1.705	...	2930, 1190, 1190
(2), (3)	8.11, 8.11, —[a]	...	752.7, 752.7, 1441, 1441, 1643, 1643, 2984, 2984, 1322, 2665, 3145
(4)	9.53, 57.0, 57.0	2.117	711, 711, 1220, 1102, 1486, 2100, 2900, 2236, 2994, 2225, 2963, 1155, 970, 1260, 1055, 1460, 725, 753, 753
(5)	49.4, 66.0, 115.5	3.175, 6.350[b]	814, 814, 725,[c] 208, 469[d]
(6)	151, 112, 263	3.175, 13.8	1200, 1200, 725,[c] 200, 200[d]
(7)	118, 244, 362	3.175, 14.1, 14.1	Same as (6)[d]
(8)	132, 427, 559	3.175, 14.8, 17.8, 13.9	Same as (6)[d]
(9)	8.66	...	1074, 1074, 1325
(10)	240.5, 240.5, —[a]	...	158.5, 158.5, 374, 1116, 1116[d]

[a] One moment of inertia cancels with one in the reactant. [b] Only those moments of inertia for internal rotation are included which do not cancel identically with an equivalent term in the reactant. [c] This frequency is included because it is much lower than the corresponding C–H stretching frequency in the reactant. [d] These vibration frequencies include only those for which cancellation cannot be made against an equivalent frequency in the reactant.

factors are listed in Table V. From the factors in Table V one obtains the calculated preëxponential factors listed in Table I. The observed pre-exponential factors are listed there for comparison.

TABLE III

PROPERTIES ASSUMED FOR THE METHYL RADICAL

I: 3.175, 1.907, 1.907; $\sigma = 3$

Vib. freq., cm.⁻¹ (taken from ammonia)

3336, 950, 3414 (twice), 1627 (twice)

TABLE IV

FORCE CONSTANTS FOR HALF-BONDS

Half-bond	k, dynes/cm.
C–H	2.55×10^5
H–H	2.55×10^5
H–Br	2.24×10^5
X–H–X bend, ergs/radian	0.164×10^{-11}

TABLE V

VALUES OF A_p FOR THE VARIOUS DEGREES OF FREEDOM IN THE DIFFERENT REACTIONS

Reaction	A_t	A_r	A_{fir}	A_v
1	6.79×10^{-26}	6.20	...	3.34
2	5.15×10^{-26}	0.606	...	1.954
3	1.325×10^{-25}	10.02	...	1.825
4	4.93×10^{-27}	0.0619	6.14	6.24
5	3.24×10^{-27}	.131	15.02	21.8
6	2.96×10^{-27}	.0116	9.83	34.4
7	2.80×10^{-27}	.00469	11.75	34.4
8	2.67×10^{-27}	.00424	11.30	34.4
9	3.59×10^{-26}	31.5	...	6.16
10	7.82×10^{-26}	4.5	...	58

Discussion.—In view of the uncertainties and errors in obtaining the experimental values of pre-exponential factors, perfect agreement is to be regarded as within a factor of two, and satisfactory agreement is within a factor of ten. For certain reactions the spread in experimental values from one worker to another is a factor of ten or more, and certain of the other reactions have not been investigated so intensively. By these standards there is excellent agreement between observed and calculated values of the pre-exponential factor for 8 out of the 9 comparisons in Table I. In particular it should be noted that this very quick and relatively easy computation gives values of the pre-exponential factor which agree with experiment and with calculations made by the much more tedious method of constructing energy surfaces.[3]

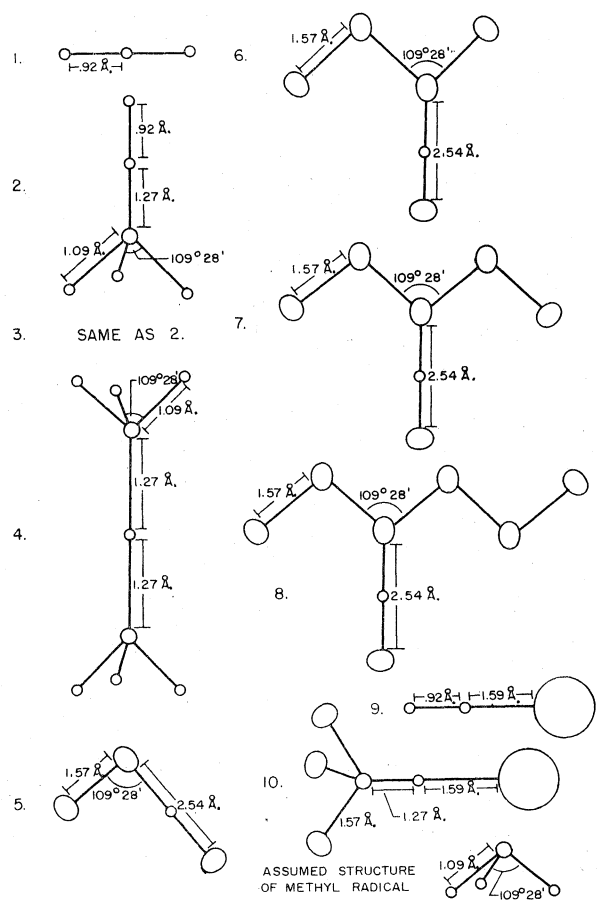

Fig. 1.—Structures of the activated complexes: small circles, H; medium circles, C; large circles, Br; ovals CH_2 or CH_3.

There may be some significance in the high values for A calcd. for the long-chain hydrocarbons, butane, pentane and hexane. If so, it is probably due to

hindered skeletal internal rotations for these activated complexes.

Finally the excellent agreement between theory and experiment for reaction 9 between Br and H_2 and the 100,000 fold discrepancy between calculated and observed factors for reaction 10

$$(CH_3)_3CH + Br \longrightarrow (CH_3)_3C + HBr$$

require special comment. We make an unqualified prediction that the observed value is wrong; in particular, we believe a reinvestigation of this reaction over a wide range of reactant pressure, degree of reaction, and pressure of additives will reveal that the over-all reaction $(CH_3)_3CH + Br_2 \rightarrow (CH_3)_3CBr + HBr$ does not follow the bromination mechanism assumed for it.[10]

Evaluation.—Kinetic data are often so uncertain that order-of-magnitude estimates of pre-exponential factors are all that one can obtain from experiment. There are many empirical rules and approximation methods in the field of molecular structure and molecular spectroscopy which, though not good enough for many purposes in their own field, are more than adequate for purposes of kinetics. The rules used here for bond distances,[5,6] for stretching force constants,[6a] and for moments of inertia for internal rotation[4] appear to be cases of this type. However, we kineticists must await developments for comparable rules for barriers to internal rotation and for either a Badger's rule for bending force constants or, more likely, an adequate empirical classification of bending frequencies. With such rules, kinetic pre-exponential factors should be calculable within a factor of four or so, without undue labor, even for complicated reactant molecules. At present these calculations appear to be valid within, perhaps, a factor of about 40. It might be remarked that for practical purposes this situation is a considerable improvement over the case as stated recently by Trotman-Dickenson[11] relative to reaction 10.

(11) A. F. Trotman-Dickenson, "Gas Kinetics," Academic Press, Inc., New York, N. Y., 1955, p. 194, line 13.

STANFORD, CAL.

PART FOUR: CARBON ISOTOPE EFFECT DURING OXIDATION OF CARBON MONOXIDE WITH NITROGEN DIOXIDE

Reprinted from THE JOURNAL OF CHEMICAL PHYSICS, Vol. 26, No. 5, 1002–1006, May, 1957
Printed in U. S. A.

Carbon Isotope Effect during Oxidation of Carbon Monoxide with Nitrogen Dioxide*

HAROLD S. JOHNSTON,† WILLIAM A. BONNER, AND DAVID J. WILSON†
Department of Chemistry, Stanford University, Stanford, California

(Received August 23, 1956)

By use of naturally occurring C^{12} and C^{13} isotopes in carbon monoxide, the effect of carbon mass on the rate of the reaction

$$CO+NO_2=CO_2+NO$$

has been studied in a 15-l Vycor flask, in the temperature range 540–727°K, and at pressures between 1 and 20 mm. The rate constant for the reaction was $k=12\times10^{12}\exp(-31{,}600/RT)$ cc mole^{-1} sec^{-1}. The ratio of rate constants k_{12}/k_{13} was 1.022 at 540°K, 1.019 at 638°K, and 1.016 at 727°K. An activated complex was set up with normal bond distances and normal force constants, and with the reaction coordinate explicitly given in terms of internal coordinates with an interaction term such that the restoring force on an antisymmetric stretching symmetry coordinate is reduced to zero. By means of E. B. Wilson's *FG* matrix methods, a vibrational analysis was made of the activated complex, all vibration frequencies were determined for one species, and shifts in frequency due to isotopic substitution were computed by a perturbation method. Similarly, the ratio of effective mass of the reaction coordinate was evaluated, and calculations were checked by the Teller-Redlich product rule. The isotope rate effect was computed by Bigeleisen's formulation of the activated complex theory. For a set of force constants well within the range of normal values and for normal bond radii, calculated isotope rate ratios at all temperatures are in excellent agreement with observed ones.

INTRODUCTION

THE reaction

$$CO+NO_2=CO_2+NO, \qquad (1)$$

was found by Crist[1,2] and co-workers to be an elementary bimolecular reaction which occurs at a convenient rate in the temperature range 500–800°. This appeared to be a particularly simple and suitable case for a study of the $C^{12}-C^{13}$ isotope effect on the reaction rate, both because of the clean-cut kinetics and the molecular simplicity of the reactants, making possible a detailed theoretical analysis of the results.

EXPERIMENTAL

Materials

Nitrogen dioxide, obtained from Matheson Company, was treated with oxygen to remove nitric oxide, passed through phosphoric anhydride to remove moisture and repeatedly distilled in vacuum. No impurity could then be found in the nitrogen dioxide by means of infrared analysis; in particular no water, nitric acid, or nitrogen pentoxide was present. Absence of water or nitric acid was essential to this study in order to avoid the chain reaction

$$HO+CO=CO_2+H \qquad (2)$$

$$H+NO_2=HO+NO. \qquad (3)$$

Carbon monoxide was produced by the action of sulfuric acid on sodium formate, and it was dried and freed of carbon dioxide by passage through Dehydrite and Ascarite towers. Carbon dioxide for the blank runs was prepared by complete combustion of a small sample of the same sodium formate which was used in the preparation of carbon monoxide, using an ordinary analytical semimicro combustion apparatus. Since the $C^{12}-C^{13}$ ratio is quite variable for naturally occurring carbon, it was essential to generate the carbon monoxide for the reactant and blank from the same sodium formate sample.

Apparatus

All runs were made in a 14.5-l Vycor flask which has been fully described elsewhere.[3]

Procedure

The pressures of reactants were measured in gas pipets, and the reactants were passed together into the furnace. All runs were made with a 20-fold excess of carbon monoxide to eliminate errors due to the decomposition of nitrogen dioxide. The reaction was allowed to proceed for a time interval which would allow consumption of less than 1% of the carbon monoxide. The reaction mixture was then pumped through a trap at liquid nitrogen temperature, and the excess carbon monoxide was discarded. The temperature of the trap was raised to −135° (*n*-pentane slush), and the carbon dioxide product was distilled into a bulb at liquid nitrogen temperature. Distillation from −135° to −195° was repeated, and complete separation of carbon dioxide from dinitrogen trioxide and dinitrogen tetroxide was achieved in this way. The pressure and volume of carbon dioxide was measured in order to calculate the rate constant for the over-all reaction. By means of a ratio-recording mass spectrometer the mass ratio 45/44 was determined in order to give the relative rates of reaction of the two isotopes. At the same time the mass ratio 45/44 was determined on the carbon dioxide blank for purposes of comparison. We

* This work was supported in part by the Office of Naval Research, Contract N6onr 25131, Project NR 051246. One of us (DJW) is grateful to the National Science Foundation for a Fellowship.

† Present address: Department of Chemistry, California Institute of Technology, Pasadena, California.

[1] G. M. Calhoun and R. H. Crist, J. Chem. Phys. **5**, 301 (1937).

[2] F. B. Brown and R. H. Crist, J. Chem. Phys. **9**, 840 (1941).

[3] H. S. Johnston, Discussions Faraday Soc. **17**, 1 (1954).

are indebted to Dr. Harold Eding of Stanford Research Institute for our mass spectrometric data.

RESULTS

Duplicate runs were made at each of three temperatures, and duplicate blanks were measured. The concentrations of reactants and the mass ratios are given in Table I.

From the concentrations of reactants and the quantity of carbon dioxide produced, the rate constant for (1) was calculated from the relation

$$d[CO_2]/dt = k[NO_2][CO]. \quad (4)$$

For each isotope of carbon a chemical equation like (1) and a rate expression like (4) may be written. The ratio of these rate expressions gives

$$\frac{d[C^{12}O_2]}{d[C^{13}O_2]} = \frac{k_{12}[C^{12}O]}{k_{13}[C^{13}O]}. \quad (5)$$

Since less than 1% of the carbon monoxide was allowed to react during each run, the total amount of carbon dioxide produced may be regarded as the initial increment, $d[CO_2]$, and the isotopic composition of the reactant is essentially unchanged and is given by the blank. Thus one obtains as a good approximation

$$\frac{[C^{12}O_2]}{[C^{13}O_2]} = \frac{k_{12}[C^{12}O_2]_{\text{blank}}}{k_{13}[C^{13}O_2]_{\text{blank}}}. \quad (6)$$

The isotopic ratio (45/44) was measured directly so that the ratio of rate constants is

$$k_{12}/k_{13} = (45/44)_{\text{blank}}/(45/44). \quad (7)$$

An Arrhenius plot was made of (7) to give the difference in activation energy as

$$E_{12} - E_{13} = -20 \pm 5 \text{ cal/mole}. \quad (8)$$

An Arrhenius plot was made of k found by (4) to give an energy of activation of 31.6 kcal/mole and a pre-exponential factor $A = 12 \times 10^{12}$ cc mole^{-1} sec^{-1}.

DISCUSSION

Using the notation of Wilson, Decius, and Cross[4] we write down the Teller-Redlich product rule for an activated complex containing N atoms, r free internal rotations, and one reaction coordinate which is essentially a free translation or a vibration with no restoring force.[5]

$$\prod_{k=1}^{3N-7-r} \frac{\omega_k'}{\omega_k} = \prod_{i=1}^{3N} \left(\frac{m_i}{m_i'}\right)^{\frac{1}{2}} \left(\frac{M'}{M}\right)^{\frac{3}{2}} \left(\frac{I_x' I_y' I_z'}{I_x I_y I_z}\right)^{\frac{1}{2}} \times \left(\frac{\mu'}{\mu}\right)^{\frac{1}{2}} \prod_{j=1}^{r} \left(\frac{I_j'}{I_j}\right)^{\frac{1}{2}}, \quad (9)$$

where m is atomic mass, M is mass of the entire complex, and μ is the effective mass of the reaction coordinate, reference 5, pp. 186–189.

Using the partition-function formulation of the activated complex theory[5] for a bimolecular reaction, one gets for the ratio of rate constants for isotopic reactions

$$\frac{k}{k'} = \frac{\kappa}{\kappa'} \frac{Q^{\ddagger}/Q'^{\ddagger}}{Q/Q'} e^{-\Delta\Delta E/RT} \quad (10)$$

where $Q^{\ddagger}$ is the partition function for the activated complex with the contribution due to the reaction coordinate factored out, Q is the complete partition function for the reactant in which isotopic substitution appears, and $\Delta\Delta E$ represents the difference between complex and reactant in the difference of zero point energy, or in this case $(E^0_{12} - E^0_{13})^{\ddagger} - (E^0_{12} - E^0_{13})^{CO}$. The partition-function ratio $Q_1^{\ddagger}/Q_2^{\ddagger}$ in (10) gives rise to the following product of ratios

$$\left(\frac{\sigma'}{\sigma}\right)_{\ddagger} \left(\frac{M}{M'}\right)_{\ddagger}^{\frac{3}{2}} \left(\frac{I_x I_y I_z}{I_x' I_y' I_z'}\right)_{\ddagger}^{\frac{1}{2}} \times \prod^{r} \left(\frac{I_j}{I_j'}\right)_{\ddagger}^{\frac{1}{2}} \prod^{3N-7-r} \left(\frac{Q_v}{Q_v'}\right)_{\ddagger}, \quad (11)$$

where σ is the symmetry number and Q_v is the partition function for vibrations; there is a comparable expression for the substituted reactant. If Eq. (11) for both complex and reactant is substituted into (9) and (10), the rate expression becomes

$$\frac{k}{k'} = \left(\frac{\mu'}{\mu}\right)^{\frac{1}{2}} \frac{\prod^{3N-7-r} \left[\frac{u(1-e^{-u'})}{u'(1-e^{-u})} e^{\Delta u/2}\right]^{\ddagger} \left(\frac{\sigma'}{\sigma}\right)^{\ddagger}}{\prod^{3n-6} \left[\frac{u(1-e^{-u'})}{u'(1-e^{-u})} e^{\Delta u/2}\right] \left(\frac{\sigma'}{\sigma}\right)} \frac{\kappa}{\kappa'}, \quad (12)$$

where $u = hc\omega/kT$, N is the number of atoms in the complex, n is the number of atoms in the substituted reactant, and the terms in the denominator refer to the substituted reactant. Equation (12), of course, is

TABLE I. Experimental results.

	Reactants m/l×10⁴				
T°K	CO	NO_2	Mass ratio 45/44×10⁶	k 1. mole^{-1} sec^{-1}	k_{12}/k_{13}
540	5.1	0.35	11 068±9	0.0019	1.0218
541	7.0	0.49	11 050±13	0.0016	1.0225
638	5.8	0.29	11 093±12	0.110	1.0193
638	4.8	0.26	11 071±5	0.120	1.0188
727	5.1	0.29	11 122±14	2.7	1.0157
727	4.6	0.26	11 113±7	3.2	1.0165

[4] Wilson, Decius, and Cross, *Molecular Vibrations* (McGraw-Hill Book Company, Inc., New York, 1955), p. 184.

[5] Glasstone, Laidler, and Eyring, *Theory of Rate Processes* (McGraw-Hill Book Company, Inc., New York, 1941).

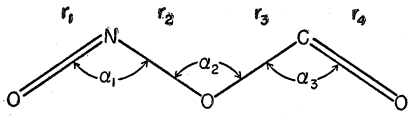

FIG. 1. Structure of the activated complex: $r_1=r_4=1.2$ A; $r_2=r_3=1.4$ A; $\alpha_1=\alpha_2=\alpha_3=120°$; planar.

Bigeleisen's[6,7] expression for the rate ratio for isotopic reactions. The only difference between Eqs. (10) and (12) is the Teller-Redlich product rule (compare reference 7, footnote 2). Whether one uses (10) or (12) depends on whether one had rather compute moments of inertia (including those for internal rotation) or mass ratio along the reaction coordinate. [Actually it is desirable to compute both sets of quantities to substitute into (9) as a check against computational errors.] Bigeleisen's formulation is considerably more convenient for computational purposes in the present case.

To use Eq. (12) one needs the mass ratio μ/μ' and the vibration frequencies for unsubstituted and substituted reactant and activated complex. These quantities are readily obtained by means of Wilson's F and G matrices,[4] provided one has a model of the activated complex. For this reaction we use the model previously proposed[8] with certain minor refinements. The activated complex was assumed to be of the planar dinitrogen trioxide structure, Fig. 1, with bond angles of 120°. The double-bond distances, 1.2 A, were taken as the sum of the double-bond radii of the elements, and the single bond distances, 1.4 A, were taken from single bond radii.[9] Partition functions for translation, rotation, and internal rotation were calculated from this model. For the vibrational analysis, a slight change was introduced in order to increase the symmetry of the unsubstituted activated complex and thus greatly simplify the calculations. The actual masses of the atoms in the activated complexes are 16–12–16–14–16 and 16–13–16–14–16. The first of these was replaced by the average-mass case 16–13–16–13–16, and the second was retained. Thus the unsubstituted complex had C_{2v} symmetry and the substituted complex was treated by a perturbation method.[10]

Force constants were assigned by analogy[11] and by use of Badger's rule.[12] Ratios of force constants were assigned as: 2, double bond stretch to single bond stretch; 10, single bond stretch to end k_α/r_1r_2; 2, end bend to center bend.[13] The magnitude of the single bond stretching force constant is 5×10^5 dynes/cm according to Badger's rule; by analogy with C—C, O—O, N—N, C—N, and C—O single-bond force constants,[11] the range $3\frac{1}{2}\times10^5$ to 6×10^5 appears to be very reasonable (we have made calculations for the values of 4, 5 and 6×10^5). The reaction coordinate was treated as before[8]; an interaction constant was introduced which reduces to zero the restoring force on the antisymmetric stretching mode involving the central oxygen atom

$$2V=k_s(r_2^2+r_3^2)+2k_s'r_2r_3+\text{other square terms.} \quad (13)$$

As k_s' approaches k_s the restoring force of the antisymmetric center stretch goes to zero, and the reaction coordinate becomes separated from the normal modes of vibration.

Out-of-plane motions for this complex are the internal rotations. A rough estimate of the barrier to internal rotation[14] indicates it to be less than RT for this complex. Thus computations are made on the assumption of free internal rotation.

With this model for the activated complex the F and G matrices[4] were set up in the usual way. The seven-by-seven FG matrix reduces to a four-by-four (A_1) and a three-by-three (B_2) which includes the reaction coordinate with zero frequency. The six nonzero frequencies and the corresponding normal modes with their normalized *eigenvectors* were found; then the shifts in frequency caused by a single isotopic substitution in the activated complex were computed by a perturbation method.[10] These frequencies and their shifts are given in Table II.

The "effective mass" along the reaction coordinate is readily calculated as a by-product of the normal-mode analysis. For the terms in (13) let $k_s'-k_s$ be ϵ, a number as close to zero as desired. The corresponding λ is so low that terms in λ^2 and higher may be neglected. In terms of F and G determinants the value of λ is[15]

$$\lambda=|G||F|/\Sigma G^{(2)}F^{(2)}, \quad (14)$$

TABLE II. Contribution of the various normal modes of vibration to the various rate factors. Q contributes to A, Q_{12}/Q_{13} contributes to k_{12}/k_{13}, and $E_{12}-E_{13}$ is given directly. T is 638°K. Force constants are 8–4–0.4–0.2.

Normal Mode	$\omega_{cm^{-1}}$	Q	$\Delta\omega^a$ cm^{-1}	$-\ln\frac{Q_{12}}{Q_{13}}$	$E_{12}-E_{13}$, cal/mole ΔE^0	$RT\theta^b$
Sym. str., mid.	1160	1.08	12.4	0.0022	17.8	−5.1
Sym. str., end	1495	1.04	12.4	0.0010	17.8	−3.2
Sym. bend, end	335	1.88	1.3	0.0027	1.9	−1.4
Mid bend	176	3.05	1.2	0.0054	1.7	−1.4
React. coord.						
Anti. sym. str., ends	1381	1.05	13.8	0.0015	19.7	−4.3
Anti. sym. bend	451	1.57	4.9	0.0063	7.0	−4.8
CO	2169	1.01	49.2	0.0008	70	−4.1
				E calc	−20.2	
				E obs	−20±5	

[a] This is a decrease in all cases.
[b] $\theta=d\ln Q/d\ln T$.

[6] J. Bigeleisen, J. Chem. Phys. **17**, 675 (1949).
[7] J. Bigeleisen and M. G. Mayer, J. Chem. Phys. **15**, 261 (1947).
[8] Herschbach, Johnston, Powell, and Pitzer, J. Chem. Phys. **25**, 736 (1956).
[9] Linus Pauling, *Nature of the Chemical Bond* (Cornell University Press, Ithaca, 1940).
[10] See reference 4, p. 188.
[11] See reference 4, pp. 175–176.
[12] R. M. Badger, J. Chem. Phys. **2**, 129 (1934); **3**, 710 (1935).
[13] These ratios are based on reference 11 and on analogy to nitrogen tetroxide and to ethers. Other ratios could be used within the range of examples from normal molecules.
[14] E. A. Mason and M. M. Kreevoy, J. Am. Chem. Soc. **77**, 5808 (1955).
[15] See reference 4, p. 68.

TABLE III. Calculated rate factors as a function of variation of force constants assumed for the activated complex.

Force constants dynes cm$^{-1}\times10^{-5}$				k_{12}/k_{13}			$E_{12}-E_{13}$	$A\times10^{-12}$
End Str.	Mid Str.	End bend	Mid bend	540°	638°	727°	cal/mole	cc m^{-1} sec^{-1} 638°[a]
8	4	0.4	0.2	1.0208	1.0180	1.0160	−20	26
10	5	0.5	0.25	1.0138	1.0124	1.0113	−10	20
12	6	0.6	0.3	1.0097	1.0092	1.0090	−3	14
observed				1.0221	1.0190	1.0161	−20±5	12

[a] Based on unity for kappa.

where $G^{(2)}$ is any two-rowed minor of $|G|$ and $F^{(2)}$ is the corresponding two-rowed minor of $|F|$, summed over all such minors.[15] For the isotopically substituted complex the expression is

$$\lambda'=|G'||F|/\Sigma G'^{(2)}F^{(2)}. \tag{15}$$

The ratio of these two terms leads to cancellation of $|F|$, and it is the ratio of effective masses μ

$$\lambda/\lambda'=\mu'/\mu. \tag{16}$$

Now, as one lets $k_s'=k_s$, some terms in $F^{(2)}$ go to zero and some others cancel out. For the present case (the reaction coordinate is number 5, the antisymmetric end stretch is 6, and the antisymmetric end bend is 7) the expression for the ratio of masses is

$$\frac{\mu}{\mu'}=\frac{|G'|}{|G|}\frac{G_{6,7}^{(2)}}{G'^{(2)}_{6,7}}, \tag{17}$$

where $G'=G+\Delta G$. The changes in G, that is, ΔG, were used in the perturbation method calculation. In (17) $|G|$ is the complete three-by-three (B_2) determinant. For the present case the value of μ_{13}/μ_{12} was 1.0095.

By the use of this value of μ'/μ and (9), a check can be made against the six planar vibration frequencies. The product of the ratio of vibration frequencies is 1.0521; the product of the ratios of atomic weights, molecular weights, one moment of inertia, and μ/μ' on the right-hand side of (9) is 1.0510. The discrepancy of 0.001 is believed to be a measure of the validity of the perturbation method for this case; it might be noted that this discrepancy is by no means negligible.

Rate constant ratios were computed[16] for three sets of force constants: 8–4–0.4–0.2, 10–5–0.5–0.25, and 12–6–0.6–0.3. The calculated curve for k_{12}/k_{13} is plotted against $1000/T$ in Fig. 2. The force constants 8–4–0.4–0.2 give a curve lying very close to the observed points at all temperatures; the other two curves miss the points and have the wrong temperature dependence. The calculated curves are very sensitive to small changes in the assigned force constants; obviously a small reduction in the lowest set of force constants would give almost perfect agreement with experiment. This adjustment is unnecessary. The primary point established is that this simple method[8] of setting up and characterizing the activated complex and reaction coordinate gives a good description of the isotope rate effect within the limits of a normal set of bond distances and force constants. In the calibration of this method of constructing activated complexes, it might be noted that the pre-exponential factor is particularly sensitive to low frequency oscillators and free internal rotations. On the other hand, these quantities have little or no effect on the isotope rate factors k/k', and $E-E'$. The high-frequency oscillators are by far the most important contributors to the isotope rate effect; this point has been made by Bigeleisen.[6] The contribution of the various frequencies to k/k' and $E-E'$ is given in Table II. A comparison of the different sets of force constants for the rate factors, A, k/k', and $E-E'$ is given in Table III. The agreement between calculated and observed pre-exponential factor is quite satisfactory for all choices of the force constants (a factor of two is precise agreement here and a factor of 10 is within experimental error).

Finally, we wish to give a short discussion emphasizing the distinction between the isotope effect contributed by the reaction coordinate and the isotope

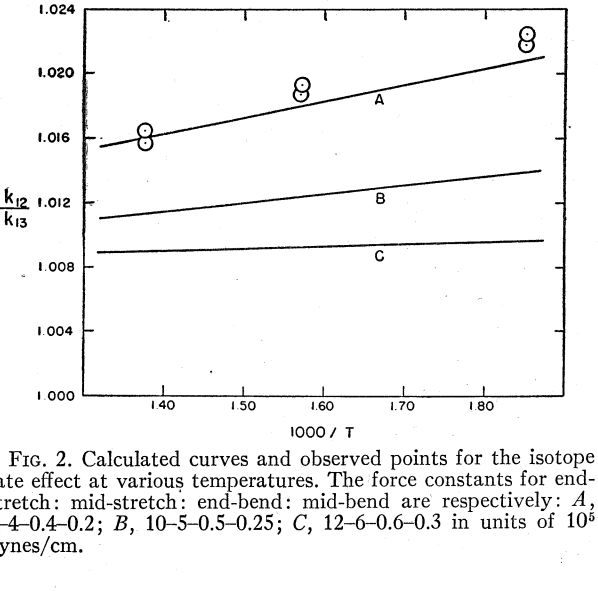

FIG. 2. Calculated curves and observed points for the isotope rate effect at various temperatures. The force constants for end-stretch: mid-stretch: end-bend: mid-bend are respectively: A, 8–4–0.4–0.2; B, 10–5–0.5–0.25; C, 12–6–0.6–0.3 in units of 10^5 dynes/cm.

[16] Bigeleisen and Mayer[7] give extensive tables of a function they call $G(u)$. This function employs the approximation, $e^{\Delta u/2}=1+\Delta u/2$. Because of the very small isotope effect observed here, we found this approximation to be extremely poor for this case. In making these computations we kept all figures to six significant figures, rounding off only at the end. Unless extreme care is taken in these computations, rounding-off errors can easily become as large as the isotope effect itself.

In these calculations the ratio of kappas was taken as one.

effect contributed by the rest of the activated complex. In terms of Bigeleisen's formulation the reaction coordinate contributes $(\mu/\mu')^{\frac{1}{2}}$ toward the isotope effect, and that is all (actually this treatment neglects the possibility of a very narrow δ, width of the top of the barrier to the reaction coordinate, and thus a significant zero-point energy in the reaction coordinate itself). The other normal modes in the activated complex contribute their product of u_i, their product of Q_i, and the zero-point energy difference, $\Sigma h\nu_i/2$. Thus isotopic substitution in atoms removed from the site of the reaction coordinate, could lead to an isotope rate effect. For the present reaction an isotope effect should be observed between CO^{16} and CO^{18}, for example.

Appendix I

Abbreviations

The following abbreviations are used in this dissertation:

mm.	millimeters of mercury
$^{o}C.$	degrees centigrade
kcal/mol.	kilocalories per mole
cc.	cubic centimeters
cm.	centimeters
$sec.^{-1}$	reciprocal seconds
mol/cc.	moles per cubic centimeter

Appendix II

Computation of the First-Order Rate Constant for a Simple Model Involving Stepwise Activation

The most general form of the Lindemann theory postulates the following mechanism:

$$\begin{aligned} A_j + M_k &\rightarrow A_i + M_l \qquad a_{jkil}, \\ A_i + M_l &\rightarrow A_j + M_k \qquad b_{jkil}, \\ A_i &\rightarrow \text{Products} \qquad c_i . \end{aligned} \tag{2.1}$$

Assume that

$$a_{jkil} = a_{jkl} \cdot \delta_{j+1,i} ,$$

$$b_{jkil} = b_{jkl} \cdot \delta_{j+1,i} ,$$

where $\delta_{m,n} = 0$ if $m \neq n$,

$\delta_{m,n} = 1$ if $m = n$.

Also assume that the states of M have their equilibrium distribution. Then, after averaging with respect to $P_l^m = \frac{M_l}{M}$, where P_l^m is the probability of the state l for the species M, and with respect to P_k^m, one finds the following expression for $\frac{dA_i}{dt}$:

$$\begin{aligned} \frac{dA_i}{dt} = {} & A_{i-1}\, a_{i-1}\, M + A_{i+1}\, b_{i+1}\, M \\ & - b_i A_i M - a_i A_i M - c_i A_i . \end{aligned} \tag{2.2}$$

Assume that

$$\frac{dA_i}{dt} = -k A_i , \tag{2.3}$$

where k is the macroscopic rate constant for the reaction. This assumption is made instead of the steady state assumption $\frac{dA_i}{dt} = 0$,

which breaks down for the case under consideration. Assumption 2.3 converts the set of differential equations 2.2 into a set of difference equations

$$0 = A_{i-1}\, a_{i-1} M + A_{i+1}\, b_{i+1} M - A_i (b_i M + a_i M + c_i - K). \tag{2.4}$$

Assume that $a_i = a$, and that the energy levels are equally spaced. Then $b_i = b$ and $a = \frac{bP_i}{P_{i-1}} = b\rho$, where $\rho = exp\left(\frac{-h\nu}{kT}\right)$; and 2.4 becomes

$$0 = b\rho M A_{i-1} + b M A_{i+1} - (b\rho M + b M + c_i - K) A_i. \tag{2.5}$$

Assume $c_i = 0$, $i < n$;

$c_i = c$, $i \geq n$, where n is the lowest quantum level at which reaction can occur. Let $A_i = \rho^{i/2} B_i$; and let

$$2 \cosh \theta'' = \frac{b M + b\rho M + c - K}{b \rho^{\frac{1}{2}} M}, \tag{2.6}$$

$$2 \cosh \theta' = \frac{b M + b\rho M - K}{b \rho^{\frac{1}{2}} M}, \tag{2.7}$$

using 2.6 or 2.7 depending on whether $i \geq n$ or $i < n$.

Then 2.5 becomes

$$0 = B_{i-1} + B_{i+1} - 2 \cosh\theta\, B_i. \tag{2.8}$$

A solution to 2.8 is

$$B_i = \alpha \sinh i\theta + \beta \cosh i\theta \tag{2.9}$$

where θ' or θ'' are used, depending on whether $i < n$ or $i \geq n$.

So $$A_i = \rho^{i/2} \left[\bar{A} \sinh i\theta' + \bar{B} \cosh i\theta' \right] \tag{2.10}$$

for the non-reactive states, and a similar expression containing θ''

and different values of the constants $\bar{A}$ and $\bar{B}$ gives the concentrations of the reactive states.

To fit the boundary conditions for the non-reactive states one proceeds as follows.

$$-k A_0 = -b\rho M A_0 + b M A_1 ,$$

so

$$A_1 = \left(\rho - \frac{k}{bM}\right) A_0 . \tag{2.11}$$

Similarly,

$$A_2 = \left[2\cosh\theta'\left(\rho - \frac{k}{bM}\right)\rho^{\frac{1}{2}} - \rho\right] A_0 . \tag{2.12}$$

Also

$$A_1 = \rho^{\frac{1}{2}}\left[\bar{A}\sinh\theta' + \bar{B}\cosh\theta'\right], \tag{2.13}$$

$$A_2 = \rho\left[\bar{A}\sinh 2\theta' + \bar{B}\cosh\theta'\right]. \tag{2.14}$$

One gets two simultaneous equations in $\bar{A}$ and $\bar{B}$ by equating 2.11 to 2.13 and 2.12 to 2.14. The solutions to these equations are

$$\bar{A} = \frac{1}{\sinh\theta'}\left\{\frac{1}{\rho^{1/2}}\left(\rho - \frac{k}{bM}\right) - \cosh\theta'\right\} A_0 , \tag{2.15}$$

$$\bar{B} = A_0 .$$

So

$$A_i = A_0\rho^{i/2}\left[\frac{\sinh i\theta'}{\sinh\theta'}\left\{\frac{1}{\rho^{1/2}}\left(\rho - \frac{k}{bM}\right) - \cosh\theta'\right\} + \cosh i\theta'\right] \tag{2.16}$$

is the desired solution for non-reactive states of A.

It is next necessary to fit the boundary conditions for the solutions A_i where $i \geq n$. It is easily verified that

$$A_{n+j} = \rho^{j/2} A_n e^{-j\theta''} \tag{2.17}$$

is the desired solution by substituting this expression into 2.5 and by noting that $\lim A_{n+j} = 0$ as $j \to \infty$ and that $A_{n+0} = A_n$.

The expression for the rate of disappearance of A is

$$-\frac{dA}{dt} = kA = c\sum_{j=0}^{\infty} A_{n+j} = c A_n \sum_{j=0}^{\infty} \left(\rho^{\frac{1}{2}} e^{-\theta''}\right)^j = \frac{c A_n}{1-\rho^{1/2} e^{-\theta''}} . \tag{2.18}$$

So

$$k = \frac{c A_n}{A} \cdot \frac{1}{1-\rho^{1/2} e^{-\theta''}} . \tag{2.19}$$

Now

$$A_0 \cong A(1-\rho) \tag{2.20}$$

if E is greater than 10 kT, as is almost always the case. So, substituting 2.16 and 2.20 into 2.19, one finds

$$k = \frac{c\rho^{n/2}(1-\rho)}{1-\rho^{1/2} e^{-\theta''}} \left[\frac{\sinh n\theta'}{\sinh \theta'} \left\{ \frac{1}{\rho^{1/2}} \left(\rho - \frac{k}{bM}\right) - \cosh\theta' \right\} + \cosh n\theta' \right] \tag{2.21}$$

where

$$2\cosh\theta' = \frac{bM + b\rho M - k}{b\rho^{1/2} M},$$

$$2\cosh\theta'' = \frac{bM + b\rho M + c - k}{b\rho^{1/2} M}.$$

At the low pressure limit $\frac{k}{bM}$ takes on its maximum value. In this region the rate of reaction is equal to the rate of activation from the (n-1)th state. So

$$K A = b P M A_{n-1}$$

and

$$\frac{K}{bM} = \frac{P A_{n-1}}{A} < P P_{n-1}.$$

Now $P_{n-1} = (1-\rho)\rho^{n-1}$, so

$$0 \leq \frac{K}{bM} \leq (1-\rho)\rho^{n}. \tag{2.22}$$

From the previous paragraph it is apparent that for reasonable values of ρ and n the quantity $\frac{k}{bM}$ is quite small over the entire pressure range. One is therefore led to expand the right-hand side of equation 2.21 in powers of $\frac{k}{bM}$ and then to drop all powers above the first. When this is done, the resulting equation can be solved for k:

$$K = \frac{2c\rho^{n}(1-\rho)}{\left[1-\rho+\frac{c}{bM}\cdot\frac{1+\rho}{1-\rho}+\sqrt{\left(1+\rho+\frac{c}{bM}\right)^{2}-4\rho}\right]}. \tag{2.23}$$

As $M \to \infty$, $k \to c\rho^{n}$, which indicates that this mechanism leads to a high-pressure limit and an activation energy of $nh\nu$ at the high-pressure limit. As $M \to 0$, $k \to bM\,\rho^{n}(1-\rho)^{2}$, so the mechanism leads to a second-order low-pressure limit and an activation energy of $nh\nu - \frac{2h\nu}{1-\exp[-h\nu/kT]}$ at the low-pressure limit.

By expanding the right-hand side of equation 2.16 in powers of $\frac{k}{bM}$ and neglecting terms of higher than first power, one finds that

$$\frac{A_m}{A_{m\,equilibrium}} = \left[1-\frac{K}{bM}\frac{\rho^{-m}}{(1-\rho)^{2}}\right], \quad m \leq n. \tag{2.24}$$

If one sets $\frac{nh\nu}{kT} = \frac{E}{RT} = 30$, $n = 30$, $\rho = e^{-1}$; the values of this ratio, $A_m/A_{m_{equil.}}$ are tabulated for a few values of m and $\frac{k}{bM}$ in the following table:

	$\frac{k}{bM}$ 0	1×10^{-15}	3	5	7	9	37.4
m							
30	1.000	.973	.920	.866	.813	.759	.000
29	1.000	.990	.971	.951	.931	.911	.632
28	1.000	.996	.989	.982	.975	.967	.865
27	1.000	.999	.996	.993	.991	.988	.950
26	1.000	1.000	.999	.998	.997	.996	.982
25	1.000	1.000	1.000	.999	.999	.998	.993

The last column on the right corresponds to the low-pressure limit. It is therefore seen that in the low-pressure region there is appreciable depletion of the first few energy levels below the critical level.

It is of interest to compare plots of k/k_∞ obtained by this mechanism with plots of k/k_∞ obtained by using a single term $\frac{a}{b + c/M}$ of the Lindemann type. If one lets $x = \frac{bM}{c}$,

$$\frac{K}{K_\infty} = \frac{2(1-\rho)}{\left[1-\rho + \frac{1}{x}\cdot\frac{1+\rho}{1-\rho} + \sqrt{\left(1+\rho+\frac{1}{x}\right)^2 - 4\rho}\right]} \qquad (2.25)$$

for the mechanism discussed here, and

$$\frac{K_L}{K_\infty} = \frac{1}{\left[1 + \frac{1}{x}\cdot\frac{1}{(1-\rho)^2}\right]} \qquad (2.26)$$

for a Lindemann expression, where the constants in $\frac{a}{b + c/M}$ have been

chosen to give 2.25 and 2.26 the same slope as $x \longrightarrow 0$.

Log plots of k/k_∞ and k_L/k_∞ are shown in figures 5 and 6 for $\rho = e^{-1}$ and $\rho = .99$.

It appears that this mechanism, in spite of its formal differences from the most simple form of the Lindemann theory, gives results that are practically indistinguishable from those of the Lindemann theory.

An attempt is currently being made to analyze the step-wise mechanism 2.1 using more realistic forms for the functions b_i and c_i.

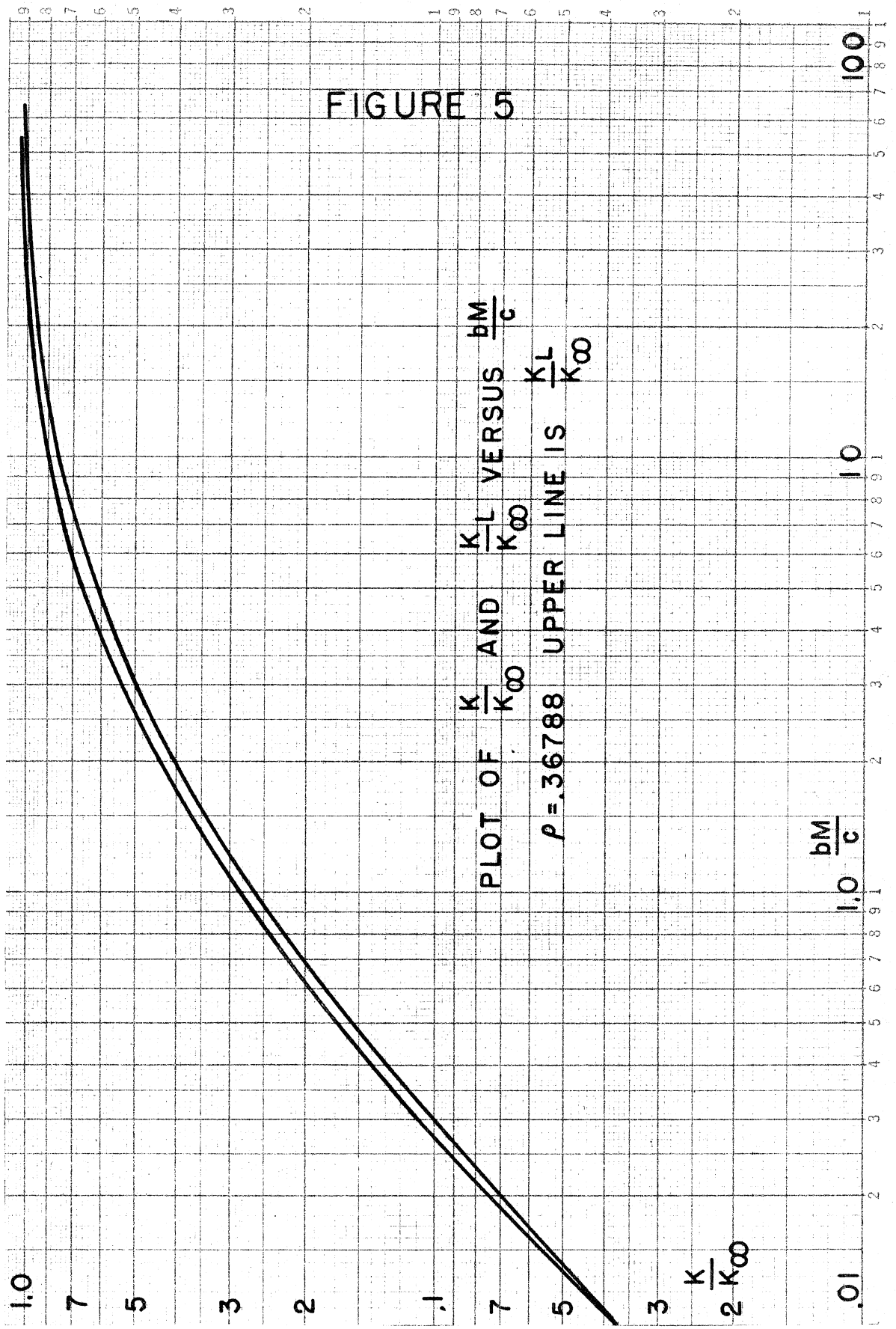
FIGURE 5
PLOT OF $\frac{K}{K_\infty}$ AND $\frac{K_L}{K_\infty}$ VERSUS $\frac{bM}{c}$
$\rho = .36788$ UPPER LINE IS $\frac{K_L}{K_\infty}$
$\frac{K}{2K_\infty}$
$\frac{bM}{c}$
1.0
.1
.01
1.0
10
100

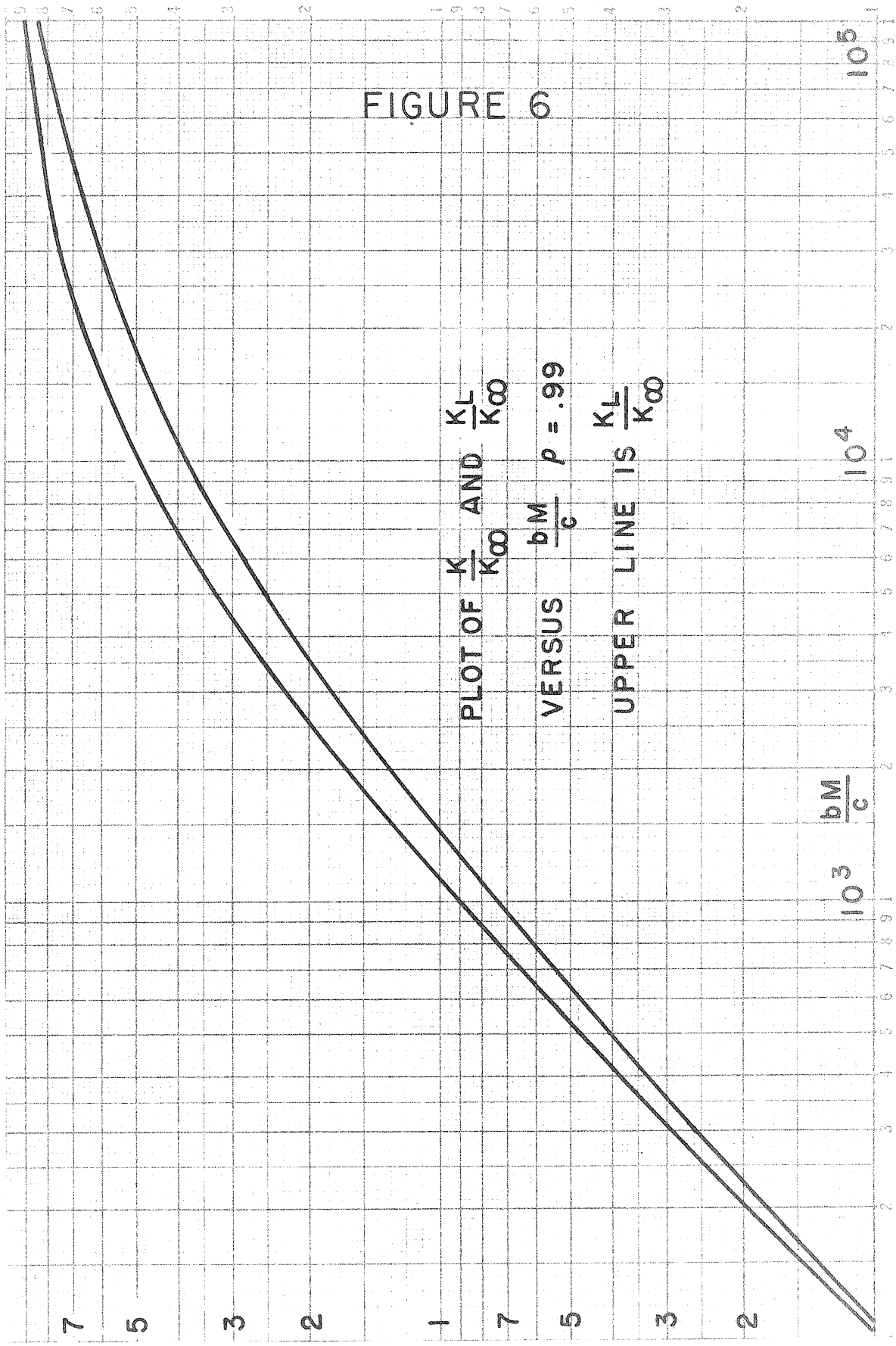
PLOT OF $\frac{K}{K_\infty}$ AND $\frac{K_L}{K_\infty}$
VERSUS $\frac{bM}{c}$ $\rho = .99$
UPPER LINE IS $\frac{K_L}{K_\infty}$
10^3 $\frac{bM}{c}$ 10^4 10^5
7 5 3 2 1 7 5 3 2

FIGURE 6

Appendix III

Analysis of the Steady State Assumption for a Unimolecular Reaction (15)

The mechanism to be considered is

$$A \rightarrow B \qquad k_1,$$

$$B \rightarrow A \qquad k_2,$$

$$B \rightarrow C \qquad k_3.$$

($B = A_i^*$; $k_1 = a_{im}M$; $k_2 = b_{im}M$; $k_3 = c_i$ in the notation used earlier.)

Then

$$\frac{dA}{dt} = \dot{A} = -k_1 A + k_2 B, \tag{3.1}$$

$$\dot{B} = k_1 A - (k_2 + k_3) B. \tag{3.2}$$

Differentiate equation 3.2:

$$\ddot{B} = k_1 \dot{A} - (k_2 + k_3) \dot{B}. \tag{3.3}$$

Use equations 3.2 and 3.3 to eliminate A and $\dot{A}$ from equation 3.1, obtaining

$$\ddot{B} + (k_1 + k_2 + k_3) \dot{B} + k_1 k_3 B = 0. \tag{3.4}$$

A solution of equation 3.4 which equals zero at $t = 0$ is

$$B = C'\left(-e^{-m^+ t} + e^{-m^- t}\right),$$

where $$m^{\pm} = \frac{(k_1 + k_2 + k_3) \pm \sqrt{(k_1 - k_3)^2 + k_2(k_2 + 2k_1 + 2k_3)}}{2}.$$

Assume that $k_1 \ll k_2$. Then $m^+ \cong k_2 + k_3$ and $m^- \cong k_1 k_3/(k_2 + k_3)$.

So $$B \cong c' \left\{ \exp\left[\frac{-k_1 k_3 t}{k_2 + k_3} \right] - \exp\left[-(k_2 + k_3) t \right] \right\},$$

and after a very short time $\left(t > \frac{1}{k_2 + k_3} \right)$

$$B \cong c' \exp\left[\frac{-k_1 k_3 t}{k_2 + k_3} \right], \tag{3.5}$$

$$\dot{B} \cong -\frac{k_1 k_3}{k_2 + k_3} B. \tag{3.6}$$

Substituting equation 3.6 in equation 3.2 gives

$$\left[\frac{(k_2 + k_3)^2 - k_1 k_3}{k_2 + k_3} \right] B \cong k_1 A.$$

Since $k_1 \ll k_2$,

$$(k_2 + k_3) B \cong k_1 A,$$

and $$B \cong \frac{k_1 A}{k_2 + k_3}. \tag{3.7}$$

The steady state assumption is

$$\dot{B} = 0 = k_1 A - (k_2 + k_3) B,$$

giving $$B = \frac{k_1 A}{k_2 + k_3}$$

which is identical with equation 3.7.

Appendix IV

Equality of Relative Efficiencies at All Pressures for the Case $b_{im} = b_m f_i$

$$R^{\circ}(N/M) = \frac{\sum_i b_m f_i P_i}{\sum_i b_m f_i P_i} = \frac{b_n}{b_m} \frac{\sum_i f_i P_i}{\sum_i f_i P_i} = b_n / b_m . \tag{4.1}$$

If $k_m = k_n$,

$$\sum_i \frac{P_i c_i b_m f_i M}{b_m f_i M + c_i} = \sum_i \frac{P_i c_i b_n f_i N}{b_n f_i N + c_i},$$

$$\sum_i \left(\frac{P_i c_i b_m f_i M}{b_m f_i M + c_i} - \frac{P_i c_i b_n f_i N}{b_n f_i N + c_i} \right) = 0, \tag{4.2}$$

$$(b_m M - b_n N) \sum_i \frac{P_i c_i^2 f_i}{(b_m f_i M + c_i)(b_n f_i N + c_i)} = 0.$$

Now

$$\sum_i \frac{P_i c_i^2 f_i}{(b_m f_i M + c_i)(b_n f_i N + c_i)} > 0 . \tag{4.3}$$

Therefore

$$b_m M = b_n N \tag{4.4}$$

if $k_m = k_n$.

The proofs that the differential and integral relative efficiencies are equal to $\frac{b_n}{b_m}$ involve substituting 4.4 into the expression for the given relative efficiency, factoring out $\frac{b_n}{b_m}$, and observing that the summations left in the numerator and denominator are identical.

$$R^d(N/M) = \frac{b_n \sum_i \frac{P_i c_i^2 f_i}{(b_n f_i N + c_i)^2}}{b_m \sum_i \frac{P_i c_i^2 f_i}{(b_m f_i M + c_i)^2}}, \tag{4.5}$$

and $b_n N = b_m M$,

so
$$R^d(N/M) = \frac{b_n}{b_m} . \tag{4.6}$$

Also,

$$R^i(N/M) = \frac{b_n \sum_i \frac{P_i c_i^2 f_i}{L_i(M,N)}}{b_m \sum_i \frac{P_i c_i^2 f_i}{L_i(M,N)}} = \frac{b_n}{b_m}, \tag{4.7}$$

$$L_i(M,N) = (b_m f_i M + c_i)(b_n f_i N + c_i) .$$

The procedure for $R^f(N/M)$ is almost as simple:

$$0 = \sum_i \frac{(M b_m - N b_n) f_i P_i c_i^2}{L_i(M+\Delta M, N+\Delta N)} = \sum_i \frac{(\Delta N b_n - \Delta M b_m) f_i P_i c_i^2}{L_i(M+\Delta M, N+\Delta N)} . \tag{4.8}$$

So

$$0 = (\Delta N b_n - \Delta M b_m) \cdot \sum_i \frac{f_i P_i c_i^2}{L_i(M+\Delta M, N+\Delta N)} , \tag{4.9}$$

Since the summation is always positive,

$$\Delta N b_n - \Delta M b_m = 0 , \tag{4.10}$$

$$R^f(N/M) = \frac{\Delta M}{\Delta N} = \frac{b_n}{b_m} . \tag{4.11}$$

Appendix V

Physical Interpretation of $RT^2 \frac{\partial \log R^0(N/M)}{\partial T}$

The most general possible form of the Lindemann mechanism is

$$\begin{aligned} A_j + M_k &\rightarrow A_i^* + M_\ell \qquad a^m_{jki\ell}, \\ A_i^* + M_\ell &\rightarrow A_j + M_k \qquad b^m_{jki\ell}, \\ A_i^* &\rightarrow \text{Products} \qquad c_i, \end{aligned} \tag{5.1}$$

where the subscripts denote quantum states of the molecules involved. The rate of disappearance of A is given by

$$\frac{-dA}{dt} = K_m A = \sum_i c_i A_i^*. \tag{5.2}$$

If one makes the steady state assumption $\frac{dA_i^*}{dt} = 0$, an expression can be obtained for A_i^*:

$$0 = \sum_{j,k,\ell} \left(a^m_{jki\ell} A_j M_k \right) - \sum_{j,k,\ell} \left(b^m_{jki\ell} M_\ell A_i^* \right) - c_i A_i^*.$$

So

$$A_i^* = \frac{\sum_{j,k,\ell} \left(a^m_{jki\ell} A_j M_k \right)}{\sum_{j,k,\ell} \left(b^m_{jki\ell} M_\ell \right) + c_i}. \tag{5.3}$$

Therefore

$$K_m = \frac{1}{A} \sum_i \frac{c_i \sum_{j,k,\ell} \left(a^m_{jki\ell} A_j M_k \right)}{\sum_{j,k,\ell} \left(b^m_{jki\ell} M_\ell \right) + c_i}. \tag{5.4}$$

Denote $\frac{A_j}{A}$ by P_j^a, $\frac{M_k}{M}$ by P_k^m, etc. Then

$$K_m = \sum_i \frac{c_i \sum_{j,k,\ell} \left(a^m_{jki\ell} P_j^a P_k^m \right) M}{\sum_{j,k,\ell} \left(b^m_{jki\ell} P_\ell^m \right) M + c_i} . \tag{5.5}$$

The quantities a^m_{jkil}, b^m_{jkil}, and c_i are truly constant -- they contain no dependence on temperature or on rate of reaction. The P's, however, may depend on both of these variables. It is assumed that averages over the states of M and over the nonreactive states of A (i.e., over the index j) are equilibrium averages, so that the quantities P_j^a are given by the equation

$$P_j^a = \frac{\exp\left(-\epsilon_j^a/kT\right)}{\sum_g \exp\left(-\epsilon_g^a/kT\right)} , \tag{5.6}$$

with a similar formula for P_ℓ^m.

Consider the low-pressure limit, at which $\sum_{j,k,\ell} \left(b^m_{jki\ell} P_\ell^m \right) M \ll c_i$ for all i. In this region

$$\begin{aligned} K_m &= M \sum_{j,k,i,\ell} a^m_{jki\ell} P_j^a P_k^m , \\ K_n &= N \sum_{j,k,\ell} a^n_{jki\ell} P_j^a P_k^n . \end{aligned} \tag{5.7}$$

Therefore

$$R^\circ(N/M) = \frac{\sum_{j,k,i,\ell} a^n_{jki\ell} P_j^a P_k^n}{\sum_{j,k,\ell} a^m_{jki\ell} P_j^a P_k^m} . \tag{5.8}$$

Denote

$$\sum_{i,\ell} a^{n}_{jki\ell} \quad \text{by} \quad a^{n}_{jk} \,, \qquad \sum_{i,\ell} a^{m}_{jki\ell} \quad \text{by} \quad a^{m}_{jk} \,. \tag{5.9}$$

On substituting 5.9 and 5.6 in 5.8, one finds

$$R^{\circ}(N/M) = \frac{\sum_{j,k,\ell} \exp\left[-\left(\epsilon_j^{a}+\epsilon_k^{n}+\epsilon_\ell^{n}\right)/kT\right] a^{n}_{jk}}{\sum_{j,k,\ell} \exp\left[-\left(\epsilon_j^{a}+\epsilon_k^{m}+\epsilon_\ell^{n}\right)/kT\right] a^{m}_{jk}} \,. \tag{5.10}$$

If one then differentiates log $R^{\circ}(N/M)$ with respect to 1/T, one finds, after regrouping terms, that

$$\frac{\partial \log R^{\circ}(N/M)}{\partial \frac{1}{T}} = \frac{1}{k}\left\{ \frac{-\sum_\ell P_\ell^{m} \sum_{j,k} \left(\epsilon_j^{a}+\epsilon_k^{n}\right) P_j^{a} P_k^{n} a^{n}_{jk} - \sum_\ell P_\ell^{m} \epsilon_\ell^{m} \sum_{j,k} P_j^{a} P_k^{n} a^{n}_{jk}}{\sum_\ell P_\ell^{m} \sum_{j,k} P_j^{a} P_k^{m} a^{n}_{jk}} \right. \tag{5.11}$$

$$\left. + \frac{\sum_\ell P_\ell^{n} \sum_{j,k} \left(\epsilon_j^{a}+\epsilon_k^{m}\right) P_j^{a} P_k^{m} a^{m}_{jk} + \sum_\ell P_\ell^{n} \epsilon_\ell^{n} \sum_{j,k} P_j^{a} P_k^{m} a^{m}_{jk}}{\sum_\ell P_\ell^{n} \sum_{j,k} P_j^{a} P_k^{m} a^{m}_{jk}} \right\}$$

where k is the gas constant.

Equation 5.11 can be rewritten in the following way by making use of the definition of an average:

$$\frac{\partial \log R^{\circ}(N/M)}{\partial \frac{1}{T}} = \frac{1}{k}\left\{ -\left[\langle \epsilon^{a}+\epsilon^{n} \rangle^{*} - \langle \epsilon^{a}+\epsilon^{n} \rangle^{e} \right] \right. \tag{5.12}$$

$$\left. + \left[\langle \epsilon^{a}+\epsilon^{m} \rangle^{*} - \langle \epsilon^{a}+\epsilon^{m} \rangle^{e} \right] \right\} .$$

$\langle\ \rangle^{*}$ indicates averaging over the distribution of the molecules which get activated, and $\langle\ \rangle^{e}$ denotes averaging over the equilibrium distributions.

Appendix VI

Computation of the Quantities ℓ_{ma}

A. Amdur's Potential

Amdur's potential is of the form

$$V_1 = \frac{a}{r^b} \tag{6.1}$$

where r is the intermolecular distance, and a and b are experimentally determined constants. It is desired to match this function and its slope to the exponential potential

$$V_2 = H e^{-r/\ell} \tag{6.2}$$

at a given value E of the potential energy. In particular, one would like to determine ℓ in terms of a, b and E.

$$\left.\frac{-V_1}{\frac{dV_1}{dr}}\right|_{V_1=E} = \left.\frac{-V_2}{\frac{dV_2}{dr}}\right|_{V_2=E} = \ell, \tag{6.3}$$

since $\left.\frac{dV_1}{dr}\right|_{E=V_1} = \left.\frac{dV_2}{dr}\right|_{E=V_2}$ and $V_1 = V_2 = E$.

So

$$\ell = \frac{1}{b}\left(\frac{a}{E}\right)^{\frac{1}{b}} = \frac{r'}{b}, \text{ where } r' = \left(\frac{a}{E}\right)^{1/b}. \tag{6.4}$$

B. Lennard-Jones 6-12 Potential

The Lennard-Jones 6-12 potential is of the form

$$V_1 = 4\epsilon\left[\left(\frac{\sigma}{r}\right)^{12} - \left(\frac{\sigma}{r}\right)^{6}\right] \tag{6.5}$$

where r is the intermolecular distance, σ is a collision diameter, and

ϵ is the depth of the potential well.

As above,

$$\left.\frac{-V_1}{\frac{dV_1}{dr}}\right|_{V_1=E} = \left.\frac{-V_2}{\frac{dV_2}{dr}}\right|_{V_2=E} = \ell , \tag{6.3}$$

$$\ell = \frac{r'}{6}\,\frac{\left[\left(\frac{\sigma}{r'}\right)^6 - 1\right]}{\left[2\left(\frac{\sigma}{r'}\right)^6 - 1\right]} , \tag{6.6}$$

where $V_1(r') \equiv E$ and

$$r' = \left[\frac{2}{1+\sqrt{1+E/\epsilon}}\right]^{1/6}\sigma . \tag{6.7}$$

Alternatively,

$$\ell = \frac{\left[\frac{2}{1+\sqrt{1+E/\epsilon}}\right]^{1/6}\left[\sqrt{1+E/\epsilon}-1\right]}{12\sqrt{1+E/\epsilon}} . \tag{6.8}$$

Appendix VII

Temperature Gradients in Reaction Cells

Benson (43) has pointed out the importance of considering the magnitudes of temperature gradients in reaction cells, and has derived a formula for estimating the maximum temperature difference in a spherical cell. His work, however, neglected the temperature dependence of the rate of the reaction being studied. In this appendix formulas are developed for cylinders, slabs, and spheres; and the temperature dependence of the reaction rate is taken into account.

A. Temperature Gradients in a Cylindrical Cell

Consider a cylindrical cell of radius a and length 2h in which chemical reaction is occurring. It is desired to compute an upper limit for the maximum temperature difference between the cell walls and the interior of the cell.

If one assumes that heat is transferred by conduction only, the differential equation governing the temperature in a reacting mixture is (43)

$$\frac{\partial T}{\partial t} = \frac{K \nabla^2 T}{\rho C_v} + \frac{\mathcal{R} H}{\rho C_v} \qquad (7.1)$$

where K = coefficient of thermal conductivity,

ρ = density,

C_v = specific heat per unit mass,

$\mathcal{R}$ = specific rate of reaction, and

H = heat of reaction.

Consider the steady state case, where $\frac{\partial T}{\partial t} = 0$; and assume that $\mathcal{R}$ is independent of time. Also assume that K, E, and H are independent

of T.

$$\begin{aligned} \mathcal{R} &= f\,(\text{concentrations}) \cdot e^{-E/RT} \\ &= A'' e^{-E/RT} \end{aligned} \tag{7.2}$$

where A" is a constant, E is the activation energy, and R and T have their usual meaning.

If one expands $\mathcal{R}$ in a Taylor's series about T_o, the cell wall temperature, and neglects terms of order $(T - T_o)^2$ and higher, one finds that

$$\mathcal{R} = A'' e^{-E/RT_o}\left(1 + \frac{E}{RT_o^2}\tau\right), \tag{7.3}$$

where $\tau = T - T_o$. The physical assumption made here is that $\frac{\tau E}{RT_o^2} \ll 1$. Then $\mathcal{R} = A' + B'\tau$, where $A' = A'' e^{-E/RT_o}$ and $B' = \frac{A'' E\, e^{-E/RT_o}}{RT_o^2}$. The steady-state equation

$$K\nabla^2 T + \mathcal{R}H = 0, \qquad T = T_o \text{ on the boundary} \tag{7.4}$$

becomes

$$\nabla^2\tau + \frac{HA'}{K} + \frac{HB'\tau}{K} = 0, \tag{7.5}$$

$$\tau = 0 \text{ on the boundary.}$$

If one lets $\tau_1 = \tau + \frac{A'}{B'} = \tau + \frac{RT_o^2}{E}$,

then

$$\nabla^2\tau_1 + \frac{HA'E}{KRT_o^2} e^{-E/RT_o}\tau_1 = 0 \tag{7.6}$$

and $\tau_1 = \frac{RT_o^2}{E}$ on the boundary. Define $\beta = \frac{H\mathcal{R}(T_o)E}{KRT_o^2}$

Then 7.6 becomes

$$\nabla^2\tau_1 + \beta\tau_1 = 0. \tag{7.7}$$

In cylindrical coordinates and in the absence of ϕ - dependence, the differential equation 7.7 is

$$\frac{\partial^2 \tau_1}{\partial r^2} + \frac{1}{r}\frac{\partial \tau_1}{\partial r} + \frac{\partial^2 \tau_1}{\partial z^2} + \beta \tau_1 = 0 . \tag{7.8}$$

If one assumes $\tau_1 = R(r) \cdot Z(z)$, this equation can be separated into two ordinary differential equations:

$$R'' + \frac{1}{r} R' + \lambda R = 0 \tag{7.9}$$

and

$$Z'' - (\lambda - \beta) Z = 0 . \tag{7.10}$$

In the limiting case of an infinitely long cell, $\tau_1 = R(r)$, and equation 7.8 becomes

$$R'' + \frac{1}{r} R' + \beta R = 0 . \tag{7.11}$$

Solutions to this equation which satisfy the boundary condition are

$$\tau_1 = \frac{R T_0^2}{E} \frac{J_0(\sqrt{\beta}\, r)}{J_0(\sqrt{\beta}\, a)} , \quad \beta > 0 \tag{7.12}$$

and

$$\tau_1 = \frac{R T_0^2}{E} \frac{I_0(\sqrt{-\beta}\, r)}{I_0(\sqrt{-\beta}\, a)} , \quad \beta < 0 \tag{7.13}$$

where $J_0(x)$ and $I_0(x)$ are the Bessel function and the modified Bessel function of zeroth order and first kind.

So

$$\tau = \frac{R T_0^2}{E} \left[\frac{J_0(\sqrt{\beta}\, r)}{J_0(\sqrt{\beta}\, a)} - 1 \right] , \quad \beta > 0 \tag{7.14}$$

$$\tau = \frac{R T_0^2}{E} \left[\frac{I_0(\sqrt{-\beta}\, r)}{I_0(\sqrt{-\beta}\, a)} - 1 \right] , \quad \beta < 0 ; \tag{7.15}$$

and

$$\tau^* = \frac{RT_0^2}{E}\left[\frac{1}{J_0(\sqrt{\beta}a)} - 1\right], \beta > 0, \tag{7.16}$$

$$\tau^* = -\frac{RT_0^2}{E}\left[1 - \frac{1}{I_0(\sqrt{-\beta}a)}\right], \beta < 0, \tag{7.17}$$

where $|\tau^*|$ is the maximum difference between the temperature at the wall and the temperature at an interior point.

For small values of the argument,

$$J_0(x) \cong 1 - \frac{x^2}{4} + \frac{x^4}{64}, \tag{7.18}$$

$$I_0(x) \cong 1 + \frac{x^2}{4} + \frac{x^4}{64}; \tag{7.19}$$

and

$$\frac{1}{J_0(x)} \cong 1 + \frac{x^2}{4} + \frac{3}{64}x^4, \tag{7.20}$$

$$\frac{1}{I_0(x)} \cong 1 - \frac{x^2}{4} + \frac{3}{64}x^4. \tag{7.21}$$

So

$$\tau^* \cong \frac{H\mathcal{R}(T_0)a^2}{4K}\left[1 + \frac{3}{16}\frac{H\mathcal{R}(T_0)Ea^2}{KRT_0^2}\right]. \tag{7.22}$$

If one considers the steady-state case where $\mathcal{R}$, K, E, and H do not depend on T, the equation for an infinitely long cylinder is

$$\frac{d^2T}{dr^2} + \frac{1}{r}\frac{dT}{dr} + \frac{\mathcal{R}H}{K} = 0,$$

or

$$\frac{d}{dr}(rT') + \frac{\mathcal{R}Hr}{K} = 0. \tag{7.23}$$

Integrate from 0 to r and divide by r:

$$T' + \frac{r}{2}\frac{RH}{K} = 0. \tag{7.24}$$

Integrate from 0 to r:

$$T(r) - T(0) = -\frac{r^2 RH}{4K}, \tag{7.25}$$

and

$$T(r) = T_0 + \frac{RH}{4K}(a^2 - r^2), \tag{7.26}$$

$$\tau^* = \frac{a^2 RH}{4K}. \tag{7.27}$$

In the case of a cell of length 2h,

$$R'' + \frac{1}{r}R' + \lambda R = 0, \tag{7.9}$$

$$Z'' - (-\beta + \lambda)Z = 0. \tag{7.10}$$

So

$$R_n = J_0(\sqrt{\lambda_n}\, r), \tag{7.28}$$
$$Z_n = \cos k(\sqrt{-\beta + \lambda_n}\, z)$$

give one set of solutions, the parameter of which can be chosen to cause the solutions to vanish at r = a. If one lets $\lambda = -\alpha + \beta$, equations 7.9 and 7.10 become

$$R'' + \frac{1}{r}R' - (\alpha - \beta)R = 0, \tag{7.29}$$

$$Z'' + \alpha Z = 0. \tag{7.30}$$

So

$$R_n = I_0(\sqrt{\alpha_n - \beta}\, r), \tag{7.31}$$
$$Z_n = \cos(\sqrt{\alpha_n}\, z)$$

give another set of solutions, the parameter of which can be chosen to cause the solutions to vanish at $z = \pm h$.

These two sets of solutions, one set vanishing on the side of the cylinder and the other vanishing on the ends, are then used to construct τ_1 .

Consider solution 7.28. Choose λ_n such that $J_0(\sqrt{\lambda_n}\, a) = 0$.

$$\tau_{11} = \sum_{n=1}^{\infty} A_n J_0(\sqrt{\lambda_n}\, r) \cosh(\sqrt{-\beta+\lambda_n}\, z), \tag{7.32}$$

$$\tau_{11}(r, \pm h) = \sum_{n=1}^{\infty} A_n J_0(\sqrt{\lambda_n}\, r) \cosh(\sqrt{-\beta+\lambda_n}\, h) = \frac{R T_0^2}{E}. \tag{7.33}$$

From reference (44), p. 164,

$$A_n \cosh(\sqrt{-\beta+\lambda_n}\, h) = \frac{R T_0^2}{E} \cdot \frac{z}{a} \cdot \frac{1}{\sqrt{\lambda_n}\, J_1(\sqrt{\lambda_n}\, a)}, \tag{7.34}$$

So

$$\tau_{11} = \frac{2 R T_0^2}{E a} \sum_{n=1}^{\infty} \frac{J_0(\sqrt{\lambda_n}\, r) \cosh(\sqrt{-\beta+\lambda_n}\, z)}{\sqrt{\lambda_n}\, J_1(\sqrt{\lambda_n}\, a) \cosh(\sqrt{-\beta+\lambda_n}\, h)}. \tag{7.35}$$

Consider solution 7.31. Choose α_n such that $Z(\pm h) = 0$. Then

$$R_n = I_0(\sqrt{\alpha_n - \beta}\, r), \quad Z_n = \cos(\sqrt{\alpha_n}\, z) \tag{7.31}$$

where

$$\alpha_n = \frac{(2n-1)^2 \pi^2}{4h^2}.$$

Then

$$\frac{R T_0^2}{E} = \sum_{n=1}^{\infty} B_n I_0(\sqrt{\alpha_n - \beta}\, a) \cos(\sqrt{\alpha_n}\, z), \tag{7.36}$$

and (44)

$$\beta_n I_0(\sqrt{\alpha_n-\beta}\,a) = \frac{RT_0^2}{E}\cdot\frac{4}{\pi}\cdot\frac{(-1)^{n-1}}{(2n-1)}. \tag{7.37}$$

Therefore

$$\tau_{12} = \frac{RT_0^2}{E}\cdot\frac{4}{\pi}\sum_{n=1}^{\infty}\frac{(-1)^{n-1}}{(2n-1)}\cdot\frac{I_0(\sqrt{\alpha_n-\beta}\,r)\cos(\sqrt{\alpha_n}\,z)}{I_0(\sqrt{\alpha_n-\beta}\,a)}. \tag{7.38}$$

Now

$$\tau = \tau_{11}+\tau_{12}-\frac{RT_0^2}{E} = \tau_1-\frac{RT_0^2}{E}; \tag{7.39}$$

so

$$\tau = \frac{RT_0^2}{E}\left\{-1+2\sum_{n=1}^{\infty}\frac{J_0(\sqrt{\lambda_n}\,r)\cosh(\sqrt{-\beta+\lambda_n}\,z)}{a\sqrt{\lambda_n}\,J_1(\sqrt{\lambda_n}\,a)\cosh(\sqrt{-\beta+\lambda_n}\,h)}\right.$$
$$\left.+\frac{4}{\pi}\sum_{n=1}^{\infty}\frac{(-1)^{n-1}I_0(\sqrt{\alpha_n-\beta}\,r)\cos(\sqrt{\alpha_n}\,z)}{(2n-1)\,I_0(\sqrt{\alpha_n-\beta}\,a)}\right\}. \tag{7.40}$$

τ^* is then obtained by setting $r = z = 0$.

This solution is valid only when all of the following conditions are fulfilled:

(a). $$\left|\frac{H\,\mathcal{R}(T_0)E}{K\,RT_0^2}\right| < \frac{x_1^2}{a^2}, \frac{\pi^2}{4h^2}, \tag{7.41}$$

where $x_1 = 2.405$ is the first root of $J_0(x)$;

(b). $$|\tau^*| \ll \frac{RT_0^2}{E}; \tag{7.42}$$

and (c). H, K and E are independent of temperature.

B. Temperature Gradients in an Infinite Slab of Width 2a

In this case the differential equation 7.4 is

$$\frac{d^2\tau}{dx^2} + \frac{\mathcal{R}H}{K} = 0, \tag{7.43}$$

If one assumes that K, $\mathcal{R}$, H and E are independent of T, this equation can be integrated twice and the boundary conditions fitted to give

$$\tau(x) = \frac{\mathcal{R}H(a^2-x^2)}{2K}, \quad \tau^* = \frac{\mathcal{R}Ha^2}{2K} \tag{7.44}$$

If one takes

$$\mathcal{R} \cong A' + B'\tau, \tag{7.45}$$

as was done in the first part of A above, the differential equation to be solved is

$$\frac{d^2\tau}{dx^2} + \frac{H}{K}(A' + B'\tau) = 0, \qquad \tau(\pm a) = 0. \tag{7.46}$$

Let $\tau_1 = \tau + \frac{A'}{B'}$, $\tau_1(\pm a) = \frac{A'}{B'} = \frac{RT_0^2}{E}$.

Then

$$\frac{d^2\tau_1}{dx^2} + \beta\tau_1 = 0. \tag{7.47}$$

So

$$\tau_1 = c\cos\sqrt{\beta}\,x, \quad \beta = \frac{H\,\mathcal{R}(T_0)E}{KRT_0^2}. \tag{7.48}$$

Fitting the boundary condition, one finds

$$\tau = \frac{RT_0^2}{E}\left[\frac{\cos(\sqrt{\beta}\,x)}{\cos(\sqrt{\beta}\,a)} - 1\right], \tag{7.49}$$

$$\tau^* = \frac{RT_0^2}{E}\left[\frac{1}{\cos(\sqrt{\beta}\,a)} - 1\right]$$

for $\beta > 0$; and

$$\tau = -\frac{RT_0^2}{E}\left[1 - \frac{\cosh(\sqrt{-\beta}\,x)}{\cosh(\sqrt{-\beta}\,a)}\right],$$

$$\tau^* = -\frac{RT_0^2}{E}\left[1 - \frac{1}{\cosh(\sqrt{-\beta}\,a)}\right] \tag{7.50}$$

for $\beta < 0$.

If one expands either 7.49 or 7.50 in powers of βa^2, one finds the approximate formula

$$\tau^* = \frac{H\mathcal{R}(T_0)a^2}{2K}\left[1 + \frac{5}{12}\,\frac{HE\mathcal{R}(T_0)a^2}{KRT_0^2}\right]. \tag{7.51}$$

C. Temperature Gradients in a Spherical Cell of Radius a (43, 45)

Benson (43) finds, for the case where $\mathcal{R}$, H and K are independent of temperature,

$$\tau = \frac{\mathcal{R}H}{6K}(a^2 - r^2),$$
$$\tau^* = \frac{\mathcal{R}H}{6K}a^2. \tag{7.52}$$

If one takes

$$\mathcal{R} \cong A' + B'\tau, \tag{7.45}$$

as was done previously, the differential equation to be solved is

$$\frac{1}{r^2}\frac{d}{dr}\left(r^2\frac{d\tau}{dr}\right) + \frac{H}{K}\left[A' + B'\tau\right] = 0 \tag{7.53}$$

Let $\tau_1 = \tau + \frac{RT_0^2}{E}$, $\tau_1(a) = \frac{RT_0^2}{E}$.

Then

$$\frac{d}{dr}\left(r^2\frac{d\tau_1}{dr}\right) + \beta r^2\tau_1 = 0. \tag{7.54}$$

Assume a solution of the form

$$\tau_1 = \sum_{n=0}^{\infty} a_n r^n. \tag{7.55}$$

It is then found that

$$a_{2n} = \frac{(-\beta)^n a_0}{(2n+1)!}, \quad a_{2n+1} = 0. \tag{7.56}$$

From this it is apparent that

$$\tau_1 = C \frac{\sin(\sqrt{\beta}\, r)}{r} \text{ or } \tau_1 = C \frac{\sinh(\sqrt{-\beta}\, r)}{r}. \tag{7.57}$$

After fitting the boundary conditions, one finds

$$\tau = \frac{R T_0^2}{E}\left[\frac{a}{r}\frac{\sin(\sqrt{\beta}\, r)}{\sin(\sqrt{\beta}\, a)} - 1\right], \ \beta > 0,$$
$$\tau = \frac{R T_0^2}{E}\left[\frac{a}{r}\frac{\sinh(\sqrt{-\beta}\, r)}{\sinh(\sqrt{-\beta}\, a)} - 1\right], \ \beta < 0, \tag{7.58}$$

If one sets $r = 0$ and expands $\tau(0)$ in powers of βa^2, one finds

$$\tau^* \cong \frac{R(T_0) H a^2}{6K}\left[1 + \frac{7}{60}\frac{H E R(T_0) a^2}{R T_0^2 K}\right] \tag{7.59}$$

for all β.

Appendix VIII

Experimental Data

This appendix contains the experimental data of this investigation. Plots of k versus M are shown in figures 7 through 25.

Table IV lists the rate constants, corrected for reactant gas effect, obtained in this investigation, and the experimental conditions under which they were obtained. The column in Table IV labeled M contains the concentrations of foreign gas in units of 10^{-8} mol/cc. The column labeled $\underline{M}$ contains the equivalent concentration of foreign gas $\left[R^{o}(M/NO_2Cl) \cdot M \right]$ in the same units. Volpe's values (6) of $R^{o}(M/NO_2Cl)$ were used.

FIGURE 7

Plot of k versus M.
NO_2Cl alone at 205°C.

⊢——+——⊣ Cordes' work

\+ Runs made after exposure of the cell to air

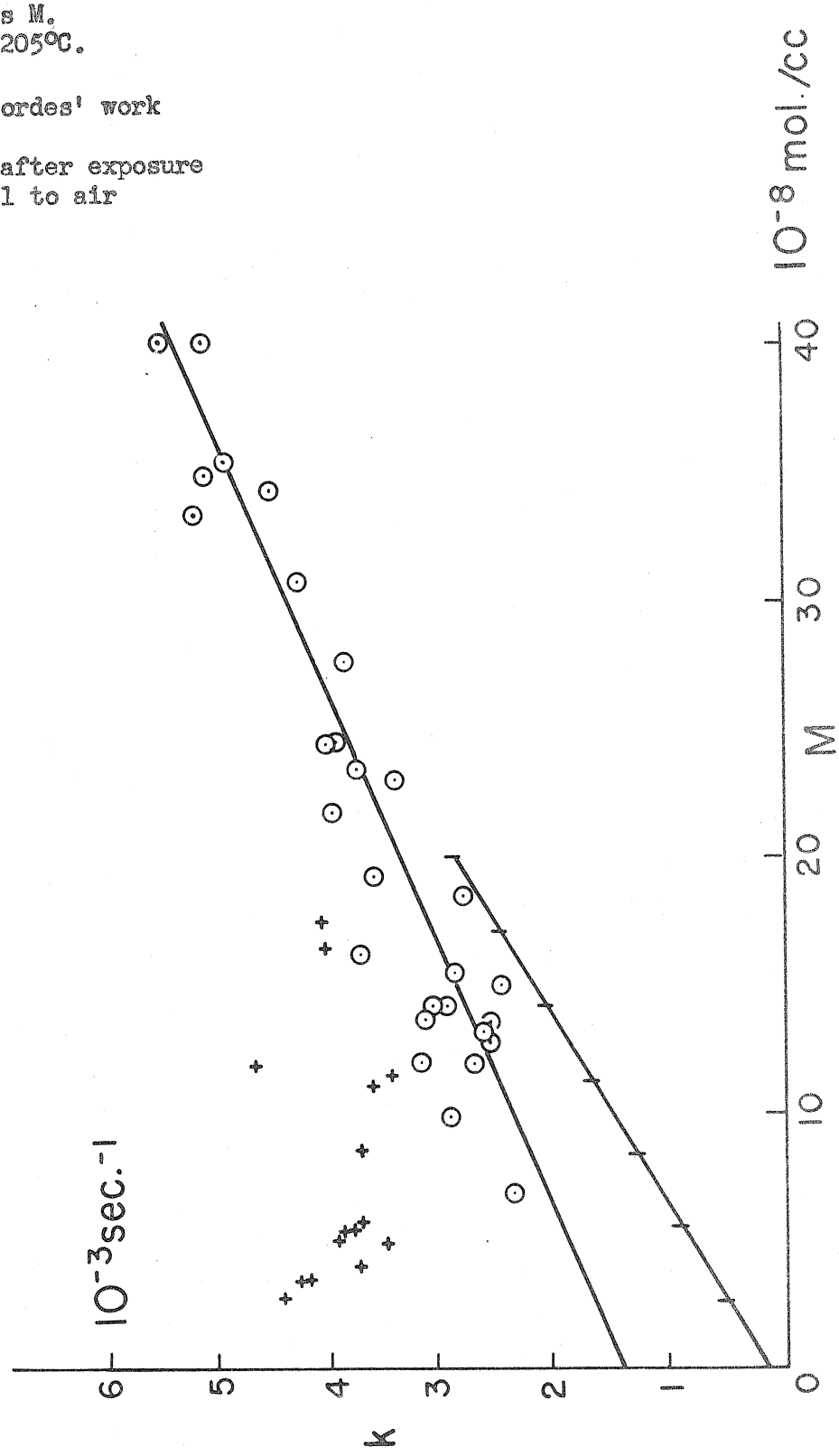

FIGURE 8

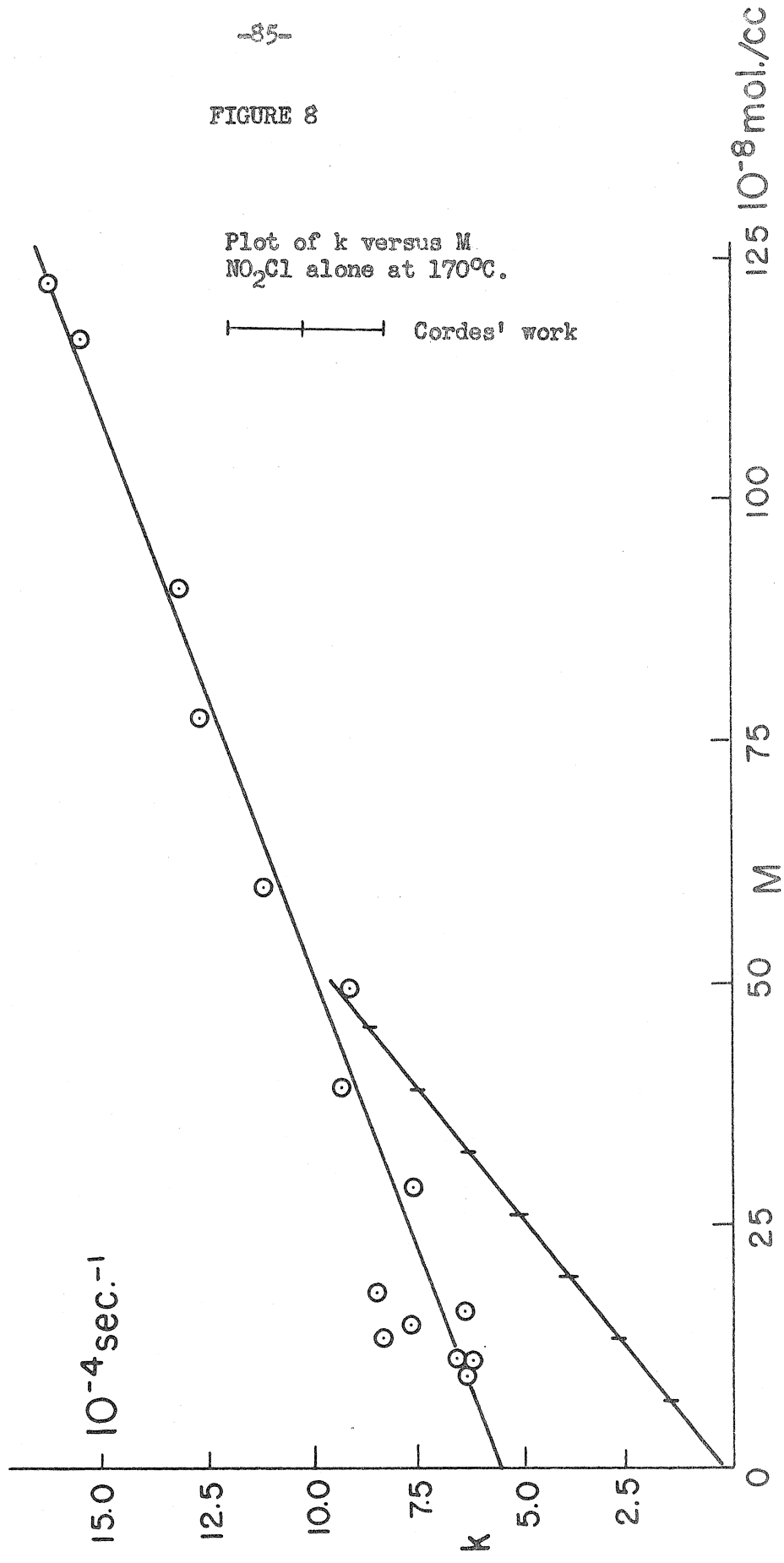
Plot of k versus M
NO_2Cl alone at 170°C.
Cordes' work
k
10^{-4} sec.$^{-1}$
15.0
12.5
10.0
7.5
5.0
2.5
0
25
50
75
100
125
M
10^{-8} mol./cc

FIGURE 9

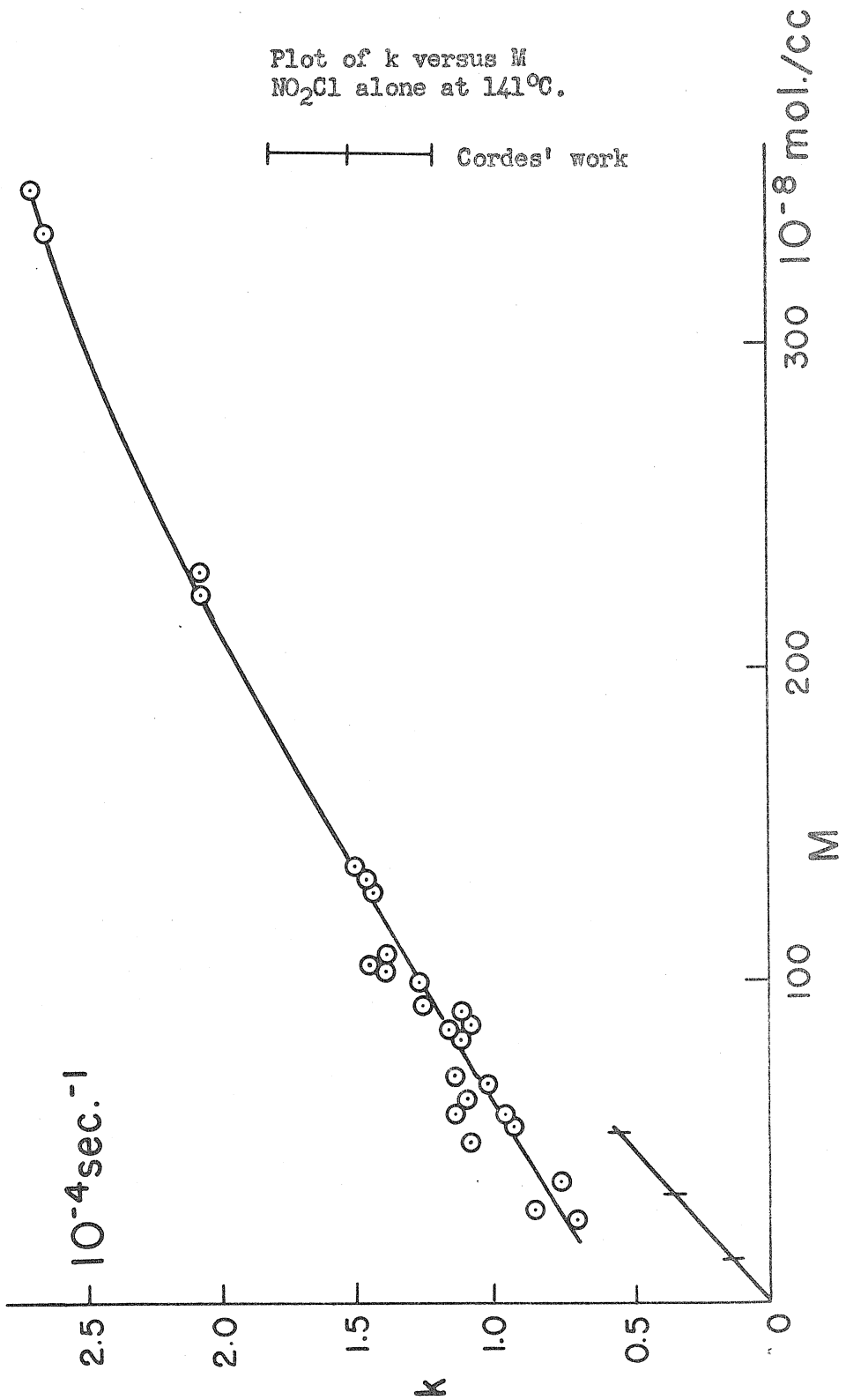
Plot of k versus M
NO_2Cl alone at 141°C.
Cordes' work
k
10^{-4} sec.$^{-1}$
2.5
2.0
1.5
1.0
0.5
0
100
200
300
M
10^{-8} mol./cc

FIGURE 10

Plot of k versus M
CO_2 and NO_2Cl at 205°C.

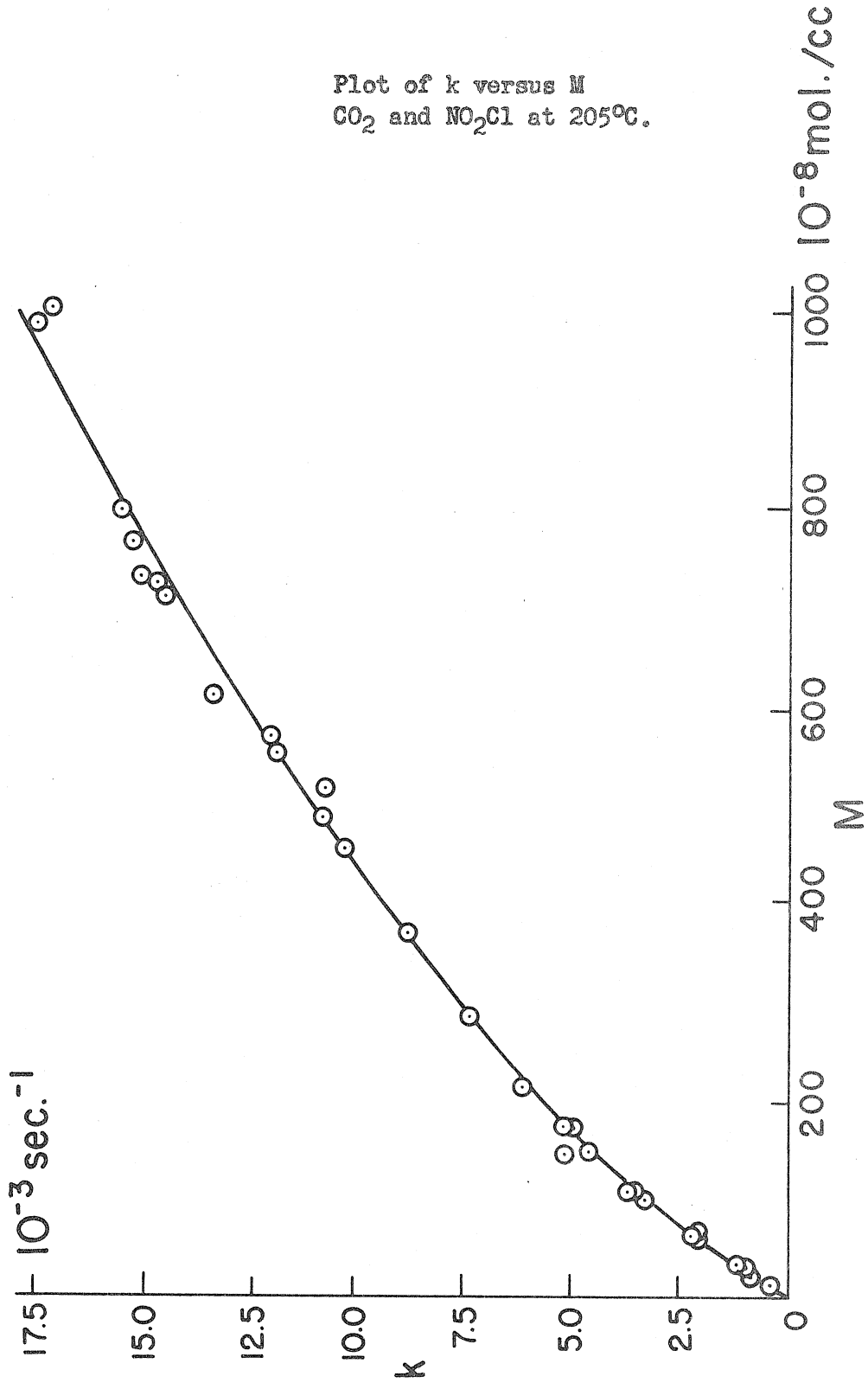

FIGURE 11

Plot of k versus M
CO and NO_2Cl at 205°C.

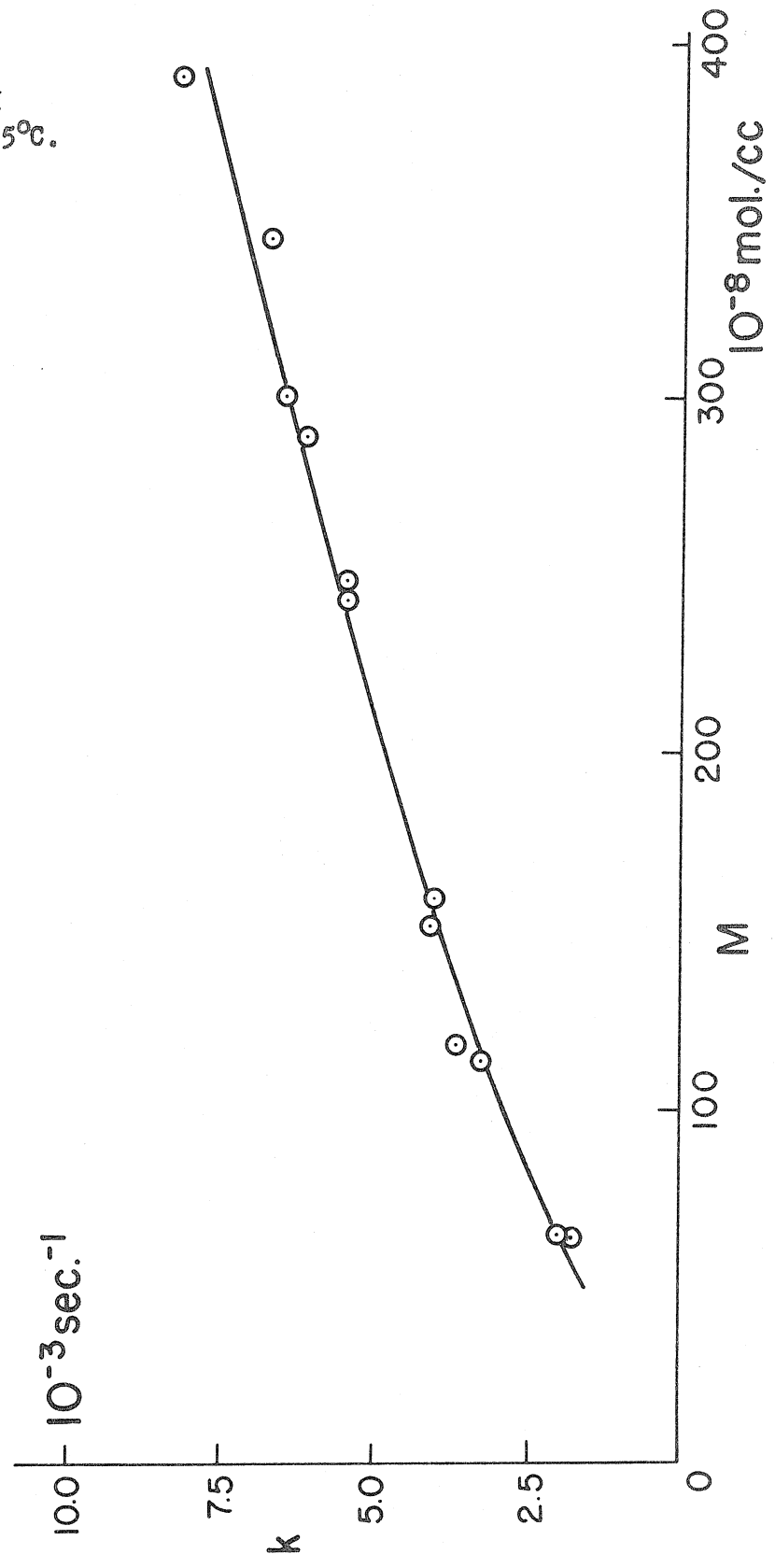

FIGURE 12

Plot of k versus M
He and NO_2Cl at 205°C.

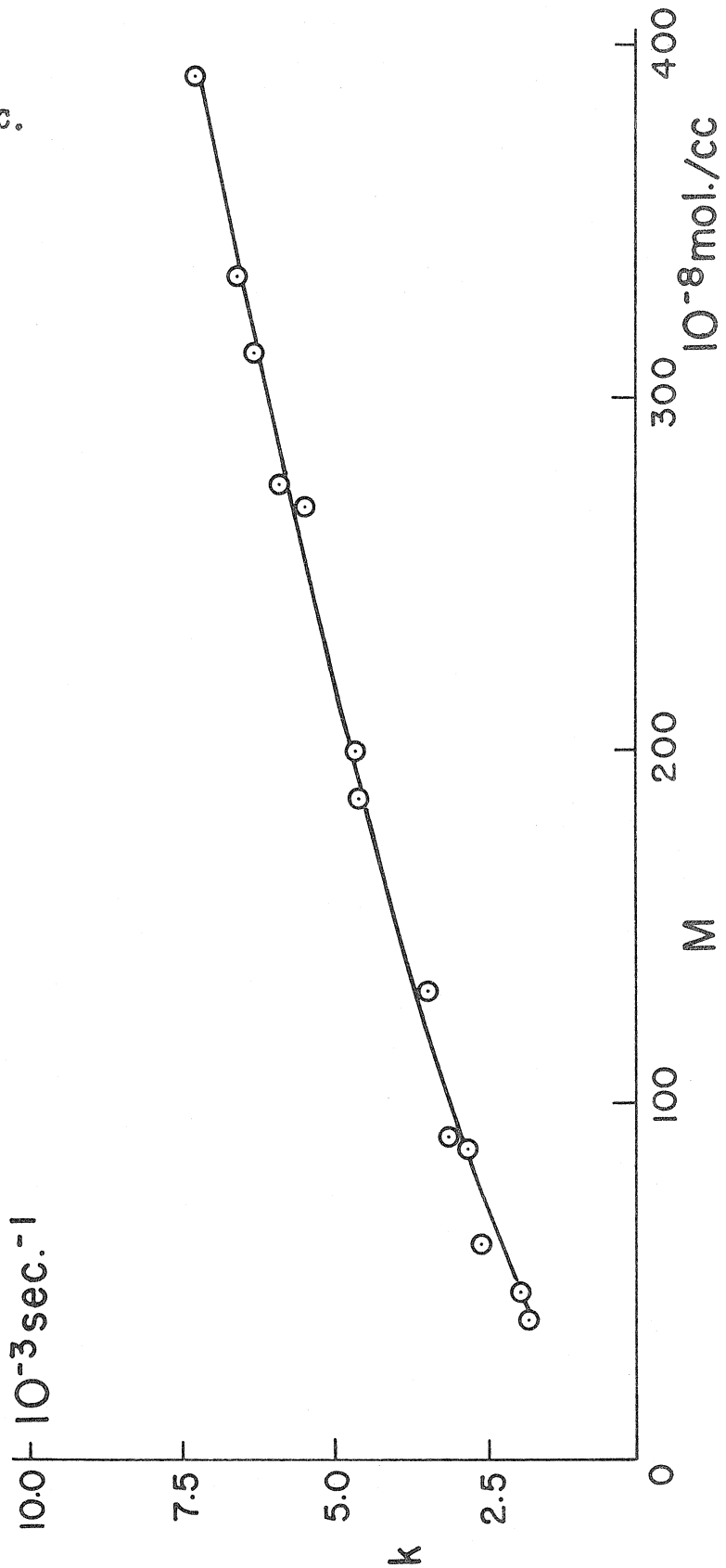

FIGURE 13

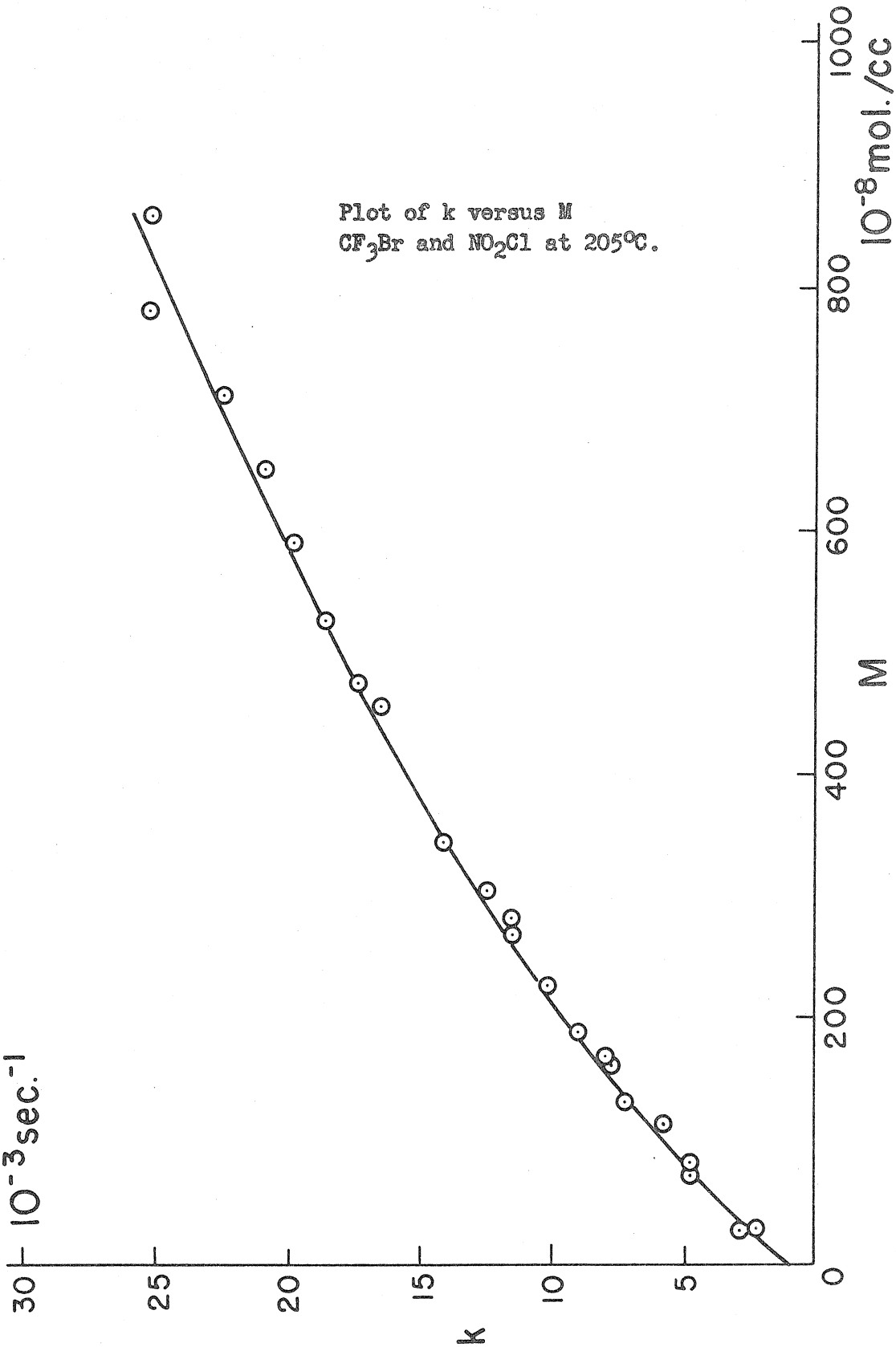
Plot of k versus M
CF_3Br and NO_2Cl at 205°C.
k
10^{-3} sec.$^{-1}$
M
10^{-8} mol./cc
0
5
10
15
20
25
30
200
400
600
800
1000

FIGURE 14

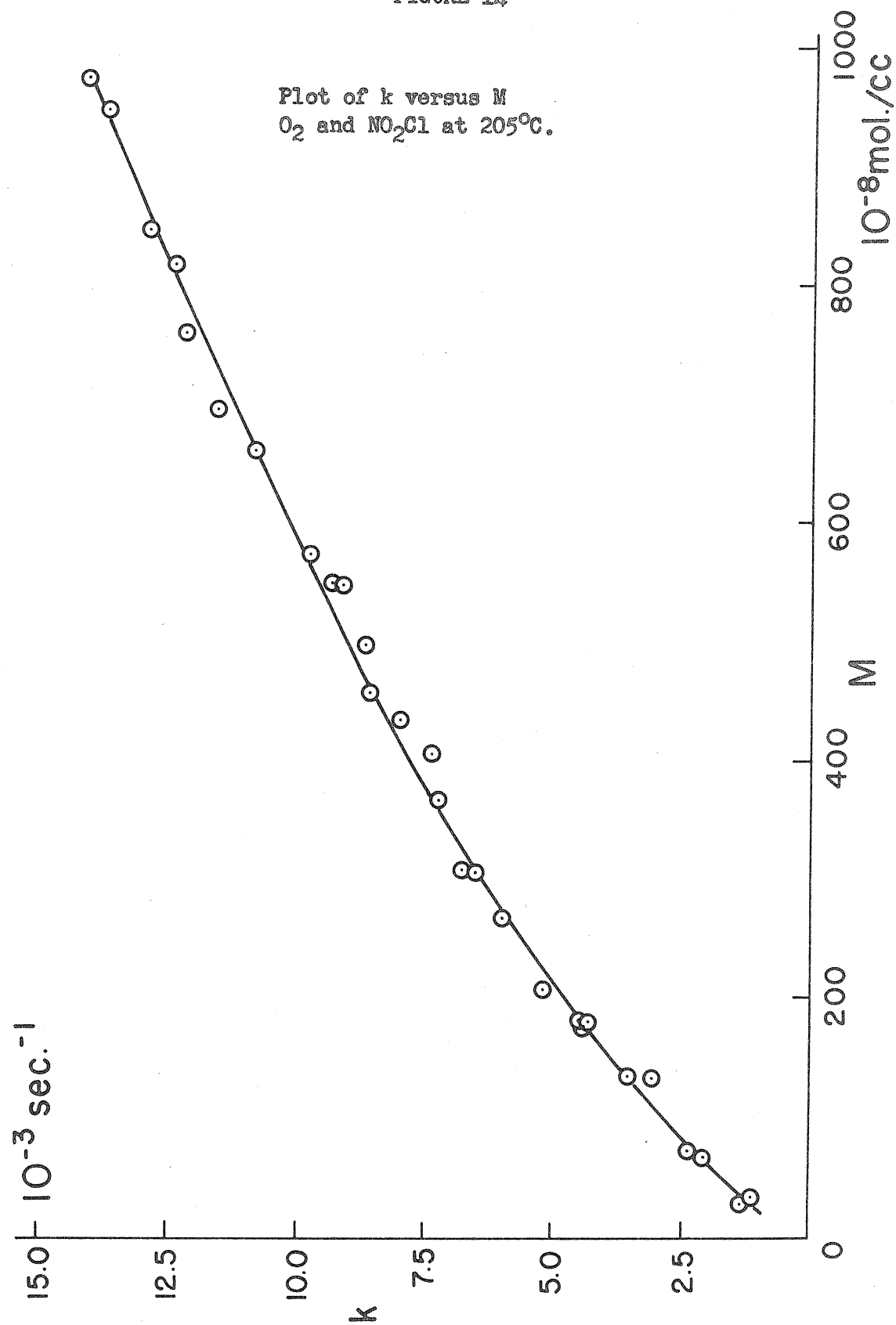
Plot of k versus M
O_2 and NO_2Cl at 205°C.
15.0
12.5
10.0
7.5
5.0
2.5
k
10^{-3} sec.$^{-1}$
0
200
400
600
800
1000
M
10^{-8}mol./cc

FIGURE 15

Plot of k versus M
CCl_4 and NO_2Cl at 205°C.

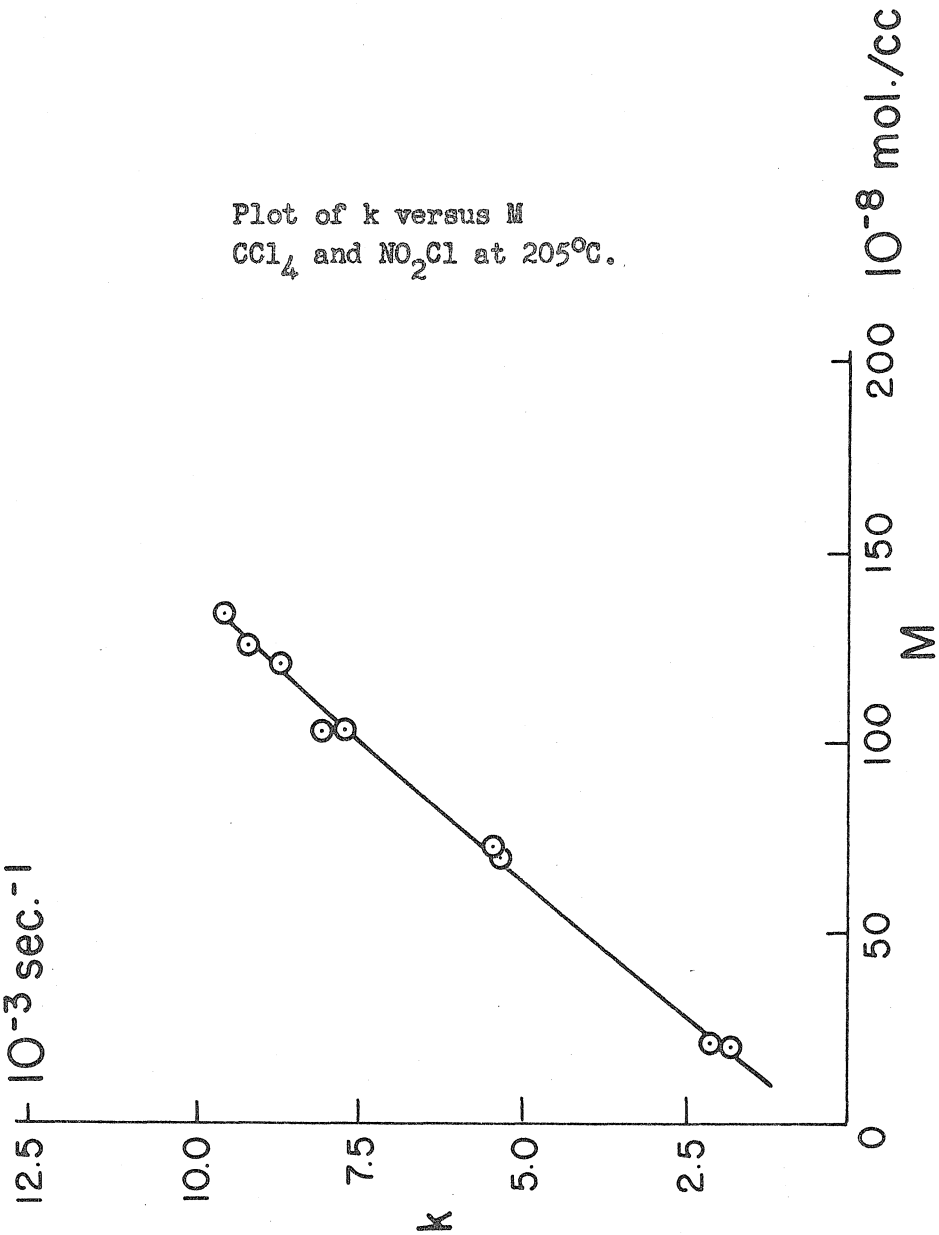

FIGURE 16

Plot of k versus M
$CClF_3$ and NO_2Cl at 205°C.

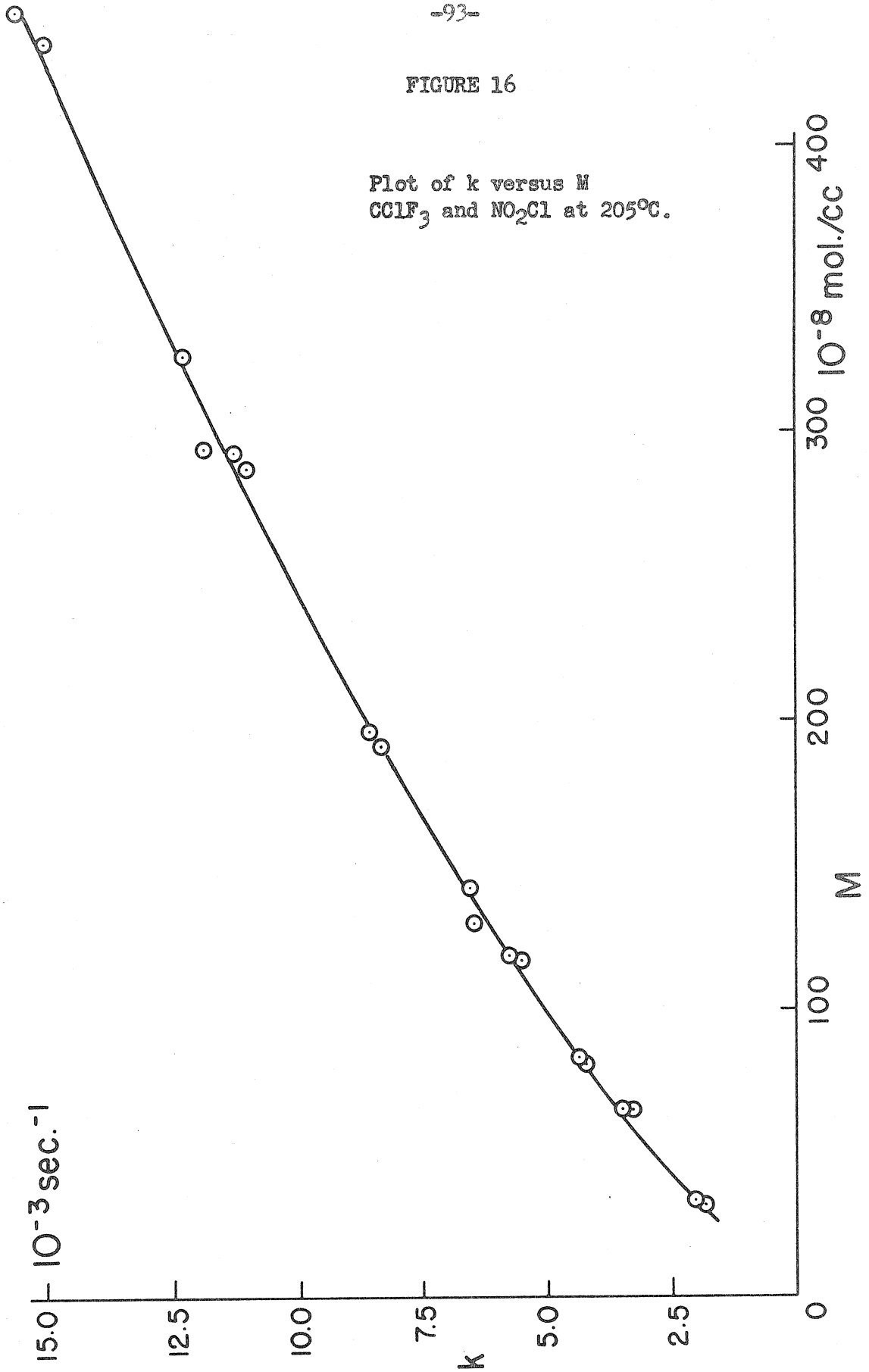

FIGURE 17

Plot of k versus M
A and NO_2Cl at 205°C.

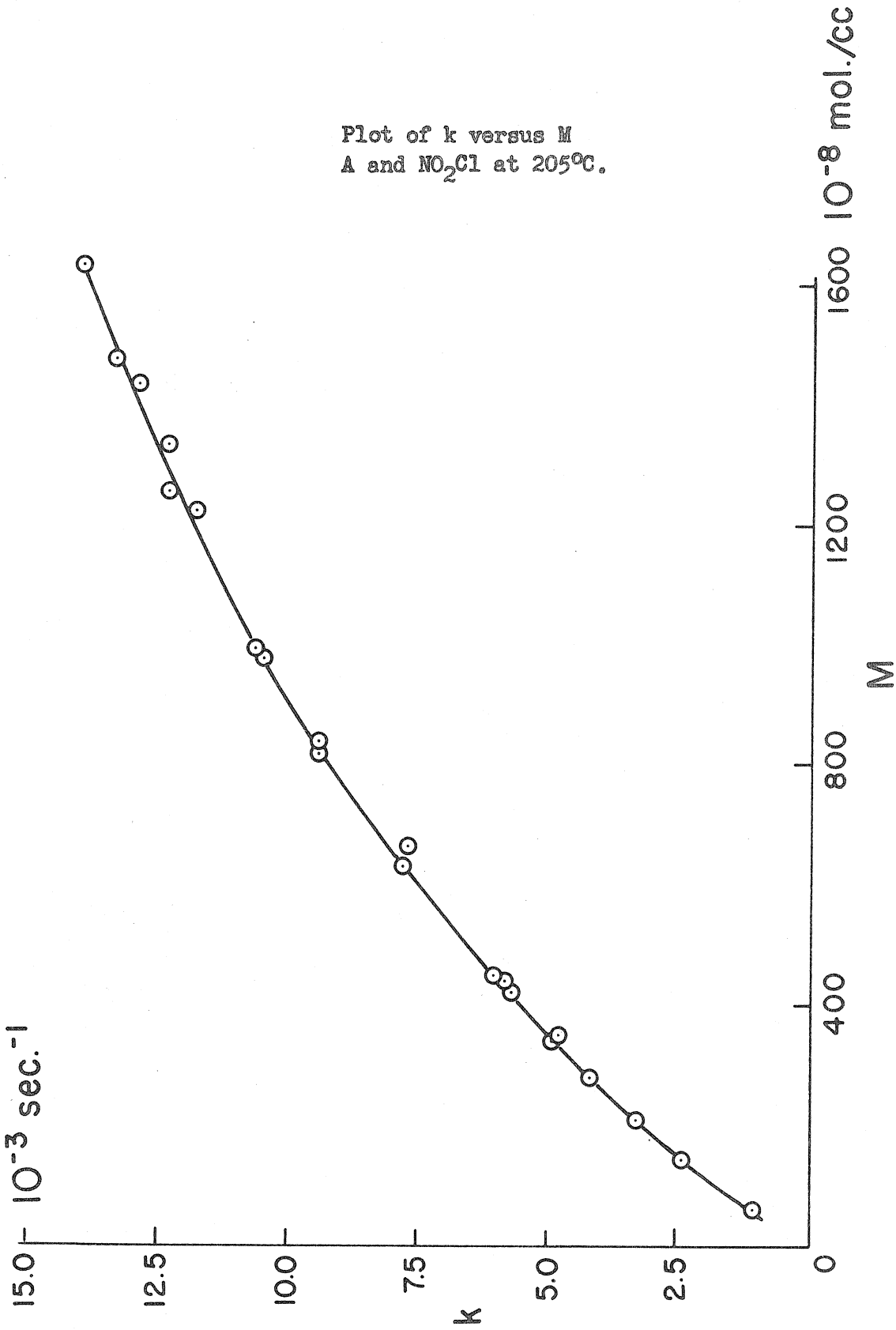

FIGURE 18

Plot of k versus M
$C_2Cl_2F_4$ and NO_2Cl at 205°C.

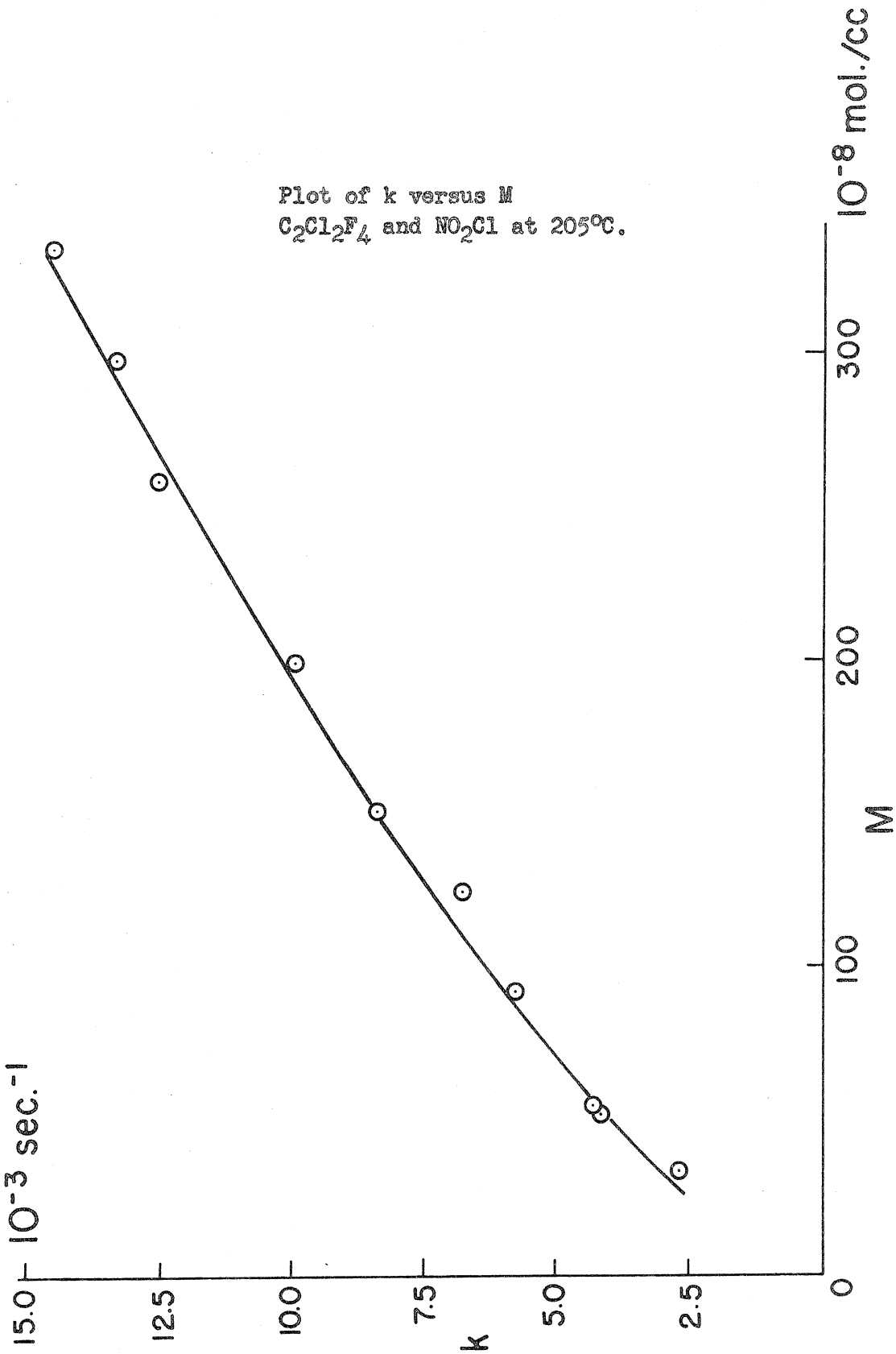

FIGURE 19

Plot of k versus M
CCl_2F_2 and NO_2Cl at 170°C.

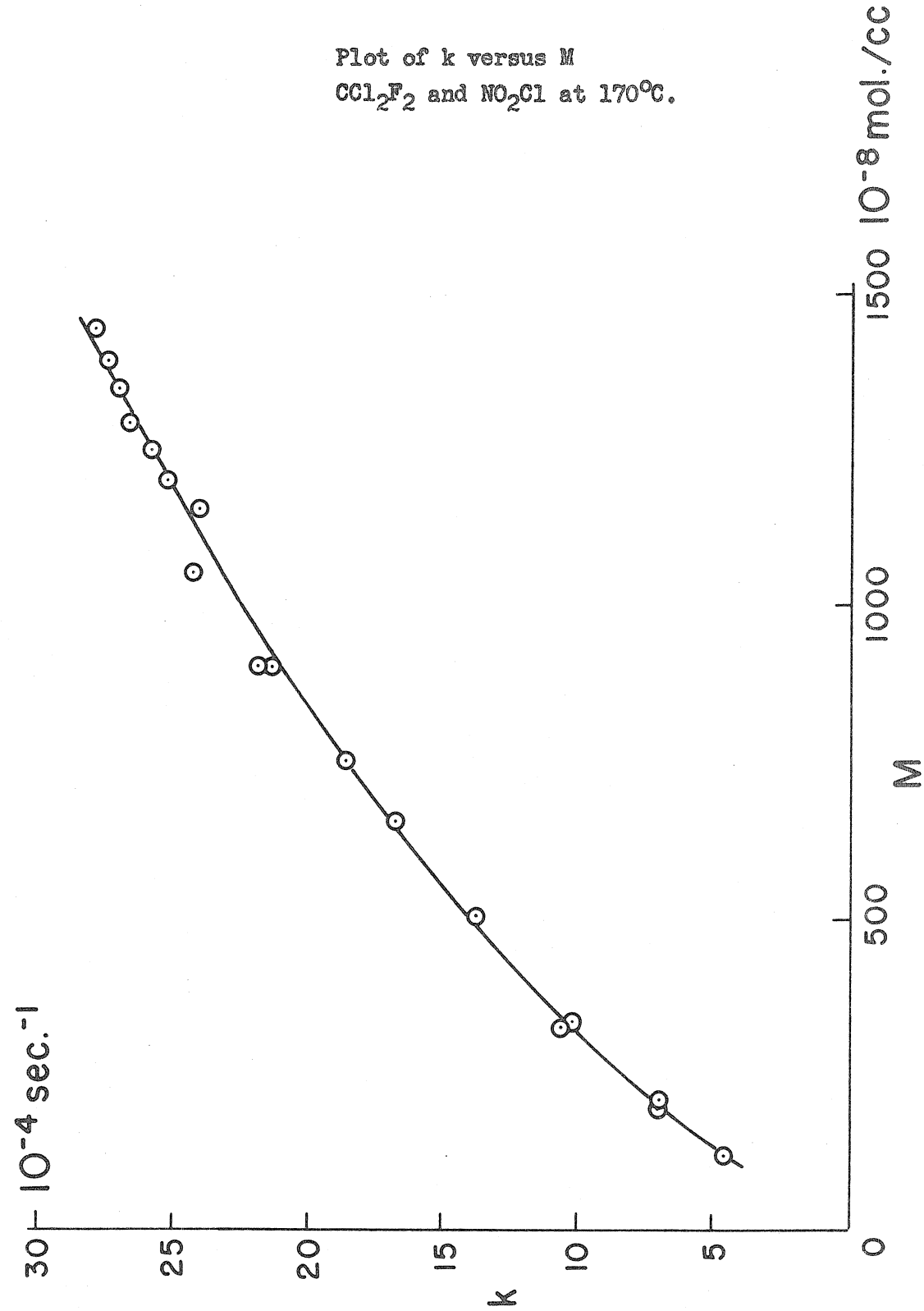

FIGURE 20

Plot of k versus M
CO_2 and NO_2Cl at 170°C.

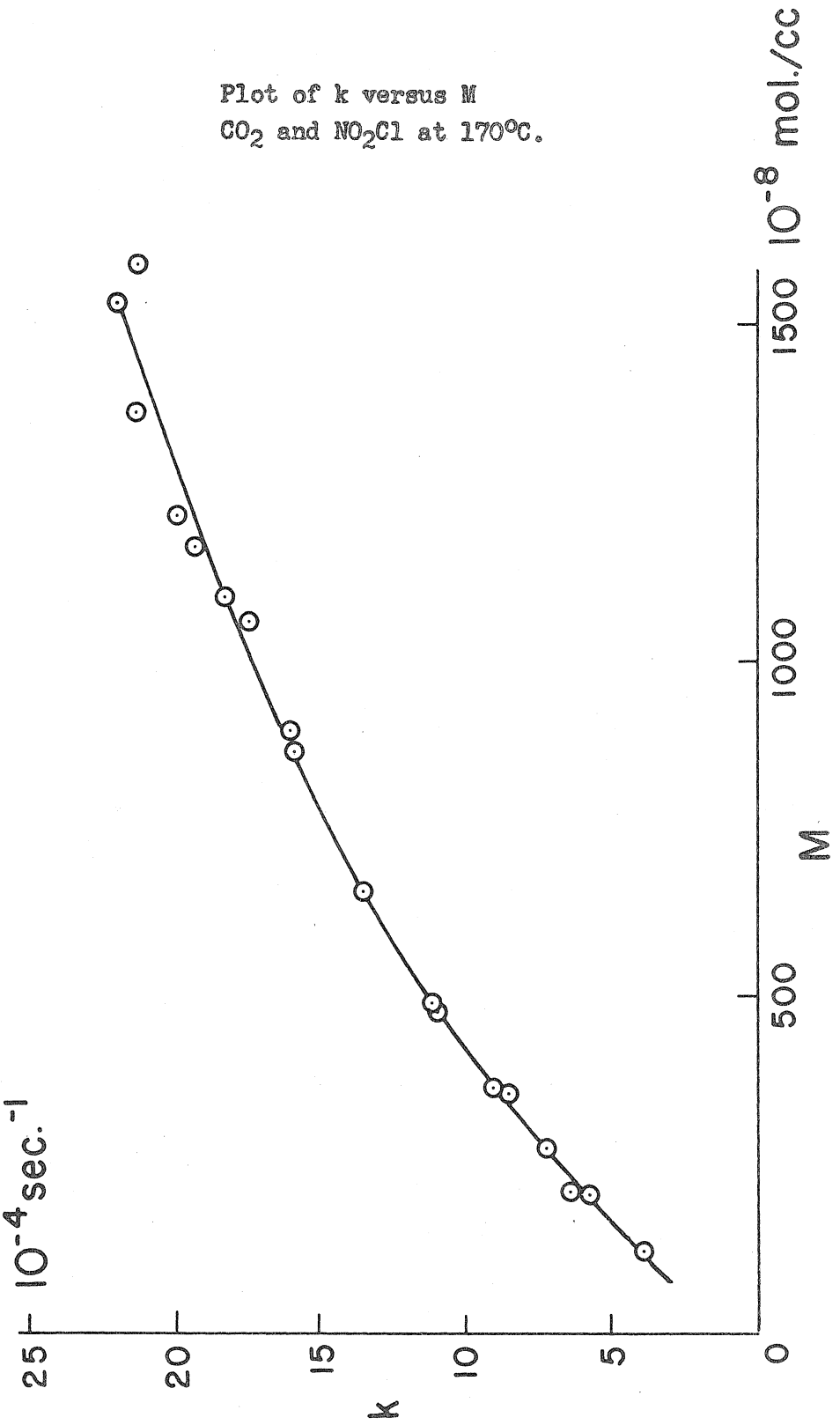

FIGURE 21

Plot of k versus M
A and NO_2Cl at 170°C.

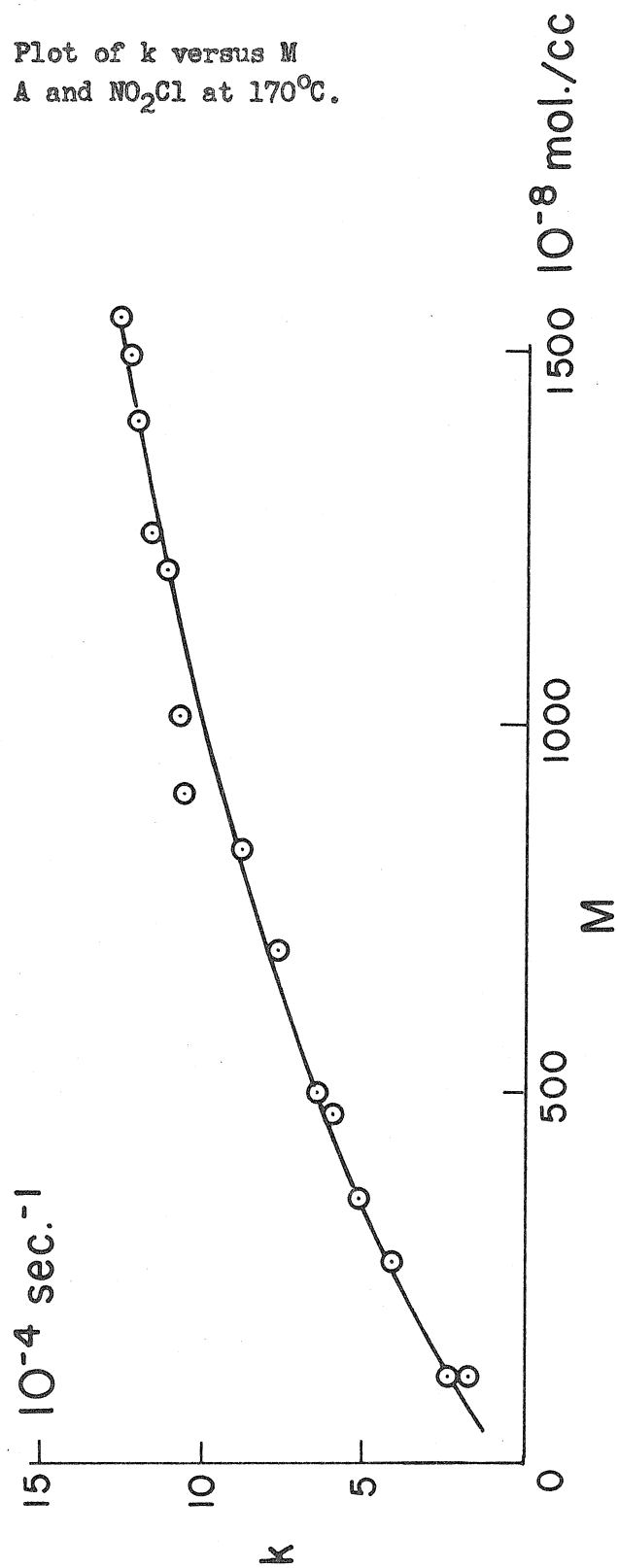

FIGURE 22

Plot of k versus M
A and NO_2Cl at 141°C.

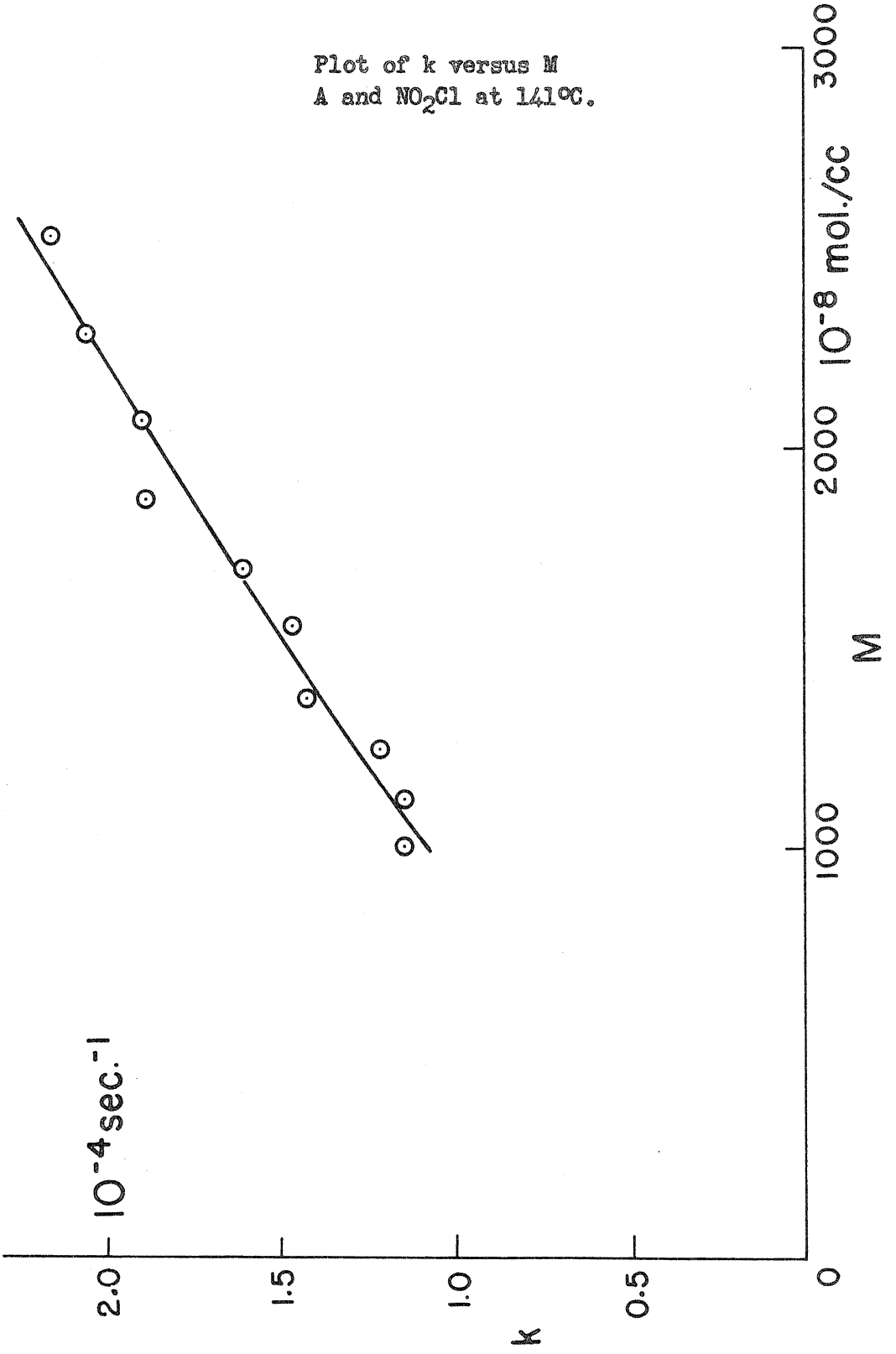

FIGURE 23

Plot of k versus M
CO_2 and NO_2Cl at 141°C.

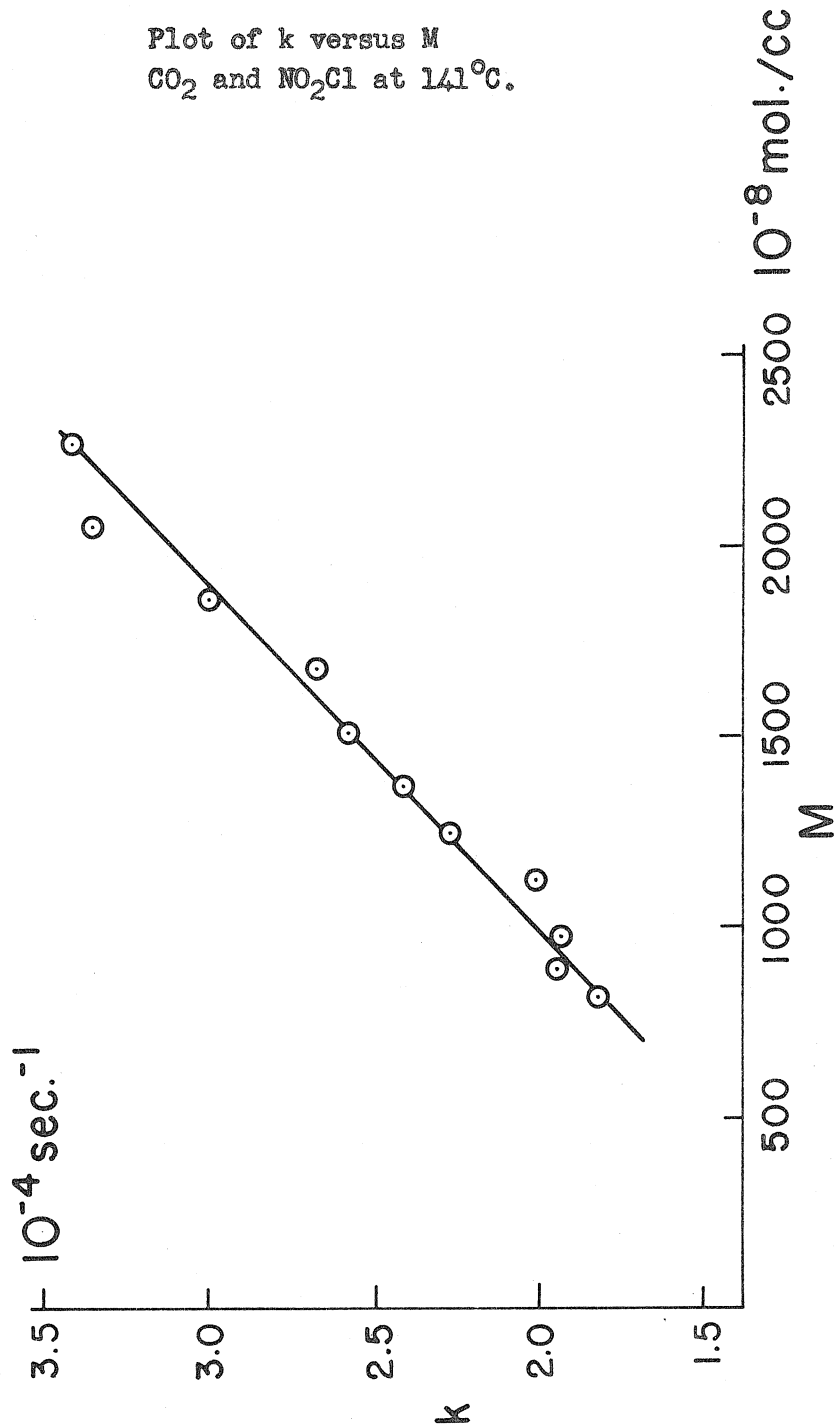

FIGURE 24

Plot of k versus M
CCl_2F and NO_2Cl at 141°C.

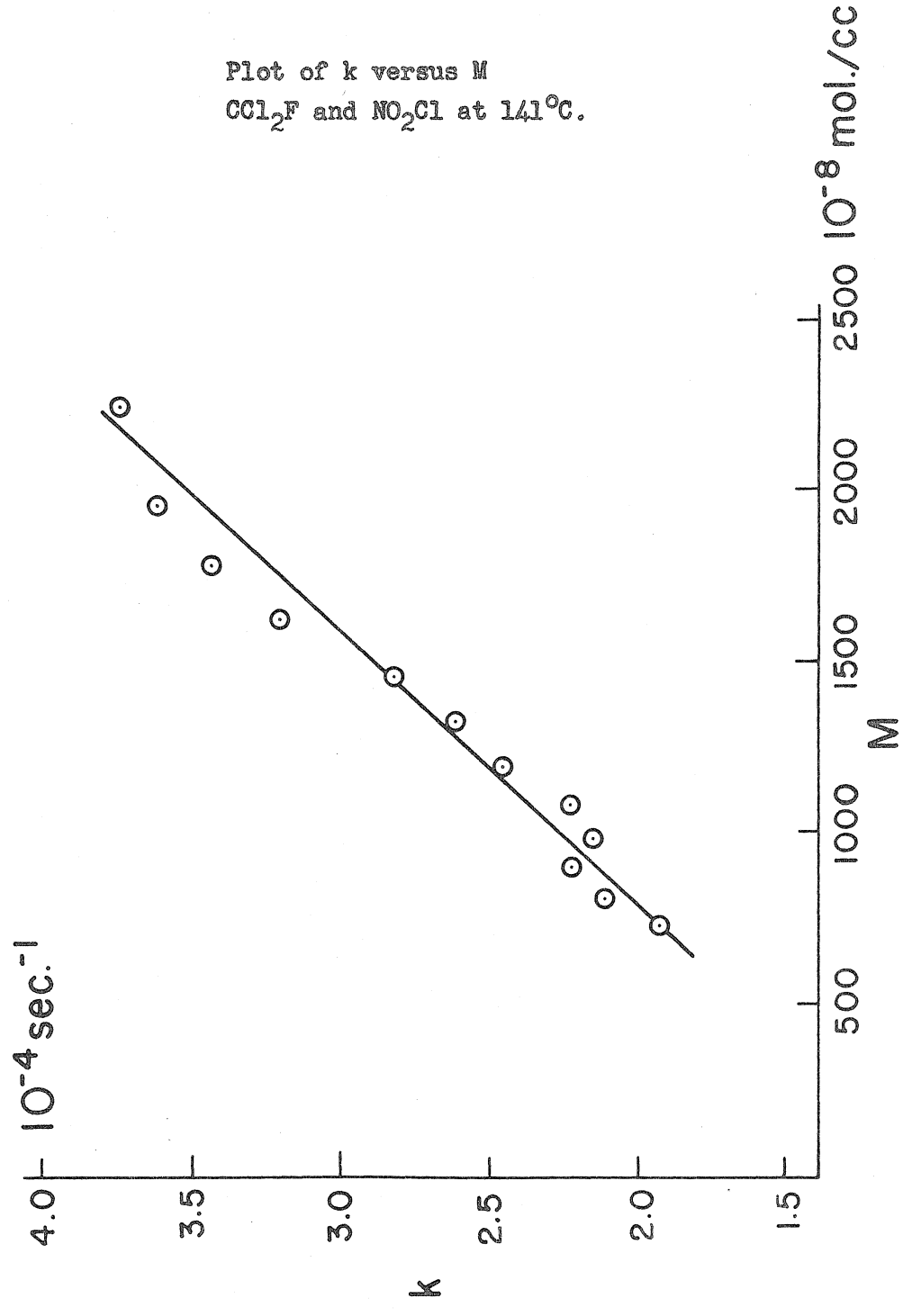

FIGURE 25

Plot of k versus M
O_2 and NO_2Cl at 141°C.

\+ Runs made after exposure of the cell to air

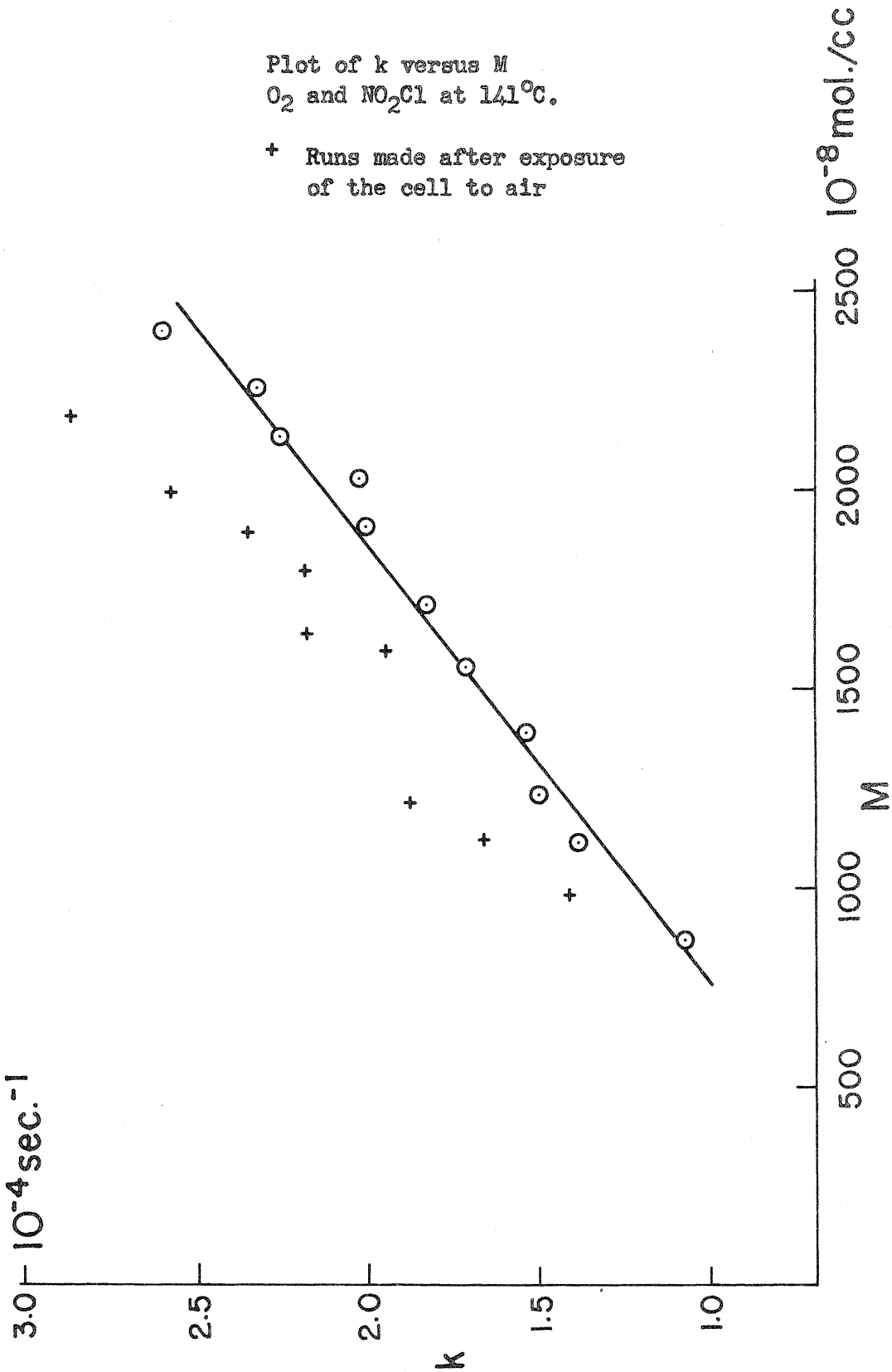

Table IV

Experimental Data

Temp.	Foreign Gas	M	$\underset{\sim}{M}$	K
141.0°C.	CO_2	804	$300 \cdot 10^{-8}$ mol/cc.	$1.82 \cdot 10^{-4}$ sec^{-1}
		890	332	1.94
		979	365	1.94
		1108	413	2.01
		1240	463	2.26
		1370	511	2.40
		1510	563	2.58
		1680	627	2.67
		1860	694	3.00
		2055	767	3.34
		2260	843	3.42
141.0°C.	CCl_2F_2	723	354	1.91
		800	391	2.10
		888	434	2.21
		980	479	2.14
		1070	523	2.21
		1192	583	2.44
		1320	645	2.60
		1460	714	2.81
		1620	792	3.18
		1780	870	3.41
		1960	958	3.59
		2250	1100	3.73
141.0°C.	A	1020	215	1.15
		1125	237	1.15
		1250	264	1.22
		1380	291	1.43
		1560	329	1.47
		1700	359	1.61
		1875	396	1.89
		2075	438	1.91
		2280	481	2.07
		2525	533	2.16

Table IV (continued)

Temp.	Foreign Gas	M	$\underset{\sim}{M}$	K
141.0°C.	O_2	880	$230 \cdot 10^{-8}$ mol/cc.	$1.08 \cdot 10^{-4}$ sec.$^{-1}$
		1110	290	1.40
		1230	321	1.52
		1395	364	1.58
		1560	407	1.74
		1710	446	1.84
		1900	496	2.02
		2015	526	2.05
		2150	561	2.28
		2260	590	2.35
		2400	626	2.63
		2525	659	2.58
141.0°C.	(NO_2Cl)	37		.76
		54		.95
		55		.95
		58		1.15
		62		1.10
		68		1.04
		70		1.13
		82		1.13
		85		1.17
		88		1.08
		91		1.12
		92		1.26
		100		1.28
		104		1.40
		106		1.48
		108		1.40
		128		1.43
		132		1.45
		135		1.50
		218		2.05
		228		2.06
		336		2.63
		348		2.67
170.1°C.	(NO_2Cl)	9.0		6.33
		10.0		6.33
		10.0		6.56
		12.5		8.48
		15.8		6.45
		38.5		9.49
		49.1		9.26
		59.2		11.17
		77.5		12.78
		90.0		13.13
		116.0		15.66
		121.5		16.31

Table IV (continued)

Temp.	Foreign Gas	M	$\underset{\sim}{M}$	K
170.1°C.	A	110	23.2 • 10^{-8} mol/cc.	1.84 • 10^{-4} $sec.^{-1}$
		115	24.3	2.46
		273	57.6	4.15
		357	75.3	5.20
		470	99.2	6.10
		500	105.5	6.49
		690	146	7.72
		825	174	8.75
		900	190	10.59
		1005	212	10.82
		1210	255	11.28
		1255	265	11.61
		1410	298	12.09
		1495	315	12.44
		1550	327	12.67
170.1°C.	CO_2	120	44.8	4.08
		200	74.6	5.76
		209	78.0	6.45
		274	102	7.32
		350	131	8.54
		365	136	8.98
		480	179	11.05
		490	183	11.28
		655	244	13.59
		870	325	15.91
		900	336	16.10
		1065	397	17.50
		1100	410	18.19
		1175	438	19.41
		1220	455	19.97
		1380	515	21.33
		1540	574	22.11
		1600	597	21.30

Table IV (continued)

Temp.	Foreign Gas	M	$\underset{\sim}{M}$	K
170.1°C.	CCl_2F_2	115	$56.2 \cdot 10^{-8}$ mol/cc.	$4.72 \cdot 10^{-4}$ sec.$^{-1}$
		190	92.9	7.02
		203	99.3	7.02
		320	156	10.78
		330	161	10.32
		501	245	13.91
		654	320	16.93
		750	367	18.56
		900	440	21.28
		1056	516	24.30
		1150	562	23.95
		1205	589	25.22
		1250	611	25.79
		1290	631	26.60
		1340	655	26.95
		1390	680	27.31
		1445	707	27.87
205.0°C.	$CBrF_3$	25		$3.11 \cdot 10^{-3}$ sec.$^{-1}$
		27		2.51
		77		4.84
		80		4.93
		112		5.99
		133		7.37
		162		7.83
		167		8.06
		188		9.10
		225		10.25
		267		11.63
		280		11.68
		304		12.51
		345		14.26
		454		16.56
		475		17.34
		524		18.54
		589		19.81
		650		20.94
		715		22.53
		785		25.29
		863		25.11

Table IV (continued)

Temp.	Foreign Gas	M	$\underset{\sim}{M}$	K
205.0°C.	He	40	$\cdot 10^{-8}$ mol/cc.	1.73 $\cdot 10^{-3}$ sec.$^{-1}$
		47		1.87
		60		2.56
		88		2.79
		91		3.04
		133		3.46
		188		4.52
		201		4.56
		270		5.44
		277		5.85
		314		6.22
		336		6.57
		391		7.19
205.0°C.	CO_2	12	4.4	.35
		20	7.5	.67
		23	8.6	.64
		26	9.7	.74
		27	10.1	.88
		58	21.6	1.93
		59	22.0	2.07
		62	23.1	1.75
		103	38.4	3.34
		108	40.3	3.45
		108	40.3	3.75
		145	54.1	5.30
		147	54.8	4.72
		178	66.4	5.27
		185	69.0	5.16
		212	79.1	6.17
		290	108.2	7.58
		368	137	8.94
		455	170	10.36
		490	183	10.99
		522	195	10.96
		555	207	11.98
		573	214	12.25
		614	229	13.73
		708	264	14.65
		722	269	14.90
		723	270	15.27
		770	287	15.59
		802	299	15.87
		985	367	17.66
		1002	374	17.36

Table IV (continued)

Temp.	Foreign Gas	M	$\underset{\sim}{M}$	K
205.0°C.	(NO_2Cl)	$6.8 \cdot 10^{-8}$ mol/cc.		$2.35 \cdot 10^{-3}$ sec.$^{-1}$
		9.7		3.00
		11.8		3.27
		11.8		2.72
		12.3		2.60
		12.6		2.63
		12.9		2.58
		13.4		3.18
		13.8		2.97
		13.8		3.00
		14.9		2.51
		15.3		2.97
		16.2		3.78
		18.3		2.86
		19.2		3.71
		21.7		4.03
		22.8		3.48
		23.3		3.83
		24.5		4.01
		24.5		4.06
		27.7		3.92
		30.4		4.29
		33.2		5.23
		34.0		4.61
		34.8		5.21
		34.9		5.02
		39.6		5.18
		40.0		5.60

Table IV (continued)

Temp.	Foreign Gas	M	$\underset{\sim}{M}$	K
205.0°C.	A	60	$12.7 \cdot 10^{-8}$ mol/cc.	$1.04 \cdot 10^{-3}$ sec.$^{-1}$
		147	31.0	2.49
		208	43.9	3.34
		280	51.1	4.19
		337	71.1	4.95
		350	73.9	4.91
		422	89.0	5.78
		440	92.8	5.88
		450	95.0	6.11
		637	134.4	7.83
		665	140.3	7.74
		815	172.0	9.35
		834	176.0	9.44
		970	204.7	10.60
		992	209.3	10.67
		1224	258.3	11.86
		1255	264.8	12.32
		1331	280.8	12.42
		1434	302.6	12.90
		1464	308.9	13.27
		1650	348.2	13.94
205.0°C.	CO	63		1.84
		63		1.85
		113		3.27
		118		3.57
		152		4.05
		159		4.08
		242		5.46
		249		5.48
		288		6.17
		299		6.47
		344		6.77
		390		8.22

Table IV (continued)

Temp.	Foreign Gas	M	$\underset{\sim}{M}$	K
205.0°C.	CCl_2F_2	46	22.5 • 10^{-8} mol/cc.	2.35 • 10^{-3} $sec.^{-1}$
		46	22.5	2.51
		48	23.5	2.26
		89	43.5	3.92
		90	44.0	4.31
		124	60.6	5.21
		127	62.1	5.44
		157	76.8	6.24
		160	78.2	6.40
		167	81.7	6.56
		169	82.6	6.82
		222	108.6	8.29
		223	109.0	7.72
		226	110.5	8.06
		226	110.5	8.34
		231	113.0	8.22
		275	134.5	9.68
		313	153.1	10.71
		359	175.6	11.68
		379	185.3	11.86
		389	190.2	12.32
		407	199.0	12.72
		453	221.5	14.05
		460	224.9	14.33
		470	229.8	13.82
		523	255.7	15.78
205.0°C.	$C_2Cl_2F_4$	36		2.74
		54		4.26
		55		4.31
		94		5.85
		126		6.84
		152		8.41
		201		10.00
		260		12.48
		300		13.31
		330		14.44

Table IV (continued)

Temp.	Foreign Gas	M	M	K
205.0°C.	$CClF_3$	32	$\cdot 10^{-8}$ mol/cc.	1.84 $\cdot 10^{-3}$ sec.$^{-1}$
		34		2.03
		65		3.29
		66		3.34
		82		4.26
		83		4.29
		117		5.51
		119		5.74
		131		6.47
		143		6.57
		192		8.34
		196		8.48
		288		10.96
		293		11.20
		295		11.82
		327		12.21
		435		14.97
		447		15.57
205.0°C.	CCl_4	19		1.84
		20		2.08
		59		5.32
		62		5.39
		102		7.60
		103		7.99
		120		8.66
		124		9.12
		134		9.51

Table IV (continued)

Temp.	Foreign Gas	M	$\underset{\sim}{M}$	K
205.0°C.	O_2	29	$7.6 \cdot 10^{-8}$ mol/cc.	$1.38 \cdot 10^{-3}$ sec.$^{-1}$
		31	8.1	1.29
		70	18.3	2.21
		72	18.8	2.33
		134	35.0	3.09
		135	35.2	3.60
		176	45.9	4.56
		180	47.0	4.61
		182	47.5	4.47
		218	56.9	5.30
		268	69.9	6.13
		308	80.4	6.59
		310	80.9	6.84
		368	96.0	7.28
		405	105.7	7.42
		435	113.5	8.09
		460	120.1	8.64
		497	129.7	8.73
		550	143.6	9.12
		550	143.6	9.33
		576	150.3	9.79
		663	173.0	10.90
		695	181.4	11.61
		759	198.1	12.14
		817	213.2	12.42
		848	221.3	12.83
		948	247.4	13.68
		975	254.5	14.30

References

1. H. J. Schumacher and G. Sprenger, Z. Elektrochem. 35, 653-655 (1929).
2. H. J. Schumacher and G. Sprenger, Z. physik. Chemie B-12, 115-131 (1931).
3. H. J. Schumacher, Chemische Gasreactionen, Edwards Bros., Inc. (1943), pp. 127-130.
4. H. F. Cordes and H. S. Johnston, J. A. C. S. 76, 4264-4269 (1954).
5. D. J. Wilson and H. S. Johnston, J. A. C. S. 75, 5763 (1953).
6. M. Volpe and H. S. Johnston, J. A. C. S. 78, 3903-3910 (1956).
7. M. Volpe and H. S. Johnston, J. A. C. S. 78, 3910-3911 (1956).
8. G. Casaletto, Doctoral Dissertation, Stanford University (1956).
9. D. Herschbach, Private Communication.
10. N. B. Slater, Proc. Roy. Soc. 194, 112-131 (1948).
11. N. B. Slater, Phil. Trans. A 246, 57-80 (1953).
12. N. B. Slater, Proc. Roy. Soc. A 218, 224-244 (1953).
13. R. L. Mills and H. S. Johnston, J.A.C.S. 73, 938-944 (1951).
14. H. S. Johnston, J. Chem. Phys. 20, 1103-1107 (1952).
15. A. A. Frost and R. G. Pearson, Kinetics and Mechanism, John Wiley and Sons, Inc. (1953).
16. R. C. Tolman, Statistical Mechanics with Applications to Physics and Chemistry, The Chemical Catalog Company, Inc. (1927).
17. L. S. Kassel, Kinetics of Homogeneous Gas Reactions, The Chemical Catalog Company, Inc. (1932).
18. H. S. Johnston, J. A. C. S. 75, 1567-1570 (1953).

19. H. S. Johnston, Third Technical Report, Section 5, Office of Naval Research Contract N 6 onr 25131, Project NR-051-246 (1953).

20. R. V. Churchill, Introduction to Complex Variables and Applications, McGraw-Hill Book Company, Inc. (1948).

21. L. S. Kassel, J. Chem. Phys. 21, 1093-1097 (1953).

22. H. S. Johnston and J. R. White, J. Chem. Phys. 22, 1969-1973 (1954).

23. H. S. Johnston and R. L. Perrine, J. A. C. S. 73, 4782-4786 (1951).

24. J. C. Giddings and H. Eyring, J. Chem. Phys. 22, 538-542 (1954).

25. H. Eyring and B. Zwolinski, J. A. C. S. 69, 2702-2707 (1947).

26. S. W. Benson, J. Chem. Phys. 19, 802-803 (1951).

27. S. W. Benson, J. Chem. Phys. 20, 1064-1069 (1952).

28. S. W. Benson and A. E. Axworthy, Jr., J. Chem. Phys. 21, 428-433 (1953).

29. C. Zener, Phys. Rev. 37, 556-569 (1931).

30. F. D. Rossini, ed., Thermodynamics and Physics of Matter, Princeton University Press (1955).

31. R. N. Schwartz, Z. I. Slawsky and K. F. Herzfeld, J. Chem. Phys. 20, 1591-1599 (1952).

32. R. N. Schwartz and K. F. Herzfeld, J. Chem. Phys. 22, 767-773 (1954).

33. C. F. Curtiss and F. T. Adler, J. Chem. Phys. 20, 249-256 (1952).

34. C. F. Curtiss, J. Chem. Phys. 21, 2045-2050 (1953).

35. E. Bauer, J. Chem. Phys. 23, 1087-1094 (1955).

36. B. Widom and S. H. Bauer, J. Chem. Phys. 21, 1670-1685 (1953).

37. I. Amdur and E. A. Mason, J. Chem. Phys. 23, 2268-2269 (1955).

38. I. Amdur and A. L. Harkness, J. Chem. Phys. 22, 664-669 (1954).

39. I. Amdur and E. A. Mason, J. Chem. Phys. 23, 415-416 (1955).

40. I. Amdur, E. A. Mason, and A. L. Harkness, J. Chem Phys. 22, 1071-1074 (1954).

41. J. O. Hirschfelder, C. F. Curtiss, and R. B. Bird, Molecular Theory of Gases and Liquids, John Wiley and Sons, Inc. (1954).

42. J. H. Wise and M. Volpe, 123rd National American Chemical Society Meeting, Los Angeles, March, 1953.

43. S. W. Benson, J. Chem. Phys. 22, 46-50 (1954).

44. R. V. Churchill, Fourier Series and Boundary Value Problems, McGraw-Hill Book Company, Inc. (1941).

45. H. F. Cordes, Doctoral Dissertation, Stanford University (1954).

Propositions

1. Bauer has suggested a hydrogen-bridge type structure for aluminum borohydride, and Ogg has relied upon this structure in interpreting the nuclear magnetic resonance spectrum of this material. It is proposed that this structure and Ogg's interpretation of this nuclear magnetic resonance spectrum are incorrect. A re-investigation of this molecule by electron diffraction would be worthwhile (1,2,3,4).

2. Control laboratories doing quantitative analysis on mixtures often over-determine the unknowns. The methods of least squares and of Lagrange's multipliers can be used to derive formulas suitable for routine use by untrained technicians for calculating the "best set" of values for the unknown component percentages in such mixtures.

3. A study of the products produced in the decomposition of the isotopically substituted cyclobutane

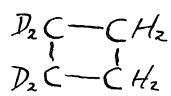

would provide information about the reaction coordinate of this decomposition.

4. Although nitryl fluoride and nitryl chloride are well-known, neither nitryl bromide nor nitryl iodide have been prepared. A method for the synthesis of nitryl bromide and a study of its thermal decomposition are proposed.

5. Trotman-Dickenson has pointed out that the data obtained by Schumacher and Frisch on the decomposition of fluorine dioxide are

totally inconsistent with Slater's theory of unimolecular reactions. It is proposed that the interpretation of these data is complicated by the effects of heterogeneity (5,6).

6. The mechanism postulated for the unimolecular decomposition of nitryl chloride (see p. 1 of this thesis) involves the formation of chlorine atoms. It is proposed to study the rate of reaction of chlorine atoms with nitryl chloride, using paramagnetic resonance.

7. The study of the effect of electronically excited atoms and molecules upon the rate of decomposition of gases whose thermal decomposition has been studied is proposed. For example, it has been observed from time to time that nitryl chloride decomposes photochemically. The study of the effect of varying concentrations of chlorine and nitrogen dioxide and of the effect of light of varying wave lengths should enable one to determine the mechanism of this reaction.

8. In the field of unimolecular reactions there are a few somewhat scandalous cases, such as nitrous oxide, nitrogen tetroxide, and mercury dialkyls, that cannot be accounted for by means of the current theories. It is proposed that these discrepancies are caused by the occurrence of limit cycles in the motion of these exceedingly non-harmonic mechanical systems (7,8).

9. It is proposed that Knox and Trotman-Dickenson's failure to find agreement between the experimental results of their work on reactions between chlorine atoms and hydrocarbons and their predictions based on activated complex theory, is caused by the

use of totally inadequate approximations in the theoretical treatment. It is suggested that the improved approximations mentioned in Part Three of this thesis be used (9).

10. An investigation by means of nuclear magnetic resonance of the rates of interconversion of isomers produced by internal hydrogen bonding in ortho-substituted phenols is proposed.

References for Propositions

1. J. Y. Beach and S. H. Bauer, J. A. C. S. 62, 3440 (1940).

2. S. H. Bauer, J. A. C. S. 72, 622, 1864 (1950).

3. R. A. Ogg, Jr., and J. D. Ray, Disc. Faraday Soc. No. 19, 239 (1955).

4. G. Silbiger and S. H. Bauer, J. A. C. S. 68, 312 (1946).

5. A. F. Trotman-Dickenson, Gas Kinetics, Academic Press, Inc., (1955), p. 73.

6. H-J. Schumacher and P. Frisch, Z. phys. Chem. 37 B, 1 (1937).

7. A. A. Andronow and C. E. Chaikin, Theory of Oscillations, Princeton University Press (1949).

8. N. Kryloff and N. Bogoliuboff, Introduction to Non-linear Mechanics, Princeton University Press (1947).

9. J. H. Knox and A. F. Trotman-Dickenson, J. Phys. Chem. 60, 1367 (1956).